OUKA
Osaka University Knowledge Archive

Title	Design of New Initiating Systems for Controlled/Living Cationic Polymerization Using Various Multidentate Ligand Frameworks
Author(s)	木越, 宣正
Citation	大阪大学, 2018, 博士論文
Version Type	VoR
URL	https://doi.org/10.18910/69377
rights	
Note	

Osaka University Knowledge Archive : OUKA

https://ir.library.osaka-u.ac.jp/

Osaka University

Design of New Initiating Systems for Controlled/Living Cationic Polymerization Using Various Multidentate Ligand Frameworks

A Doctoral Thesis

by

Sensho Kigoshi

Submitted to

the Graduate School of Science,

Osaka University

February 2018

Acknowledgements

This thesis presents the research that the author performed at the Department of Macromolecular Science, Graduate School of Science, Osaka University under the direction of Professor Sadahito Aoshima during 2011–2018.

First of all, the author would like to express the deepest appreciation to Professor Sadahito Aoshima for his continuous guidance, enthusiastic discussion, and warm encouragement throughout the author's laboratory life. The author is also deeply grateful to Professor Shokyoku Kanaoka for his kind support and insightful comments with new perspective, and Assistant Professor Arihiro Kanazawa for his convincing suggestions, stimulating discussion, and enormous help.

The author acknowledges his appreciation to Professor Akihito Hashidzume and Professor Hiroyasu Yamaguchi for careful reviewing of this thesis and fruitful comments.

The author expresses his gratitude to Associate Professor Kenichi Kuroda (University of Michigan School of Dentistry) for giving me an opportunity to study and have wonderful experiences as a visiting scholar in his group (June to August 2016).

The author would like to thank Mr. Seiji Adachi, Dr. Yasuto Todokoro, and Dr. Naoya Inazumi for NMR measurements, and Dr. Akihiro Ito for mass spectroscopy.

The author is deeply indebted to all "ORION" members; Professor Yoshio Okamoto (Nagoya University, Harbin Engineering University), Professor Mitsuo Sawamoto (Kyoto University, Chubu University), Professor Yoshitsugu Hirokawa (The University of Shiga Prefecture), Professor Masao Tanihara (Nara Institute of Science and Technology), Professor Eiji Yashima (Nagoya University), Professor Masami Kamigaito (Nagoya University), Professor Makoto Ouchi (Kyoto University), and all members of their groups for active discussions and good interactions. The author is particularly grateful to Dr. Hajime Kammiyada, Dr. Junki Tanabe, and Dr. Shinya Yamamoto for frequent discussions and friendly communications.

The author expresses his special thanks to all members of Aoshima Laboratory for useful suggestion and their friendship during the course of research. Particularly, the author is grateful to Dr. Yukari Oda (Assistant Professor, Kyushu University), Dr. Hiroaki Shimomoto (Senior Assistant Professor, Ehime University), Dr. Yasushi Ishido (Sekisui Chemical Co., Ltd.), Dr. Yu Shinke (The Yokohama Rubber

Co., Ltd.), Dr. Kira B. Landenberger (Lecturer, Kyoto University), Dr. Hayato Yoshimitsu (Kaneka Corp.), Dr. Mayuka Yamada (Mitsubishi Chemical Co., Ltd.), Dr. Koichiro Takii (JSR Corp.), Dr. Ryohei Saitoh (Mitsubishi Rayon Co., Ltd.), and Dr. Tomoya Yoshizaki (Toray Industries, Inc.) for their stimulating suggestion and encouragement. The author also thanks Dr. Norifumi Yokoyama (Fujifilm Corp.), Dr. Suzuka Matsumoto-Takii (Asahi Kasei Corp.), Mr. Shungo Kanda (Toray Industries, Inc.), and Mr. Ryohei Kimura (Toyobo Co., Ltd.) for meaningful discussion and friendship, and Mr. Hiroshi Oda (Nippon Paint Co., Ltd.), Mr. Daichi Yokota, Mr. Motoki Higuchi for their kind help and assistance. The author is also obliged to Mrs. Misato Asai-Nishiuchi and Mrs. Mariko Okamoto for their thoughtful support.

The author is grateful to the Japan Society for the Promotion of Sciences (JSPS) for JSPS Research Fellowship for Young Scientists (DC2) and a Grant-in-Aid for JSPS Fellow (16J01970) from April 2016 to March 2018.

Finally, the author expresses his heartfelt appreciation to his late father Shoshin Kigoshi, his mother Shoko Kigoshi, his brothers Shinjo Kigoshi and Kenshin Kigoshi, his grandmother Emiko Kigoshi, his fiancée Kanae Tsuji, and all his relatives for their continuous supports and considerable encouragement.

February 2018

木越 宣正

Sensho Kigoshi

Department of Macromolecular Science

Graduate School of Science

Osaka University

Contents

Chapter 1 General Introduction 1

Part I Controlled/Living Cationic Polymerization Using Tetradentate Schiff Base Ligands/Metal Chlorides Initiating Systems

Chapter 2 *In Situ* and Readily Prepared Metal Catalysts and Initiator for Living Cationic Polymerization of Isobutyl Vinyl Ether: Dual-Purpose Salphen as a Ligand Framework for $ZrCl_4$ and an Initiating Proton Source 19

Chapter 3 Salen-Type Ligand/MCl_n Initiating Systems for the Controlled Cationic Polymerization of Isobutyl Vinyl Ether: Effects of the Ligand Framework 37

Part II Catalytic Structure–Property Relationship of Complex Catalysts in Cationic Polymerization Using Initiating Systems Consisting of Bidentate Schiff Base Ligands and Metal Chlorides

Chapter 4 Appropriate Ligand Frameworks for Various Polymerization Systems 51

Chapter 5 Structure–Property Relationship of Phenoxyimine Ligands/MCl_n Initiating Systems for Cationic Polymerizations of Vinyl Ether 73

Chapter 6 Summary 95

List of Publications 99

Chapter 1

General Introduction

1. Background

1.1 Catalyst Design for Organic Synthesis

Designing metal complex catalysts is one of the most effective strategies for the development of novel synthetic methods of various organic compounds with selectivity, activity, and atom economy in both industrial and academic fields. A great advantage of metal complex catalysts is that the electric and steric features of the catalytic environment can be tuned by combining various ligands and central metals. The fine-tuning of metal catalysts improves catalytic properties, such as the activity, regio-, chemo-, enantio-, and stereoselectivities, and scope of the applicable substrates and conditions.[1–3] To develop new catalysts and metal-complex-catalyzed reactions, one needs to understand how metals and ligands influence reaction mechanisms and catalytic properties at the molecular level.

Asymmetric synthesis has been diligently studied in association with the development of metal complex catalysts for the synthesis of optically active compounds across a wide range of fields, including synthetic organic chemistry, medicinal chemistry, agricultural chemistry, and natural product chemistry.[4] Catalytic asymmetric synthesis has economic advantages, particularly on the industrial scale, because only a catalytic amount of a chiral source, such as an enzyme, chiral metal complex, and chiral organic molecule, is needed to produce considerable amounts of optically active compounds. Through tremendous research on the design of asymmetric catalysts, the following important core structures, which are called "privileged[5,6] ligands (catalysts)", have been developed: such as BINAP,[7] BINOL,[8] salen complexes,[9] BOX,[10] DuPhos,[11] TADDOL[12] (Figure 1).

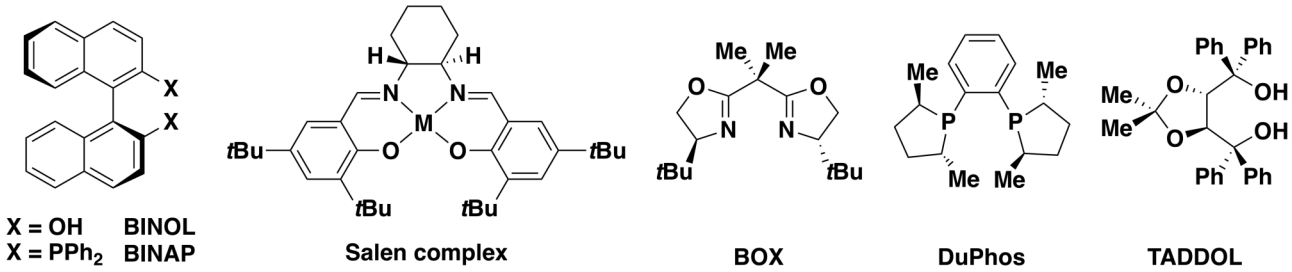

Figure 1. Selected privileged ligands and catalysts.

The catalysts with these privileged ligands are widely used for various asymmetric reactions. For example, BINAP, which was developed as an asymmetric hydrogenation catalyst (Rh-binap complex catalyst) by Noyori and co-workers in 1980s,[13] has been demonstrated as an effective ligand of catalysts for asymmetric hydrofunctionalization (hydroboration, hydrosilylation, hydroacylation, and hydroamination),

alkene isomerization (allylamines and allylalcohols), Diels-Alder reaction, Heck reaction, aldol-type reactions, etc.[14] The wide scope of applicable reactions demonstrates the importance of catalyst structures for asymmetric recognition ability. In addition, these structural features of privileged catalysts contribute to the strategic approach of catalyst design in various fields.

1.2 Polymerization Catalysts

Catalysts used in polymerization reactions require not only sufficient activity, stability and tolerance for polar groups, and versatility but also precise control of the polymer structures, such as the molecular weight, molecular weight distribution, tacticity, comonomer sequence, and composition. These demands are potentially satisfied by tuning the catalytic properties of metal complex catalysts. Indeed, catalyst design has been studied systematically in coordination polymerization,[15] radical polymerization,[16–19] and ring-opening metathesis polymerization (ROMP),[20,21] which has provided high turnover frequencies, sufficient stereoselectivities, monomer versatility, and robustness under various conditions (e.g., in aqueous media).

Theoretical understanding of ligand-structure-catalytic property relationships and the catalytic reaction mechanisms is highly efficient for the design of well-defined polymer structures. Stereospecific polymerization of olefin derivatives demonstrated the importance of the catalytic site topology for stereoselectivity. In 1954, Natta discovered a catalyst to generate isotactic polypropylene,[22] which opened the door for stereospecific polymerization. In particular, single-site polymerization catalysts, including metallocene catalysts, enable almost perfect stereocontrol, such as isotactic, syndiotactic, and hemiisotactic control, through the topological approach.[23–30] Ewen's symmetry rule properly explained the relationship between the catalyst symmetry and the stereoregularity of product polymers (Figure 2A).[26,27] Subsequently, various post-metallocene catalysts,[31–37] such as phenoxyimine-type catalysts, were developed to attain both stereocontrol and high activity (Figure 2B).[38] An advantage of phenoxyimine-type catalysts is the accessibility of various structures by a simple condensation reaction of commercially available amines and salicylaldehyde derivatives. Moreover, recent developments of metal complex catalysts, such as α-diimine palladium catalysts (Brookhart type) and phosphine-sulfonato palladium catalysts (Drent type), have realized the copolymerization of polar monomers with olefin monomers.[31,37,39–41]

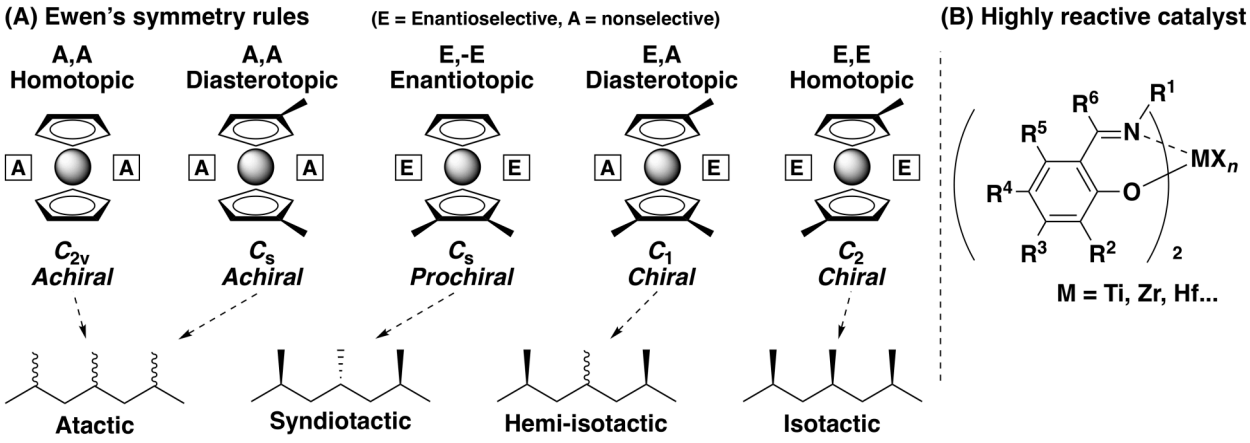

Figure 2. (A) Ewen's symmetry rules, and (B) highly reactive post-metallocene catalysts.

Lewis acid catalysts have been playing pivotal roles in various organic syntheses since the 19th century. Conventional Lewis acids, such as metal halides, have been extensively employed for fundamental organic reactions, including Friedel-Crafts, Diels-Alder, and aldol-type reactions, at the dawn of organic chemistry. Subsequently, tailored Lewis acid catalysts were developed in modern organic synthesis,[42] which allowed for improved catalytic properties, such as reactivity, selectivity, and versatility. In addition, tailored chiral catalysts achieved Lewis-acid-mediated asymmetric syntheses. More recently, various artistic catalysts were designed based on new concepts, such as combined acid systems (Brønsted-acid-assisted Lewis acid, Lewis-acid-assisted Lewis acid, Lewis-acid-assisted Brønsted acids, and Brønsted-acid-assisted Brønsted acid systems) and bifunctional catalytic systems.[43–45]

Designing metal complex catalysts used as Lewis acid catalysts in cationic polymerization is expected to contribute to the improvement of activity and stereoselectivity; however, studies on catalyst design using various ligand frameworks have been limited to selected examples. The difficulty of catalyst design in cationic polymerization partly comes from the limitation of applicable metal catalysts (Et_xAlCl_{3-x}, $SnCl_4$, $TiCl_4$, $ZnCl_2$, BCl_3, etc.); however, recent studies have demonstrated that a wide variety of metal halides are efficient for living cationic polymerizations when combined with suitable additives.[46] The narrow scope of ligands, which stems from the deactivation of strong electron-donating ligands by catalysts, is also responsible for this difficulty.[47–49] A few successful examples of catalyst design include the stereoselective cationic polymerization of vinyl ether (VE) using titanium catalysts with aryloxy ligands [$TiCl_2(OAr)_2$].[50] In addition, designed Lewis acid catalysts, such as metallocene-type catalysts and catalysts with extremely weakly coordinating counteranions, were efficient for the synthesis of polyisobutene with a very high molecular weight or highly reactive polyisobutylene with exo-olefin moieties at the chain ends.[51] In these studies, the polymerization behavior was discussed focusing on the features of the counteranions because counteranions are highly responsible for the propagation reactions through interactions with the carbocationic chain ends.

1.3 Living Cationic Polymerization

Living polymerization, which consists of initiation and propagation reactions and is free from irreversible chain-transfer and termination reactions, is highly effective for the precise control of the molecular weight, molecular weight distribution, comonomer composition, microstructure, chain-end structure, and molecular architecture. Szwarc[52] reported the first example of living polymerization in 1956 for the anionic polymerization of styrene. After this breakthrough, various living polymerization systems have been achieved via diverse mechanisms, including ring-opening, cationic, radical, metathesis, and coordination mechanisms. Precise syntheses of various functional polymers with well-defined structures have also been extensively studied along with the increasing accessibility of living polymerization techniques.[15-21,53–68]

The dynamic equilibrium of dormant and active species is the key to achieving living polymerization, particularly in cationic and radical polymerizations. The first living cationic polymerization was achieved via the HI/I_2 initiating system for the polymerization of isobutyl vinyl ether (IBVE) in 1984.[69] Subsequently, the tertiary ester/BCl_3 system was developed for the living polymerization of isobutene in 1986.[70] Both of these systems attained the livingness by constructing an appropriate equilibrium between the covalent carbon-halogen bonds (dormant species) and the growing carbocations (active species). Living cationic polymerization via the dormant-active equilibrium was subsequently achieved by various initiating systems that employed suitably nucleophilic counteranions,[71–75] weak Lewis bases,[76–79] or tetraalkylammonium salts.[47,48]

The base-assisting system (Figure 3), which employs weak Lewis bases, such as esters and ethers as additives, is superior to other systems in terms of the diversity of the applicable monomers. In the base-assisting system, weak Lewis bases contribute to adjusting the Lewis acidity of the catalysts and stabilizing the growing carbocations. Recent studies using a wide variety of metal halides in the base-assisting cationic polymerization of IBVE[46] and *p*-methoxystyrene[91] demonstrated that the nature of the central metals, such as oxo- and chlorophilicities, and the structures of counteranions highly influenced the polymerization rates and controllability.[46,90] Thus, a suitable initiating system can be designed with the use of appropriate Lewis acids and weak Lewis bases depending on the reactivity of the monomers used. Moreover, the base-assisting system will be very helpful for devising a rational strategy to develop novel complex catalysts based on the interaction between metal halides and heteroatoms.

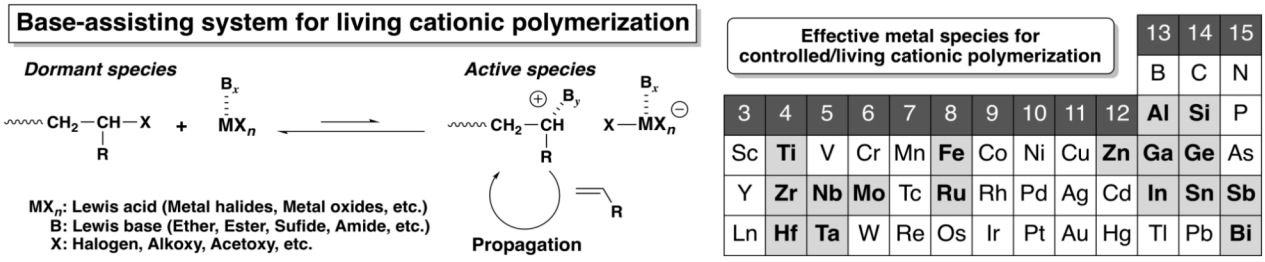

Figure 3. The base-assisting living cationic polymerization and metal species of metal halide catalysts used for the polymerization.

1.4 Design of Metal Complex Catalysts for the Cationic Polymerization of VE

The primary motivation for catalyst design in cationic polymerization was the improvement of the polymerization controllability. For example, the modification of $TiCl_4$ by alkoxy or aryloxy groups generated $TiCl_n(OR)_{4-n}$, which successfully functioned as catalysts for the controlled/living cationic polymerization of VEs,[80–83] β-pinene,[84,85] styrenes,[86–88] and indene.[89] The RO groups efficiently tune the electronic properties of the central Ti atom to exert appropriate Lewis acidity to $TiCl_n(OR)_{4-n}$. The moderation of the Lewis acidity by alcohols was also efficient for the controlled polymerization of VEs using other metal halides, such as $MoCl_5$ and $NbCl_5$.[90] Moreover, $TiCl_2(OAr)_2$ catalysts with proper aryloxy groups induced the stereospecific cationic polymerization of VEs most likely due to the generation of counteranions with appropriate steric bulkiness.[50]

Catalyst design in cationic polymerization is expected to be useful for expanding the scope of monomers, the development of environmentally benign catalytic systems, and stereocontrol. However, the systematic understanding of metal complex catalysts in cationic polymerization is insufficient because the scope of applicable ligands is very narrow. As mentioned above, relatively strong Lewis bases, such as amine/amide compounds, easily deactivate Lewis acid catalysts. Thus, previous studies of metal complex catalysts for VE polymerization have overcome this drawback through the elaborate design of ligands, additives, and reaction conditions. These are categorized into three groups as demonstrated below.

(1) Cationic Metal Complex Catalysts and Their Precursors

The first group includes cationic metal complexes, which have a positive charge at the central metal and are generally activated by activators, such as $B(C_6F_5)_3$ or methylaluminoxane (MAO), before polymerization (Figure 4).[92–98] Baird[92] reported that a combination of Cp^*TiMe_3 with a highly electrophilic borane, $B(C_6F_5)_3$, generated a methyl-bridged compound, $Cp^*TiMe_2(\mu\text{-Me})B(C_6F_5)_3$, which served as a $[Cp^*TiMe_2]^+$ supply source. This cationic species functioned as an initiator not only for the polymerizations of ethylene,[99,100] propylene,[100] 1-hexene,[101] and styrene[99] via the Ziegler-Natta process but also for the polymerizations of isobutene,[102] VE,[103] and styrene[99] via a carbocationic mechanism. In the carbocationic mechanism, the polymerization was initiated from the cationic metal center or from protons generated from the hydrolysis of the complex and/or $B(C_6F_5)_3$ by adventitious water. The propagation reaction occurred at the carbocationic chain ends accompanying counteranions such as $[XB(C_6F_5)_3]^-$ (X = Me, OR, etc.). In this process, the metal complex did not directly affect the propagation step but was responsible only for the initiation step. However, Baird's mechanism cannot fully explain the polymerization results using metal complexes categorized into this group, as exemplified by the isotactic polymerization of butyl VE by Ti complexes with tridentate amine ligands.[93] The cationic complex systems have a great potential to construct polymerization reactions with unique features; however, the partial uncertainty makes it difficult to develop a strategic approach to designing novel complexes.

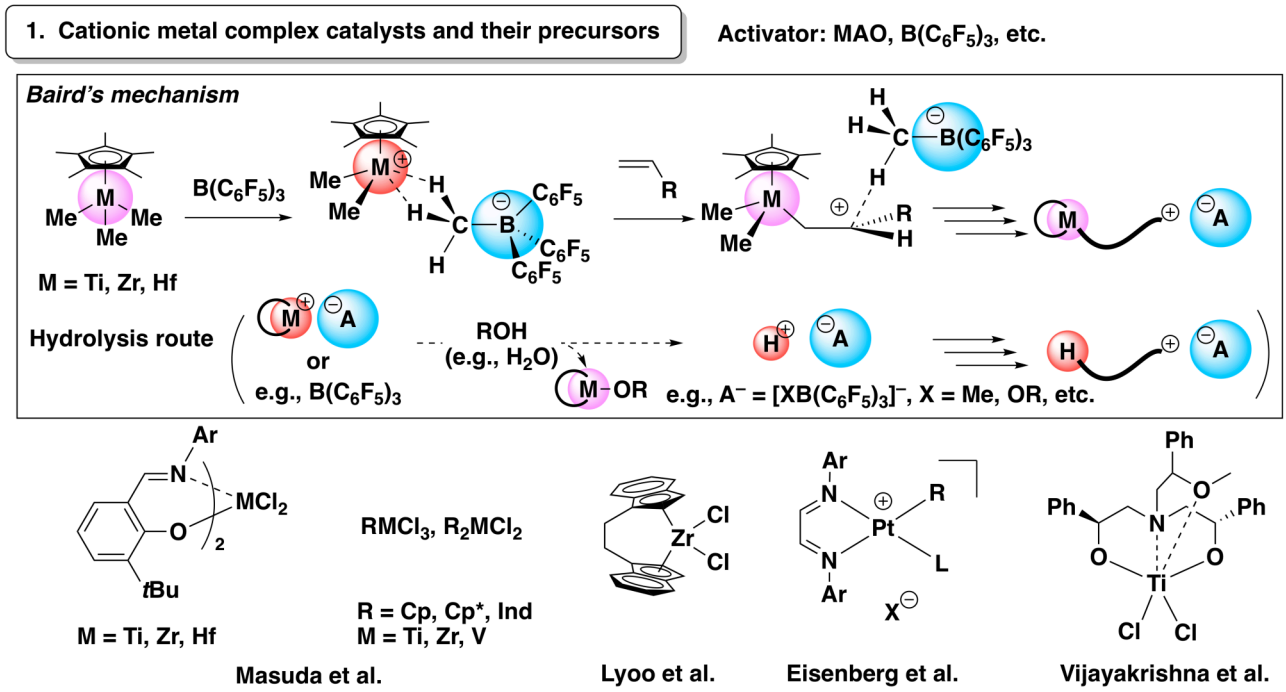

Figure 4. Cationic metal complex catalysts and their precursors used for cationic polymerization of VE.

(2) Neutral Metal Complex Catalysts

Neutral metal complexes that have vacant sites and exhibit Lewis acidity are the most widely employed for living cationic polymerization among the three groups (Figure 5). Cationogens, which are compounds with carbon-hetero atom bonds, such as carbon-halogen or carbon-acetoxy bonds, are often used in combination with neutral metal complexes in the absence[72–75] or presence of additives.[76–79] Metal complex catalysts abstract the heteroatom from the cationogen to generate the initiating cationic species and a counteranion. Propagating chains also have carbon-heteroatom bonds, which are reversibly activated via the dormant-active equilibrium as explained above. Appropriate ligands such as alcohols and acetylacetone (acac) have been employed to generate catalysts such as $TiCl_n(OR)_{4-n}$[80–83] and $M(acac)_n$[104] (M = Zn, Sn, Al, etc.). These ligands suitably moderate the Lewis acidity of the central metals by tuning the catalytic environment. Stereoselective polymerization was also feasible with $TiCl_2(OAr)_2$,[50] as described above. In addition, a facile method to generate metal complex catalysts *in situ* by mixing metal halides and ligand precursors, such as alcohols and acac, was constructed for the living cationic polymerization of VEs.[90,105,106] This method is highly expected to be useful for designing neutral metal complexes with a wide variety of ligands.

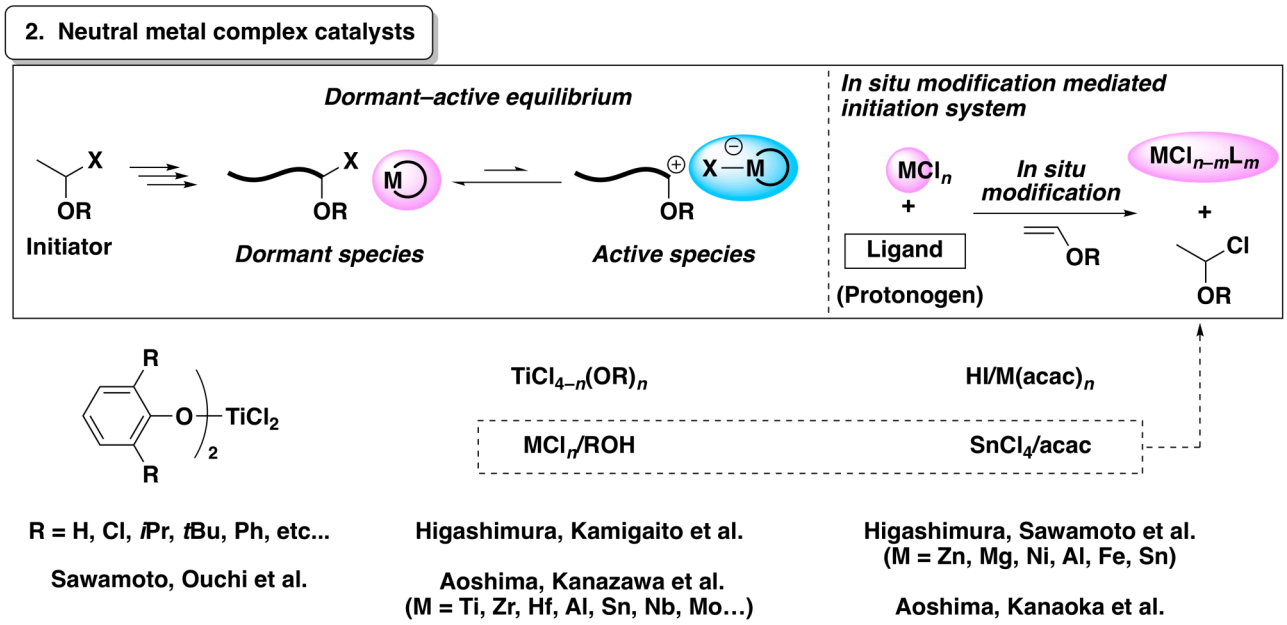

Figure 5. Neutral metal complex catalysts used for cationic polymerization of VE.

(3) Ate Complexes and Their Precursors

Ate complexes, which have a negative charge at the central metal, are prepared through reactions between a cationic source such as a trityl halide or R_3SiH and a neutral metal complex (Figure 6).[107–110] Polymerization is initiated from the cationic species generated from the cationic source. The metal species with a negative charge functions as a counteranion during polymerization. The electrostatic interactions between the growing carbocation and the ate complex likely affects the propagation reaction. In fact, the MWD of the obtained polymer was affected by the structures of niobium complexes.[107] The initiating system using ate complexes is inherently different from the system using tetraalkylammonium salts[47,48] because the anionic metal species, such as $SnCl_5^-$, act as a Lewis acid catalyst in the latter system.

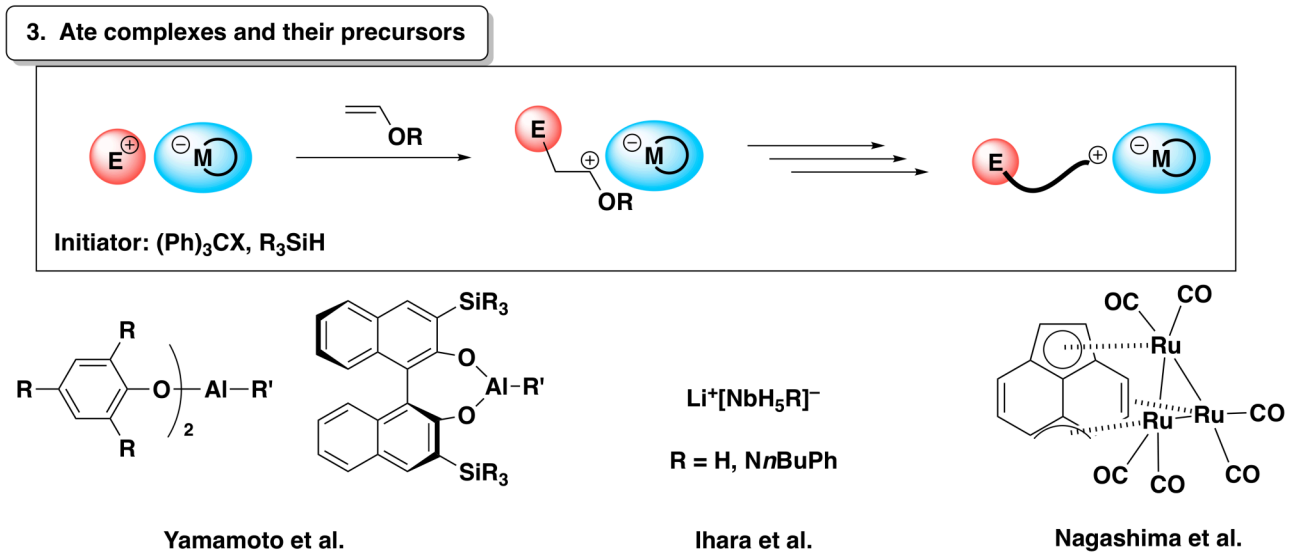

Figure 6. Ate complexes and their precursors used for cationic polymerization of VE.

2. Objective and Outline of This Thesis

The objective of this thesis is to comprehensively examine the functions and properties of metal complex catalysts in cationic polymerization. Ligand frameworks, metal species, and reaction conditions need to be elaborately designed for controlled cationic polymerization. The base-assisting system that employs neutral metal complexes as Lewis acid catalysts is a prospective candidate for the design baseline in this study because various metal species are applicable in combination with weakly Lewis basic additives, such as esters and ethers.[46] First, the author focuses on multidentate Schiff base ligands containing phenol moieties, e.g., salen and salphen ligands, because this framework is easy to synthesize and derivatize and has a relatively mild donating ability. For complex formation, a ligand and a metal halide is simply mixed *in situ* before polymerization because this method requires neither a purification process for the catalysts nor an initiator (hydrogen halides, which act as initiating species, are generated via the complexation).[90,105,106] Moreover, the author designs phenoxyimine-type ligands with a wide variety of substituents, particularly focusing on their electronic and steric features. The author also aims to explore the structure-property relationship in controlled/living cationic polymerization using metal complex catalysts with phenoxyimine-type ligands.

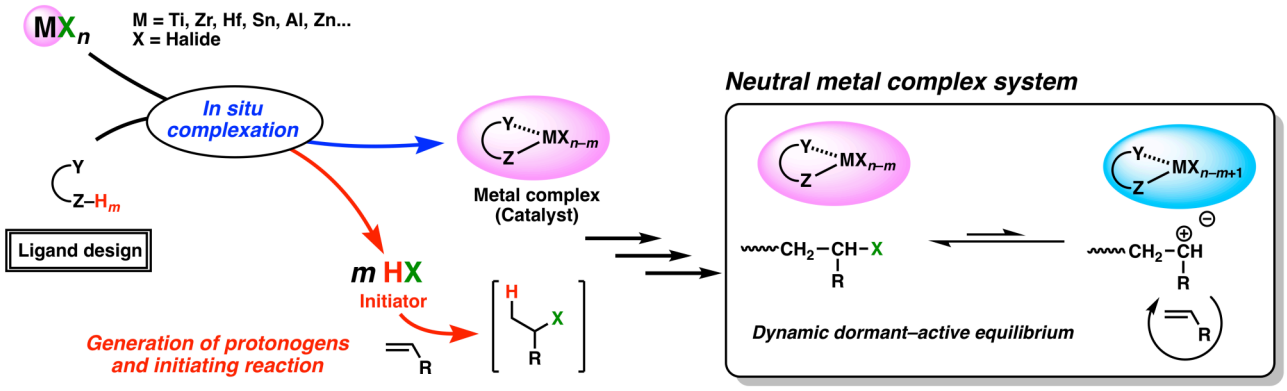

Figure 7. Methodology adopted in this thesis.

This thesis consists of two parts (Figure 8): Part I (Chapters 2 and 3) describes the development of a new methodology of the *in situ* complexation of metal complex catalysts for living cationic polymerization. In part II (Chapters 3 and 4), the structure–property relationship in controlled cationic polymerization is investigated using metal complex catalysts generated from phenoxyimine ligands containing a variety of substituents.

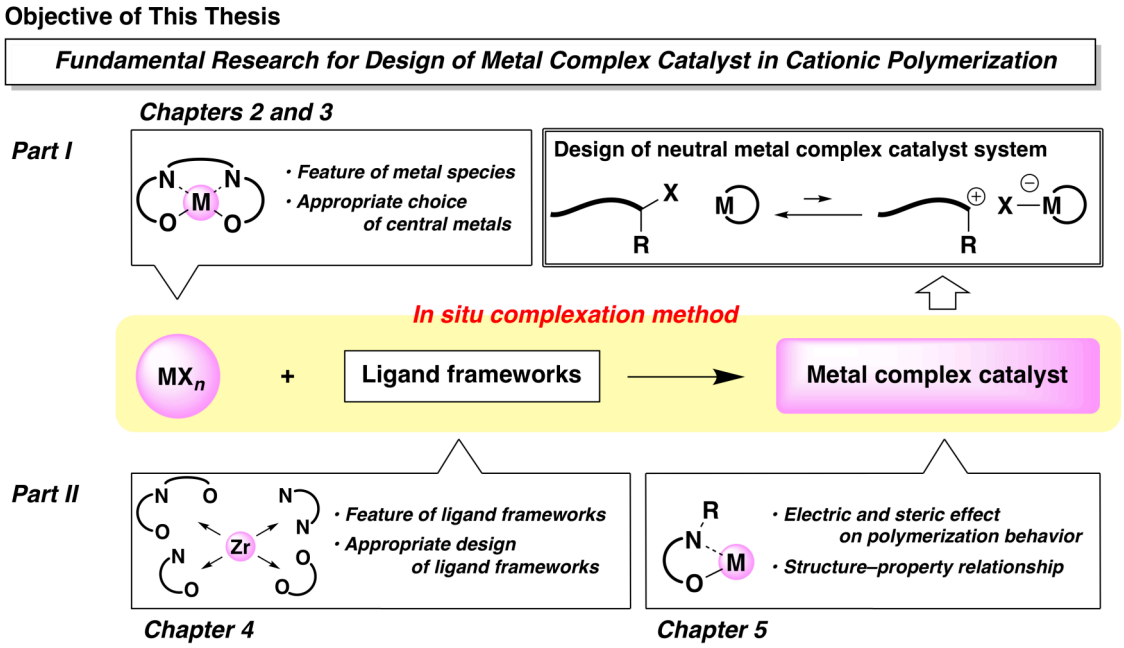

Figure 8. Outline of this thesis.

Chapter 2 describes the construction of a new strategy for the preparation of metal complex catalysts (Figure 9). Tetradentate Schiff base ligands, salphen ligands, are employed in this chapter. The salphen complex is prepared *in situ* by simply mixing the ligand and a metal chloride. The *in situ* complexation method has a dual role: the readily prepared metal complex is used as a catalyst, and *in situ* generated hydrochloric acid is used as an initiator. A series of investigations using various metal chlorides indicated that a vacant site on the central metal is important to exert Lewis acidity and relatively oxophilic metal species, such as $ZrCl_4$, are suitable for the controlled polymerization of VEs.

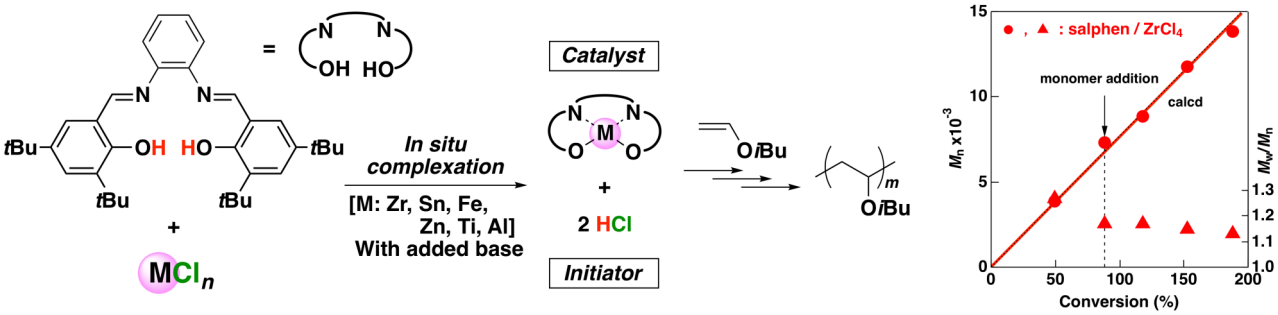

Figure 9. Salphen ligand/MCl_n initiating system for cationic polymerization of IBVE.

Chapter 3 presents the systematic investigation on the design of metal complex catalysts using salen derivatives and metal chlorides (Figure 10). The choice of the ligand structure is expected to be important for controlling the catalyst function, such as the activity and stereoselectivity. The structural effects of the complex catalysts on the polymerization rates are compared between salen and salphen ligands.

This structural feature is also important for the design of metal complex catalysts with appropriate Lewis acidities using various metal chlorides. The effect of the ligand structures on the polymerization behavior is also investigated using salen derivatives.

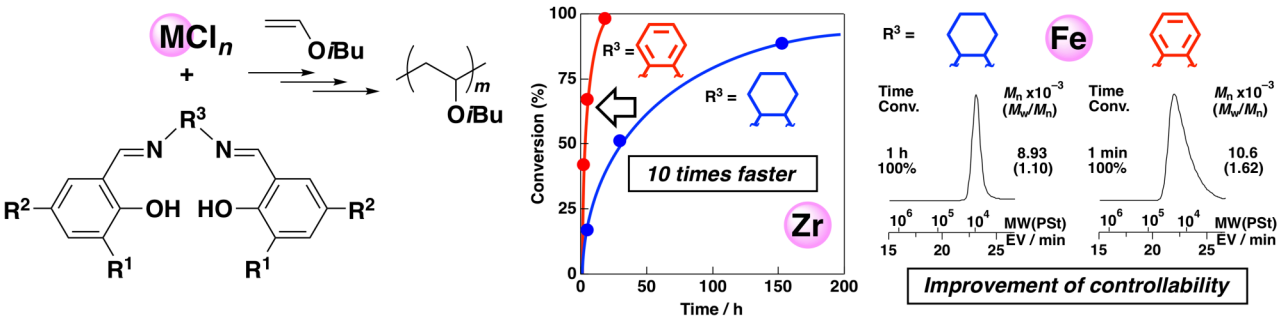

Figure 10. Salen and salphen ligands/MCl_n initiating system for cationic polymerization of IBVE.

Chapter 4 addresses the polymerization behavior using various ligand frameworks (Figure 11). Various bidentate ligand frameworks, such as phenoxyimine, pyridineimine, α-diimine, and diacetamide, are combined with $ZrCl_4$ to prepare complexes used for the polymerization of IBVE. Phenoxyimine-type ligands are demonstrated to be superior to the others in terms of the controllability of the polymerization, catalyst solubility, catalytic activity, and ease of derivatization. In addition, the phenoxyimine complexes with various metal chlorides are prepared and used for the polymerization of various monomers under various conditions.

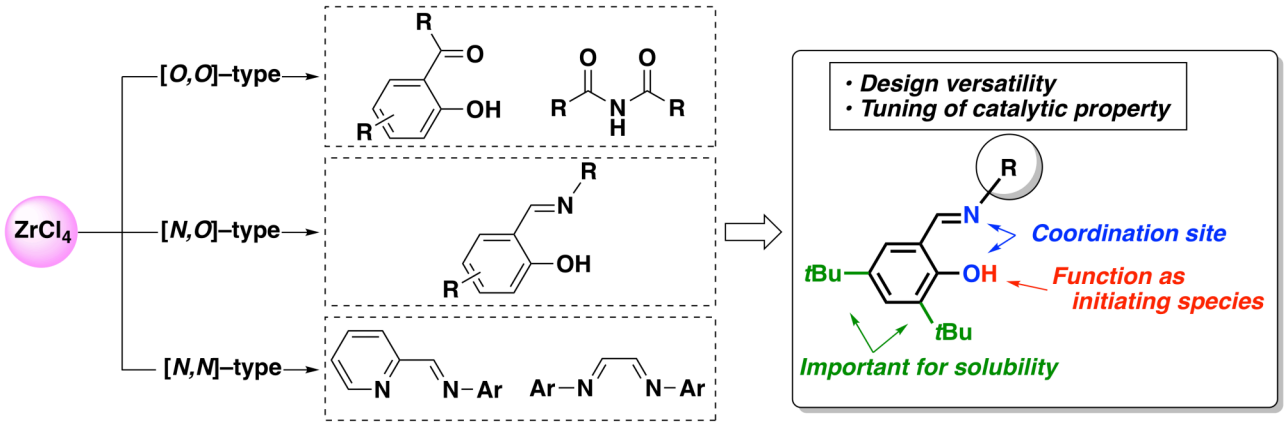

Figure 11. Various bidentate ligands/$ZrCl_4$ initiating system for cationic polymerization of IBVE.

In Chapter 5, the author investigated the structure–property relationships of the phenoxyimine ligands/MCl_n initiating systems (Figure 12). The substituent on the phenoxyimine ligand affects the catalytic properties particularly through the electron-donating and withdrawing effects. The Hammett substituent constant is suitably applied to estimate the catalytic properties. The apparent polymerization rate constants

and stereoselectivities were correlated to the Hammett substituent constant.

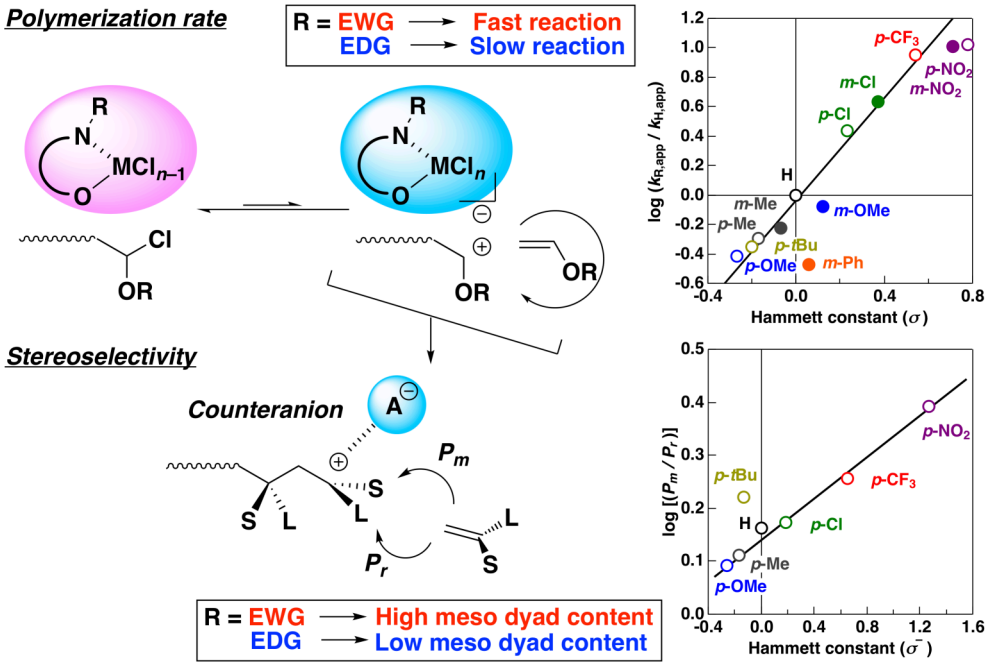

Figure 12. Structure–property relationship between phenoxyimine ligands and catalytic activity or stereoselectivity.

3. References

1. Steinborn, D; Harmsen, A. *Fundamentals of Organometallic Catalysis*; Wiley-VCH GmbH & Co. KGaA: Weinheim, 2012.
2. Beller, M; Bolm, C. *Transition Metals for Organic Snthesis*; Wiley-VCH Verlag GmbH & Co. KGaA: Weinheim, 2004.
3. Hartwig, J. F. *Organotransition Metal Chemistry: From bonding to Catalysis*; University Science Books: Sausalito, CA, 2010.
4. Ojima, I. *Catalytic Asymmetric Synthesis*, 3rd ed.; John Wiley & Sons, Inc.: Hoboken, NJ, 2010.
5. Yoon, T. P.; Jacobsen, E. N. *Science* **2003**, *299*, 1691-1693.
6. Zhou, Q.-L. *Privileged Chiral Ligands and Catalysts*; Wiley-VCH Verlag GmbH & Co. KGaA: Weinheim, 2011.
7. (a) Noyori, R. *Asymmetric Catalysis in Organic Synthesis*; John Wiley & Sons, Inc.: New York, 1994. (b) Noyori, R. *Angew. Chem. Int. Ed.* **2002**, *41*, 2008–2022.
8. (a) Brunel, J. M. *Chem. Rev.* **2007**, *107*, PR1–PR45. (b) Chen, Y.; Yekta, S.; Yudin, A. K. *Chem. Rev.* **2003**, *103*, 3155–3212. (c) Kocovsky, P.; Vyskocyl, S.; Smrcina, M. *Chem. Rev.* **2003**, *103*, 3213–3246.
9. (a) Atwood, D. A.; Harvey, M. J. *Chem. Rev.* **2001**, *101*, 37–52. (b) Katsuki, T. *Synlett* **2003**, *3*, 281–297. (c) Cozzi, P.G. *Chem. Soc. Rev.* **2004**, *33*, 410–421. (d) Katsuki, T. *Chem. Soc. Rev.* **2004**, *33*, 437–444. (e) Darensbourg, D. J.; Mackiewicz, R. M.; Phelps, A. L.; Billodeaux, D. R. *Acc. Chem. Res.* **2004**, *37,* 836–844. (f) Venkataramanan, N. S.; Kuppuraj, G.; Rajagopal, S. *Coord. Chem. Rev.* **2005**, *249*, 1249–1268. (g) McGarrigle, E. M.; Gilheany, D. G. *Chem. Rev.* **2005**, *105*, 1563–1602. (h) Baleizao, C.; Garcia, H. *Chem. Rev.* **2006**, *106*, 3987–4043. (i)

Matsumoto, K.; Saito, B.; Katsuki, T. *Chem. Commun.* **2007**, *35*, 3619–3627. (j) Darensbourg, D. J. *Chem. Rev.* **2007**, *107*, 2388–2410.

10. (a) Desimoni, G.; Faita, G.; Jørgensen, K. A. *Chem. Rev.* **2006**, *106*, 3561–3651. (b) Ghosh, A. K.; Mathivanan, P.; Cappiello, J. *Tetrahedron: Asymmetry* **1998**, *9*, 1–45. (c) Rechavi, D.; Lemaire, M. *Chem. Rev.* **2002**, *102*, 3467–3494. (d) Fraile, J. M.; Garcia, J. I.; Herrerias, C. I.; Mayoral, J. A.; Pires, E.; Salvatella, L. *Catal. Today* **2009**, *140*, 44–50. (e) Fraile, J. M.; Garcia, J. I.; Mayoral, J. A. *Coord. Chem. Rev.* **2008**, *252*, 624–646. (f) Hargaden, G. C.; Guiry, P. J. *Chem. Rev.* **2009**, *109*, 2505–2550. (g) Rasappan, R.; Laventine, D.; Reiser, O. *Coord. Chem. Rev.* **2008**, *252*, 702–714.
11. (a) Burk, M. J. *Acc. Chem. Res.* **2000**, *33*, 363–372. (b) Clark, T. P.; Landis, C. R. *Tetrahedron: Asymmetry* **2004**, *15*, 2123–2137.
12. Seebach, D.; Beck, A. K.; Heckel, A. *Angew. Chem. Int. Ed.* **2001**, *40*, 92–138.
13. Miyashita, A.; Yasuda, A. Takaya, H.; Toriumi, K.; Ito, T.; Souchi, T. Noyori, R. *J. Am. Chem. Soc.* **1980,** *102,* 7932–7934.
14. Ohkuma, T.; Kurono, N. *Privileged Chiral Ligands and Catalysts*; Zhou, Q.-L., Ed.; Wiley-VCH Verlag GmbH & Co. KGaA: Weinheim, 2011; Chapter 1.
15. Domski, G. J.; Rose, J. M.; Coates, G. W.; Boling, A. D.; Brookhart, M. *Prog. Polym. Sci.* **2007**, *32*, 30–92.
16. Kamigaito, M.; Ando, T.; Sawamoto, M. *Chem. Rev.* **2001**, *101*, 3689–3745.
17. (a) Ouchi, M.; Terashima, T.; Sawamoto, M. *Chem. Rev.* **2009**, *109*, 4963–5050. (b) Ouchi, M.; Sawamoto, M. *Macromolecules* **2017**, *50*, 2603–2614.
18. Matyjaszewski, K. *Macromolecules* **2012,** *45,* 4015–4039.
19. Rosen, B. M.; Percec, V. *Chem. Rev.* **2009**, *109*, 5069–5119.
20. Bielawski, C. W.; Grubbs, R. H. *Prog. Polym. Sci.* **2007**, *32*, 1–29.
21. (a) Schrock, R. R. *Chem. Rev.* **2009**, *109*, 3211–3226. (b) Schrock, R. R. *Acc. Chem. Res.* **2014**, *47*, 2457–2466.
22. Natta, G.; Pino, P.; Corradini, P.; Danusso, F.; Mantica, E.; Mazzanti, G.; Moraglio, G. *J. Am. Chem. Soc.* **1955**, *77*, 1708-1710.
23. Alt, H. G.; Koppl, A. *Chem. Rev.* **2000**, *100*, 1205–1221.
24. Coates, G. W. *Chem. Rev.* **2000**, *100*, 1223–1252.
25. Alt, H. G.; Licht, E. H.; Licht, A. I.; Schneider, K. J. *Coord. Chem. Rev.* **2006**, *250*, 2–17.
26. Ewen, J. A. *J. Mol. Catal. A* **1998**, *128*, 103−109.
27. Resconi, L.; Cavallo, L.; Fait, A.; Piemontresi, F. *Chem. Rev.* **2000**, *100*, 1253–1345.
28. Farina, M. *Macromol. Symp.* **1995**, *89*, 489–498.
29. van der Leek, Y.; Angermund, K.; Reffke, M.; Kleinschmidt, R.; Goretzki, R.; Fink, G. *Chem. Eur. J.* **1997**, *3*, 585–591.
30. Severn, J.; Jones, R. L. *Handbook of Transition Metal Polymerization Catalysts*; Hoff, R.; Mathers, R. T. Ed.; John Wiley & Sons, Inc.: Hoboken, NJ, 2010; Chapter 7.
31. Ittel, S. D.; Johnson, L. K.; Brookhart, M. *Chem. Rev.* **2000**, 100, 1169–1203.
32. Gibson, V. C.; Spitzmesser, S. K. *Chem. Rev.* **2003**, *103*, 283–315.
33. Takeuchi, D. *Dalton Trans.* **2010**, *39*, 311–328.
34. Guan, Z. *Chem. Asian J.* **2010**, *5*, 1058–1070.
35. Wu, J. Q.; Li, Y. S. *Coord. Chem. Rev.* **2011**, *255*, 2303–2314.
36. Baier, M. C.; Zuideveld, M. A.; Mecking, S. *Angew. Chem., Int. Ed.* **2014**, *53*, 9722–9744.
37. Berkefeld, A.; Mecking, S. *Angew. Chem., Int. Ed.* **2008**, *47*, 2538–2542.

38. (a) Matsugi, T.; Fujita, T. *Chem. Soc. Rev.* **2008**, *37*, 1264–1277. (b) Maiko, H.; Terao, H.; Iwashita, A.; Fujita, T. *Chem. Rev.* **2011**, *111*, 2363–2449.
39. Nakamura, A.; Ito, S.; Nozaki, K. *Chem. Rev.* **2009**, *109*, 5215–5244.
40. Nakamura, A.; Anselment, T. M. J.; Claverie, J.; Goodall, B.; Jordan, R. F.; Mecking, S.; Rieger, B.; Sen, A.; van Leeuwen, P. W. N. M.; Nozaki, K. *Acc. Chem. Res.* **2013**, *46*, 1438–1449.
41. Chen, E. Y.-X. *Chem. Rev.* **2009**, *109*, 5157–5214.
42. Yamamoto, H. *Lewis acids in Organic Synthesis*; Wiley-VCH Verlag GmbH: Weinheim, 2000.
43. (a) Yamamoto, H.; Futatsugi, K. *Angew. Chem. Int. Ed.* **2005**, *44*, 1924–1942. (b) Yamamoto, H. *Proc. Jpn. Acad., Ser. B* **2008**, *84*, 134–146.
44. Shibasaki, M.; Kanai, M.; Matsunaga, S.; Kumagai, N. *Acc. Chem. Res.* **2009**, *42*, 1117–1127.
45. Denmark, S. E.; Fu, J. *Chem. Rev.* **2003**, *103*, 2763–2793.
46. Kanazawa, A.; Kanaoka, S.; Aoshima, S. *Macromolecules* **2009**, *42*, 3965–3972.
47. (a) Pernecker, T.; Kennedy, J. P.; Ivan, B. *Macromolecules* **1992**, *25*, 1642–1647. (b) Pernecker, T.; Kennedy, J. P. *Polym. Bull.* **1992**, *29*, 27–33.
48. Kamigaito, M.; Maeda, Y.; Sawamoto, M.; Higashimura, T. *Macromolecules* **1993**, *26*, 1643–1649.
49. Yonezumi, M.; Takano, N.; Kanaoka, S.; Aoshima, S. *J. Polym. Sci., Part A: Polym. Chem.* **2008**, *46*, 6746–6753.
50. (a) Ouchi, M.; Kamigaito, M.; Sawamoto, M. *Macromolecules* **1999**, *32*, 6407–6411. (b) Ouchi, M.; Kamigaito, M.; Sawamoto, M. *J. Polym. Sci., Part A: Polym. Chem.* **2001**, *39*, 1060–1066. (c) Ouchi, M.; Kamigaito, M.; Sawamoto, M. *J. Polym. Sci., Part A: Polym. Chem.* **2001**, *39*, 1067–1074.
51. (a) Baird, M. C. *Chem. Rev.* **2000**, *100*, 1471–1478. (b) Shaffer, T. D.; Ashbaugh, J. R. *J. Polym. Sci., Part A: Polym. Chem.* **1997**, *35*, 329–344. (c) Bochmann, M. *Acc. Chem. Res.* **2010**, *43*, 1267–1278. (d) Jacob, S.; Pi, Z.; Kennedy, J. P. *Polym. Bull.* **1998**, *41*, 503–510. (e) Kostjuk, S. V.; Yeong, H. Y.; Voit, B. *J. Polym. Sci., Part A: Polym. Chem.* **2013**, *51*, 471–486. (f) Diebl, B. E.; Li, Y.; Cokoja, M.; Kühn, F. E.; Radhakrishnan, N.; Zschoche, S.; Komber, H.; Yeong, H. Y.; Voit, B.; Nuyken, O.; Hanefeld, P.; Walter, H.-M. *J. Polym. Sci., Part A: Polym. Chem.* **2010**, *48*, 3775–3786.
52. (a) Szwarc, M.; Levy, M.; Milkovich, R. *J. Am. Chem. Soc.* **1956**, *78*, 2656–2657. (b) Szwarc, M. *Nature* **1956**, *178*, 1168–1169.
53. Grubbs, R. B.; Grubbs, R. H. *Macromolecules* **2017**, *50*, 6979–6997.
54. (a) Hadjichristidis, N.; Pitsikalis, M.; Pispas, S.; Iatrou, H. *Chem. Rev.* **2001**, *101*, 3747–3792. (b) Polymeropoulos, G.; Zapsas, G.; Ntetsikas, K.; Bilalis, P.; Gnanou, Y.; Hadjichristidis, N. *Macromolecules* **2017**, *50*, 1253–1290.
55. Hirao, A.; Goseki, R.; Ishizone, T. *Macromolecules* **2014**, *47*, 1883–1905.
56. Penczek, S.; Cypryk, M.; Duca, A.; Kubisa, P.; Slomkowski, S. *Prog. Polym. Sci.* **2007**, *32*, 30–92.
57. Aoshima, S.; Kanaoka, S. *Chem. Rev.* **2009**, *109*, 5245–5287.
58. (a) Webster, O. W. *J. Polym. Sci., Part A: Polym. Chem.* **2000**, *38*, 2855–2860. (b) Webster, O. W. *Adv. Polym. Sci.* **2004**, *167*, 1–34.
59. Otsu, T. *J. Polym. Sci., Part A: Polym. Chem.* **2000**, *38*, 2121–2136.

60. Chiefari, J.; Chong, Y. K.; Ercole, F.; Krstina, J.; Jeffery, J.; Le, T. P. T.; Mayadunne, R. T. A.; Meijs, G. F.; Moad, C. L.; Moad, G.; Rizzardo, E.; Thang, S. H. *Macromolecules* **1998**, *31*, 5559–5562.
61. Moad, G.; Rizzardo, E.; Thang, S. H. *Polymer* **2008**, *49*, 1079–1131.
62. Perrier, S. *Macromolecules* **2017**, *50*, 7433–7447.
63. Georges, M. K.; Veregin, R. P. N.; Kazmaier, P. M.; Hamer, G. K. *Macromolecules* **1993**, *26*, 2987–2988.
64. Hawker, C. J.; Bosman, A. W.; Harth, E. *Chem. Rev.* **2001**, *101*, 3661–3688.
65. Studer, A.; Schulte, T. *Chem. Rec.* **2005**, *5*, 27–35.
66. Goto, A.; Tsujii, Y.; Fukuda, T. *Polymer* **2008**, *49*, 5177–5185.
67. Yamago, S. *Chem. Rev.* **2009**, *109*, 5051–5068.
68. Yokozawa, T.; Yokoyama, A. *Chem. Rev.* **2009**, *109*, 5595–5619.
69. Miyamoto, M.; Sawamoto, M.; Higashimura, T. *Macromolecules* **1984**, *17*, 265–268.
70. Faust, R.; Kennedy, J. P. *Polym. Bull.* **1986**, *15*, 317–323.
71. Higashimura, T.; Kojima, K.; Sawamoto, M. *Polym. Bull.* **1988**, *19*, 7–11.
72. Sawamoto, M.; Okamoto, C.; Higashimura, T. *Macromolecules* **1987**, *20*, 2693–2697.
73. Kojima, K.; Sawamoto, M.; Higashimura, T. *Macromolecules* **1989**, *22*, 1552–1557.
74. Schappacher, M.; Deffieux, A. *Macromolecules* **1991**, *24*, 2140–2142.
75. Schappacher, M.; Deffieux, A. *Macromolecules* **1991**, *24*, 4221–4223.
76. Aoshima, S.; Higashimura, T. *Polym. Bull.* **1986**, *15*, 417–423.
77. Aoshima, S.; Higashimura, T. *Macromolecules* **1989**, *22*, 1009–1013.
78. Kishimoto, Y.; Aoshima, S.; Higashimura, T. *Macromolecules* **1989**, *22*, 3877–3882.
79. Higashimura, T.; Kishimoto, Y.; Aoshima, S. *Polym. Bull.* **1987**, *18*, 111–115.
80. Kamigaito, M.; Sawamoto, M.; Higashimura, T. *Macromolecules* **1995**, *28*, 5671–5675.
81. Zhou, Y.; Faust, R.; Chen, S.; Gido, S. P. *Macromolecules* **2004**, *37*, 6716–6725.
82. Zhou, Y.; Faust, R. *Polym. Bull.* **2004**, *52*, 421–428.
83. Hadjikyriacou, S.; Faust, R. *Macromolecules* **1996**, *29*, 5261–5267.
84. (a) Lu, J.; Kamigaito, M.; Sawamoto, M.; Higashimura, T.; Deng, Y. X. *J. Polym. Sci., Part A: Polym. Chem.* **1997**, *35*, 1423–1430. (b) Lu, J.; Kamigaito, M.; Sawamoto, M.; Higashimura, T.; Deng, Y. X. *Macromolecules* **1997**, *30*, 22–26.
85. Li, A.-L.; Zhang, W.; Liang, H.; Lu, J. *Polymer* **2004**, *45*, 6533–6537.
86. Hasebe, T.; Kamigaito, M.; Sawamoto, M. *Macromolecules* **1996**, *29*, 6100–6103.
87. Li, D.; Faust, R. *Macromolecules* **1995**, *28*, 1383–1389.
88. Sipos, L.; Som, A.; Faust, R. *Biomacromolecules* **2005**, *6*, 2570–2582.
89. (a) Thomas, L.; Polton, A.; Sigwalt, P. *Macromolecules* **1992**, *25*, 5886–5892. (b) Thomas, L.; Tardi, M.; Polton, A.; Sigwalt, P. *Macromolecules* **1993**, *26*, 4075–4082. (c) Thomas, L.; Polton, A.; Tardi, M.; Sigwalt, P. *Macromolecules* **1995**, *28*, 2105–2111.
90. Kanazawa, A.; Kanaoka, S.; Aoshima, S. *Macromolecules* **2010**, *43*, 2739–2747.
91. Kanazawa, A.; Shibutani, S.; Yoshinari, N.; Konnno, T.; Kanaoka, S.; Aoshima, S. *Macromolecules* **2012**, *45*, 7749–7757.
92. Baird, M. C. *Chem. Rev.* **2000**, *100*, 1471–1478.
93. (a) Sudhakar, P.; Vijayakrishna, K. *Polymer* **2009**, *50*, 783–788. (b) Sudhakar, P.; Vijayakrishna, K. *Polym. Int.* **2009**, *58*, 1362–1365. (c) Sudhakar, P.; Vijayakrishna, K. *ChemCatChem* **2010**, *2*, 649–652.

94. Kawaguchi, T.; Sanda, F.; Masuda, T. *J. Polym. Sci., Part A: Polym. Chem.* **2002**, *40*, 3938–3943.
95. (a) Kim, I.; Ha, Y. S.; Ha, C.-S. *Macromol. Rapid Commun.* **2004**, *25*, 1069–1072. (b) Kim, I.; Ha, Y. S.; Ha, C.-S. *Macromol. Rapid Commun.* **2003**, *24*, 949–951.
96. (a) Albeitz, P. J.; Yang, K.; Eisenberg, R. *Organometallics,* **1999,** *18,* 2747–2749. (b) Albietz, P. J.; Jr.; Yang, K.; Lachiicotte, R. J.; Eisenberg, R. *Organometallics* **2000,** *19,* 3543–3555.
97. Kwon, O. W.; Noh, S. K.; Lyoo, W. S. *J. Appl. Polym. Sci.* **2008**, *107*, 1487–1492.
98. (a) Chen, Y.-C.; Reddy, K. R.; Liu, S.-T. *J. Organomet. Chem.* **2002**, *656*, 199–202. (b) Chen, C.-L.; Chen, Y.-C.; Liu, Y.-H.; Peng, S.-M.; Liu, S.-T. *Organometallics* **2002**, *21*, 5382–5385.
99. Wang, Q.; Quyoum, R.; Gillis, D. J.; Tudoret, M.-J.; Jeremic, D.; Hunter, B. K.; Baird, M. C. *Organometallics* **1996**, *15*, 693–703.
100. Ewart, S. W.; Sarsfield, M. J.; Tremblay, T. L.; Williams, E. F.; Baird, M. C. *Organometallics* **1998**, *17*, 1502–1510.
101. Murray, M. C.; Baird, M. C. *J. Mol. Catal.* **1998**, *128*, 1–4.
102. Barsan, F.; Baird, M. C. *J. Chem. Soc., Chem. Commun*. **1995**, 1065–1066.
103. Wang, Q.; Baird, M. C. *Macromolecules* **1995**, *28*, 8021–8027.
104. Sawamoto, M.; Kojima, K.; Higashimura, T. *Makromol. Chem.* **1991**, *192*, 2479–2486.
105. Kanazawa, A.; Kanaoka, S.; Aoshima, S. *J. Polym. Sci., Part A: Polym. Chem.* **2010**, *48*, 2509–2516.
106. Kanaoka, S.; Nakayama, S.; Aoshima, S. *Kobunshi Ronbunshu* **2011,** *68,* 349–351.
107. Ihara, E.; Yoshida, N.; Ikeda, J.; Itoh, T.; Inoue, K. *J. Polym. Sci., Part A: Polym. Chem.* **2006,** *44,* 2636–2641.
108. Oishi, M.; Yamamoto, H. *Bull. Chem. Soc. Jpn.* **2001**, *74*, 1–10.
109. (a) Nagashima, H.; Itonaga, C.; Yasuhara, J.; Motoyama, Y.; Matsubara, K. *Organometallics* **2004**, *23*, 5779–5786. (b) Harada, N.; Nishikata, T.; Nagashima, H. *Tetrahedron* **2012**, *68*, 3243–3252.
110. (a) Crivello, J. V.; Rajaraman, S. K. *J. Polym. Sci., Part A: Polym. Chem.* **1997,** *35,* 1579–1591. (b) Crivello, J. V.; Rajaraman, S. K. *J. Polym. Sci., Part A: Polym. Chem.* **1997,** *35,* 1593–1604. (c) Crivello, J. V.; Rajaraman, S. K. *J. Polym. Sci., Part A: Polym. Chem.* **1997,** *35,* 1985–1997. (d) Crivello, J. V.; Rajaraman, S. K. *Macromol. Symp.* **1998,** *132,* 37–43.

Part I

Controlled/Living Cationic Polymerization Using Tetradentate Schiff Base Ligands/Metal Chlorides Initiating Systems

Chapter 2

In Situ and Readily Prepared Metal Catalysts and Initiator for Living Cationic Polymerization of Isobutyl Vinyl Ether: Dual-Purpose Salphen as a Ligand Framework for $ZrCl_4$ and an Initiating Proton Source

Introduction

The expansion of the scope of substrates or monomers in organic reactions or polymerization is often sparked by the development of new metal catalysts with well-designed ligands. For example, various elaborately designed polymerization catalysts have enhanced tolerance towards polar groups and catalytic activity, widening the choice of polymerizable monomers in the field of olefin metathesis polymerization,[1,2] transition metal-catalyzed living radical polymerization or atom-transfer radical polymerization (ATRP),[3–5] and the coordination polymerization of polar vinyl monomers.[6–8] This explosive growth in precise organic synthesis and polymerization can be attributed to the variable and/or controllable activity of metal complex catalysts with various carefully designed ligands. Their diverse activity is attained by tuning the electron density of the central metals and/or the redox potential of the complexes through the interaction of the designed ligands with the central metals.

The rather limited scope of monomers in cationic polymerization for high polymers may be improved if well-defined metal catalysts with various ligands are available. A distinct opportunity for the utility of designed metal complexes as catalysts in cationic polymerization was shown by the recent development of initiating systems for base-assisting living cationic polymerization.[9] These systems consist of a metal halide and an externally-added base, the interaction of which is a key to successful living polymerization.[9] Among various combinations, an alcohol or acetylacetone with an appropriate metal halide permitted *in situ* ligand exchange, generating a real catalytic species inducing living polymerization.[10,11] These results encouraged the author to pursue the goal of designing metal complex catalysts for precise polymer synthesis using cationic polymerization. Despite the potency of metal complex catalysts, catalyst design using various ligands has been limited in cationic polymerization,[9,12,13] although ligand design or *in situ* complex formation was demonstrated to be effective for achieving the stereoselective cationic polymerization of alkyl vinyl ethers[14] or styrene derivatives.[15,16]

The difficulty in the use of metal-complex catalysts for cationic polymerization lies in maintaining sufficient catalytic activity with a highly nucleophilic ligand and/or preventing the termination. In fact, the amount of nucleophilic additive is a decisive factor for controlled polymerization, particularly when an ammonium salt or an amine/amide compound is employed as the additive.[17–19] The polymerization is readily inhibited by an excess of such relatively strong nucleophilic additives, even if their absolute concentration is very low. In addition, the previous study has showed that an alkoxy group on certain Lewis

acid catalysts dissociates from the central metal to react with the propagating carbocation.[10] Hence, catalyst design to date in this field has focused on relatively simple compounds containing alkoxy or phenoxy groups.[10,11,14,20]

To circumvent the abovementioned problems, the use of a Schiff base ligand would be effective because the chelating effect of the ligand is expected to suppress any ligand exchange reactions that may lead to the deactivation of the polymerization. Furthermore, a family of Schiff base ligands, known as one of the most useful ligands, can coordinate with many different metals,[21,22] yielding catalysts capable of achieving a variety of synthetic transformations. In particular, various transition metals are available for complex formation with Schiff base ligands, which permits the precise tuning of catalytic activity[23] based upon the unique properties of each transition metal. Another feature of the ligand is that the electronic and geometric characteristics of catalysts are readily adjusted[22,24] because Schiff base ligands are prepared by a condensation reaction between aldehydes and amines with various substituents. In this study, therefore, the author examines catalyst design using a chelating Schiff base ligand for the cationic polymerization of a vinyl ether.

As a first step toward catalyst design, an *in situ* complexation method is investigated for catalyst modification using a salphen ligand [*N,N′*-bis(3,5-di-*tert*-butylsalicylidene)-1,2-phenylenediamine, **1**]. The salphen ligand, a tetradentate Schiff base ligand, is easily synthesized by the condensation of equivalent quantities of a specific salicylaldehyde and 1,2-phenylenediamine. A salphen complex is synthesized simply by mixing the ligand and a metal chloride in dichloromethane, and the resulting solution is directly added to a monomer solution in toluene. In addition, the ligand performs another role: during complex formation, HCl is generated and can function as a protonogen, or an initiator, for the cationic polymerization of a vinyl ether (VE) (Scheme 1). Furthermore, salphen derivatives with various substituents (ligands **2**–**6**) are used for the cationic polymerization using the ligand/$ZrCl_4$ initiating systems. The polymerization behavior likely depends on the electronic and steric properties of subsitituents and solubilities of the generated catalysts.

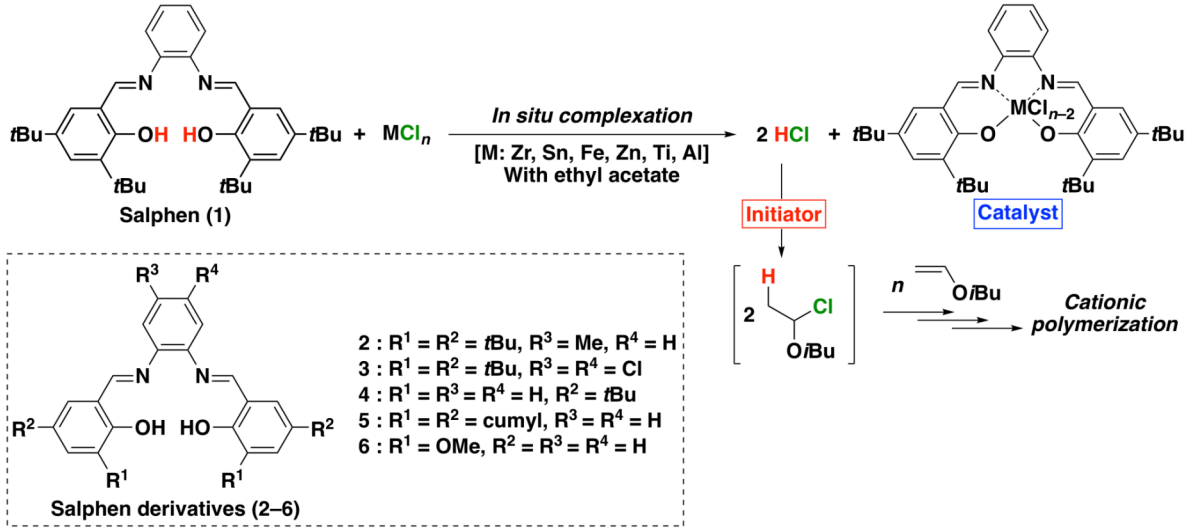

Scheme 1. Cationic polymerizations using salphen ligands and metal chlorides.

Experimental

Materials

Isobutyl VE (IBVE; TCI; >99.0%), ethyl acetate (Wako; >99.5%), and heptane (Nacalai Tesque; >99.0%) were distilled twice over calcium hydride before use. Toluene (Wako; 99.5%) and dichloromethane (CH_2Cl_2, Wako; 99.9%) were dried using solvent purification columns (Glass Contour). The preparation of 1-(isobutoxy)ethyl chloride [IBVE–HCl; $CH_3CH(O\mathit{i}Bu)Cl$] was accomplished via the addition reaction of IBVE with dry HCl, according to the reported method.[25] Commercially available $SnCl_4$ (Aldrich; 1.0 M solution in heptane), $ZnCl_2$ (Aldrich; 1.0 M solution in diethyl ether), and $TiCl_4$ (Aldrich; 1.0 M solution in dichloromethane) were used without further purification. An $FeCl_3$ stock solution in diethyl ether was prepared from anhydrous $FeCl_3$ (Aldrich; 99.99%). Stock solutions of $AlCl_3$ and $ZrCl_4$ in ethyl acetate were prepared from anhydrous $AlCl_3$ (Aldrich; 99%) and $ZrCl_4$ (Aldrich; 99.99%), respectively. All chemicals except dichloromethane and toluene were stored in brown ampules under dry nitrogen.

Synthesis of Salphen Ligands

_N,N′_-Bis(3,5-di-_tert_-butylsalicylidene)-1,2-phenylenediamine (1)

The ligand was prepared using a similar method to that described in the literature.[26] A methanol solution (3 ml) of 1,2-diaminobenzene (0.49 g, 4.55 mmol) was added to a methanol solution (15 ml) of 3,5-di-*tert*-butylsalicylaldehyde (2.14 g, 9.12 mmol) while stirring under a nitrogen atmosphere at room temperature. The mixed solution was heated under reflux for 5 h, and the reaction mixture was then cooled to room temperature. After filtration, the solid fraction was washed twice with cold methanol and dried under reduced pressure. Furthermore, the product was purified by recrystallization from ethyl acetate. The ligand was obtained as a yellow solid (1.01 g, 21%). ^{1}H NMR (500 MHz, $CDCl_3$, 30 °C): δ 13.51 (2H, s, OH), 8.65 (2H, s, N=C*H*), 7.44 (2H, m, C*H*-phenol), 7.31 (2H, m, C*H*-phenylene), 7.23 (2H, m, C*H*-phenylene), 7.21 (2H, m, C*H*-phenol), 1.43, 1.32 (18H, s, *t*Bu). ^{13}C NMR (125 MHz, $CDCl_3$, 30 °C): δ 164.7 (N=*C*H), 158.6 (*C*–OH), 142.8 (*ipso*-phenylene), 140.3, 137.2, 118.4 (*ipso*-phenol), 128.2, 127.3, 126.8, 119.8 (phenol and phenylene), 35.1, 34.2 (CMe$_3$), 31.5, 29.5 (CMe_3).

_N,N′_-Bis(3,5-di-_tert_-butylsalicylidene)-4-methyl-1,2-phenylenediamine (2)

A procedure similar to **1** but with the use of 4-methyl-1,2-diaminobenzene and two equivalents of 3,5-di-*tert*-butylsalicylaldehyde gave a yellow solid. ^{1}H NMR (500 MHz, $CDCl_3$, 30 ºC): δ 13.59 (1H, s, OH), 13.55 (1H, s, OH), 8.65 (2H, s, N=C*H*), 7.43 (2H, m, C*H*-Ph), 7. 20 (2H, m, C*H*-Ph), 7.16–7.10 (2H, m, C*H*-Ph), 7.04 (1H, s, C*H*-Ph), 2.42 (3H, s, CH_3-Ph), 1.43 (18H, s, *t*Bu), 1.32 (18H, s, *t*Bu).

_N,N′_-Bis(3,5-di-_tert_-butylsalicylidene)-4,5-dichloro-1,2-phenylenediamine (3)

A procedure similar to **1** but with the use of 4,5-dichloro-1,2-diaminobenzene (0.78 g, 4.42 mmol) and 3,5-di-*tert*-butylsalicylaldehyde (2.07 g, 8.84 mmol) with a few drops of trifluoroacetic acid gave a yellow solid (1.03 g, 38%). ^{1}H NMR (500 MHz, $CDCl_3$, 30 ºC): δ 13.13 (2H, s, OH), 8.63 (2H, s, N=C*H*),

7.47 (2H, d, C*H*-Ph), 7. 34 (2H, s, C*H*-Ph), 7.22 (2H, d, C*H*-Ph), 1.42 (18H, s, *t*Bu), 1.32 (18H, s, *t*Bu).

***N,N′*-Bis(5-*tert*-butylsalicylidene)-1,2-phenylenediamine (4)**

A procedure similar to **1** but with the use of 1,2-diaminobenzene (0.47 g, 4.37 mmol) and 5-*tert*-butylsalicylaldehyde (1.56 g, 8.74 mmol) gave a crystalline orange solid. ^{1}H NMR (500 MHz, $CDCl_3$, 30 °C): δ 12.81 (2H, s, O*H*), 8.63 (2H, s, N=C*H*), 7.41 (2H, m, C*H*-Ar), 7.35 (2H, m, C*H*-Ar), 7.32 (2H, m, C*H*-Ar), 7.22 (2H, m, C*H*-Ar), 6.98 (2H, m, C*H*-Ar), 1.31 (18H, s, *t*Bu).

3,5-Di-cumylsalicylaldehyde

The aldehyde compound was prepared according to the literature procedure.[27] ^{1}H NMR (500 MHz, $CDCl_3$, 30 ºC): δ 11.24 (1H, s, OH), 9.76 (1H, s, O=C*H*), 7.5–7.1 (12H, m, C*H*-Ph), 1.73 (6H, s, *t*Bu), 1.64 (6H, s, *t*Bu).

***N,N′*-Bis(3,5-di-cumylsalicylidene)-1,2-phenylenediamine (5)**

A procedure similar to **1** but with the use of 1,2-diaminobenzene and 3,5-di-cumyl-salicylaldehyde gave the ligand. ^{1}H NMR (500 MHz, $CDCl_3$, 30 ºC): δ 12.97 (2H, s, OH), 8.44 (2H, s, N=C*H*), 7.3–7.0 (28H, m, C*H*-Ph), 1.70 (24H, s, *t*Bu).

***N,N′*-Bis(3-methoxysalicylidene)-1,2-phenylenediamine (6)**

A procedure similar to **1** but with the use of 1,2-diaminobenzene (0.56 g, 5.14 mmol) and 3-methoxysalicylaldehyde (1.57 g, 10.3 mmol) gave an orange solid (0.67 g, 41%). ^{1}H NMR (500 MHz, $CDCl_3$, 30 °C): δ 13.12 (2H, s, O*H*), 8.62 (2H, s, N=C*H*), 7.33 (2H, m, C*H*-Ar), 7.19 (2H, m, C*H*-Ar), 6.96–7.02 (4H, m, C*H*-Ar), 6.86 (2H, m, C*H*-Ar), 3.89 (6H, s, O*Me*).

Polymerization Procedure

The following is a typical polymerization procedure. A glass tube equipped with a three-way stopcock was dried using a heat gun (Ishizaki; PJ-206A; blow temperature approximately 450 °C) under dry nitrogen for 10 min before use. Toluene (3.30 ml), heptane (0.25 ml), ethyl acetate (0.45 ml), and IBVE (0.50 ml) were added successively into the tube using dry syringes. In another tube, a metal chloride solution was added to a salphen ligand in dichloromethane/ethyl acetate (9/1 v/v), and the solution was kept at 0 °C for at least 30 min to achieve quantitative complexation. The polymerization was initiated by the addition of the complex solution (0.50 ml; 50 mM) to the monomer solution at the polymerization temperature. The reaction was terminated by the addition of methanol containing a small amount of aqueous ammonia solution. The quenched reaction mixture was diluted with hexane and washed successively with dilute hydrochloric acid, aqueous NaOH solution, and water. The organic layer was evaporated under reduced pressure at 50 °C to remove the remaining volatile compounds. The product was dried in vacuo for at least 6 h at room temperature. The monomer conversion was determined by gas chromatography (column packing material: PEG-20M-Uniport B; GL Sciences Inc.) using heptane as an internal standard.

Characterization

The molecular weight distribution (MWD) of the polymers was measured by gel permeation chromatography (GPC) in chloroform at 40 °C with polystyrene gel columns [TSKgel GM_{HHR-M} × 2 or 3 (exclusion limit molecular weight = 4×10^6; based size = 5 μm; column size = 7.8 mm I.D. × 300 mm); flow rate = 1.0 mL/min] connected to a Tosoh DP-8020 pump, a CO-8020 column oven, a UV-8020 ultraviolet detector, and an RI-8020 refractive-index detector. The number-average molecular weight (M_n) and polydispersity ratio [weight-average molecular weight/number-average molecular weight (M_w/M_n)] were calculated from the chromatographs with respect to 16 polystyrene standards (Tosoh; M_n = 577–1.09×10^6, $M_w/M_n \leq 1.1$). The ^1H and ^{13}C NMR spectra of the obtained polymers were recorded in $CDCl_3$ at 30 ºC using a JEOL JNM-ECA 500 spectrometer (500.16 MHz for ^1H and 125.77 MHz for ^{13}C) and a JEOL JNM-ECA 400 spectrometer (399.78 MHz for ^1H and 100.53 MHz for ^{13}C).

Results and Discussion

The polymerization was conducted in toluene using an as-prepared salphen complex solution, obtained simply by mixing equivalent amounts of a metal chloride and **1** at 0 °C in the presence of ethyl acetate in dichloromethane. The advantage of this method over a common, previously reported method[22] is the greatly facilitated synthetic procedure without purification and the *in situ* generation of toxic HCl as a proton source, as observed with the systems using alcohol or acetylacetone in conjunction with metal chlorides.[10,11]

The choice of metal halide was crucial for achieving controlled polymerization. Among the metal halides examined, $ZrCl_4$ combined with the ligand catalyzed the polymerization in the best-controlled manner (Table 1, entry 1). The reaction proceeded quantitatively at a moderate rate[28] in a homogeneous system in the presence of ethyl acetate as an added base[29] in toluene at 0 °C. The obtained polymers had narrow MWDs, which shifted toward higher molecular weight regime with increasing monomer conversion. It is noteworthy that their M_n values increased linearly with the conversion along the theoretical line calculated using the molar ratio of IBVE to the phenoxy groups in **1**[30,31] (Figure 1). These results also

Table 1. Cationic polymerization of IBVE using MCl_n and **1**[a]

entry	MCl_n	time	conv (%)[b]	$M_n \times 10^{-3}$ (calcd)[c]	$M_n \times 10^{-3}$ (obs)[d]	M_w/M_n[d]	meso dyad (%)[e]
1	$ZrCl_4$	18.5 h	98	7.6	7.3	1.15	66
2	$SnCl_4$	20 min	94	7.3	10.5	1.37	65
3	$FeCl_3$	5 s	90	7.0	11.5	1.57	61
4	$ZnCl_2$	6 h	97	7.5	17.3	1.94	60
5	$TiCl_4$	168 h	12	0.9	n.d.	n.d.	n.d.
6	$AlCl_3$	430 h	2	0.2	n.d.	n.d.	n.d.

[a] $[IBVE]_0$ = 0.76 M, $[MCl_n]_0$ = 5.0 mM, $[\mathbf{1}]_0$ = 5.0 mM, [ethyl acetate] = 1.0 M, [heptane] = 5.0 vol% in toluene at 0 ºC. [b] Determined by gas chromatography. [c] Based on the amounts of **1**.[30] [d] Determined by GPC (polystyrene standards). [e] Determined by ^{13}C NMR analysis (see Figure 5 for the spectra).

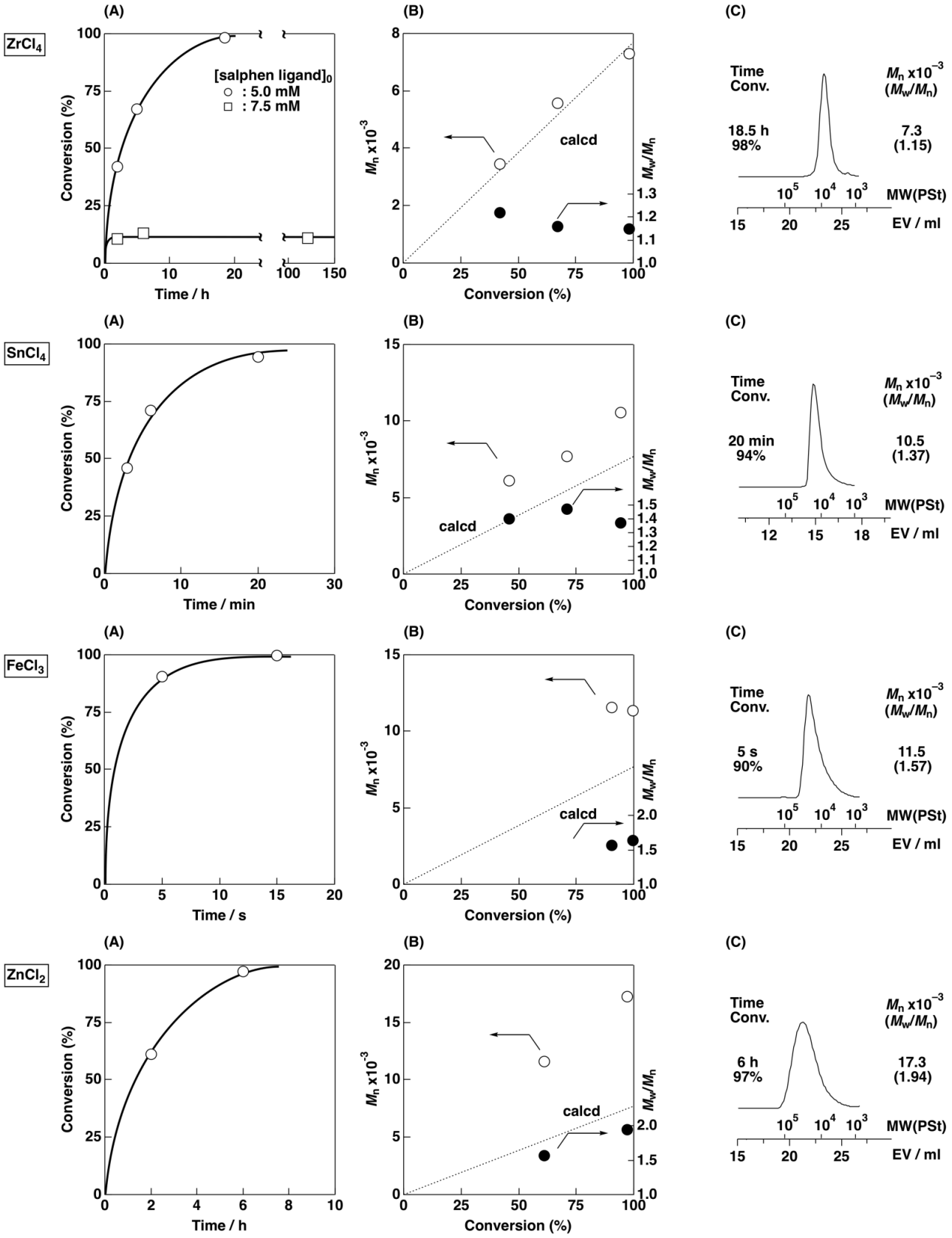

Figure 1. (A) Time–conversion curves for the polymerization, (B) M_n (dotted line: calculated M_n) and M_w/M_n and (C) MWD curves for poly(IBVE)s obtained using the **1**/MCl_n initiating systems ($[IBVE]_0$ = 0.76 M, $[MCl_n]_0$ = 5.0 mM, $[\mathbf{1}]_0$ = 5.0 mM (circle) or 7.5 mM (square), [ethyl acetate] = 1.0 M, [heptane] = 5.0 vol% in toluene at 0 ºC).

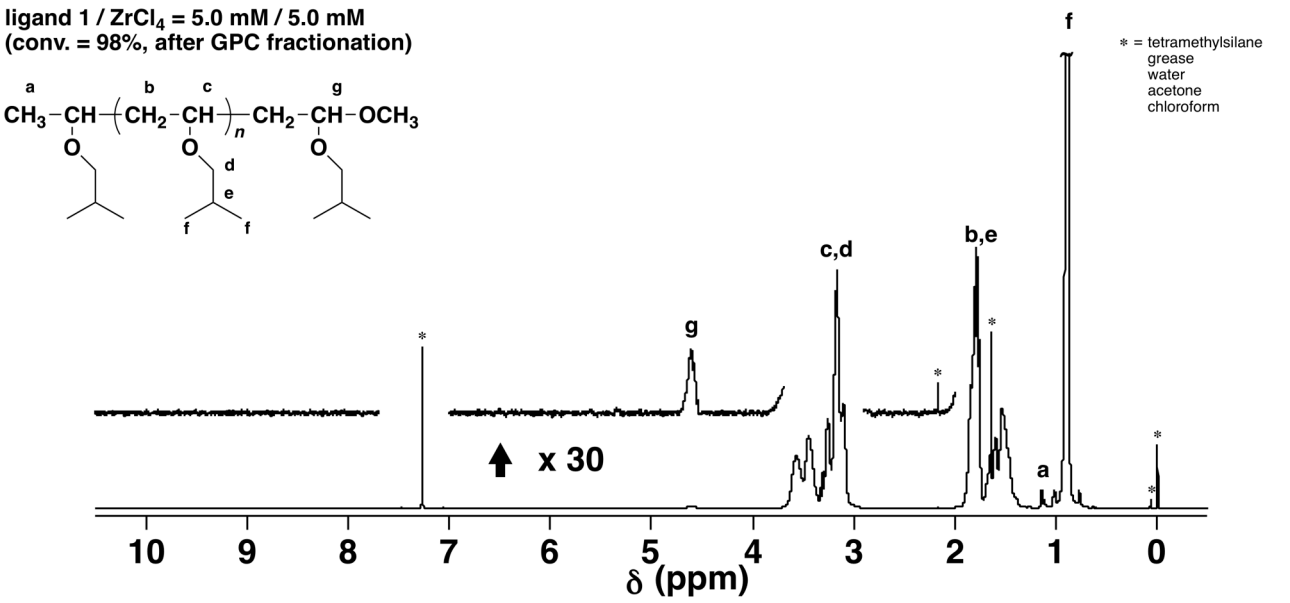

Figure 2. ^{1}H NMR spectrum of poly(IBVE) obtained using the **1**/$ZrCl_4$ initiating system ($[IBVE]_0$ = 0.76 M, $[ZrCl_4]_0$ = 5.0 mM, $[\mathbf{1}]_0$ = 5.0 mM, [ethyl acetate] = 1.0 M, [heptane] = 5.0 vol% in toluene at 0 ºC; 500 MHz in $CDCl_3$ at 30 ºC; signal integral ratio: a/g = 3.00/1.02).

indicate the quantitative formation of the metal complex from the mixture of **1** and $ZrCl_4$ along with a protonogen to initiate polymerization (Scheme 1). ^{1}H NMR analysis of the product polymer also showed the complete suppression of undesired side reactions[32,33] during the polymerization (Figure 2).

Several common metal chloride catalysts induced uncontrolled or no polymerization (Table 1, entries 2–6). The combination of $SnCl_4$, $FeCl_3$, or $ZnCl_2$ with **1** induced uncontrolled polymerization. The GPC profiles of the products obtained with these metal chlorides had broad MWDs with noticeable tailing (Figure 1). The M_n values of the polymers obtained from the **1**/$SnCl_4$ and $ZnCl_2$ systems increased linearly, although they were higher than the calculated values. The higher M_n values likely result from a smaller proton source concentration (HCl) due to insufficient complex formation. The tailing of the MWDs also suggests the occurrence of termination/transfer reactions caused by the unreacted ligand molecules. In sharp contrast, no polymerization occurred for the combination of **1** with $TiCl_4$ or $AlCl_3$. The inactivity is attributable to the absence of vacant sites that exhibit Lewis acidity on the central metals, as opposed to the Zr-salphen complexes [**1**–$ZrCl_2$], which have a labile coordination (a vacant) site because of their ability to form seven-coordinate structures[34–38] (Scheme 2). Therefore, metal chlorides can be classified into three groups according to their polymerization behavior: catalysts inducing living/controlled polymerization mediated by living/long-lived species ($ZrCl_4$); uncontrolled polymerization ($SnCl_4$, $FeCl_3$, and $ZnCl_2$); and no reaction ($TiCl_4$ and $AlCl_3$).

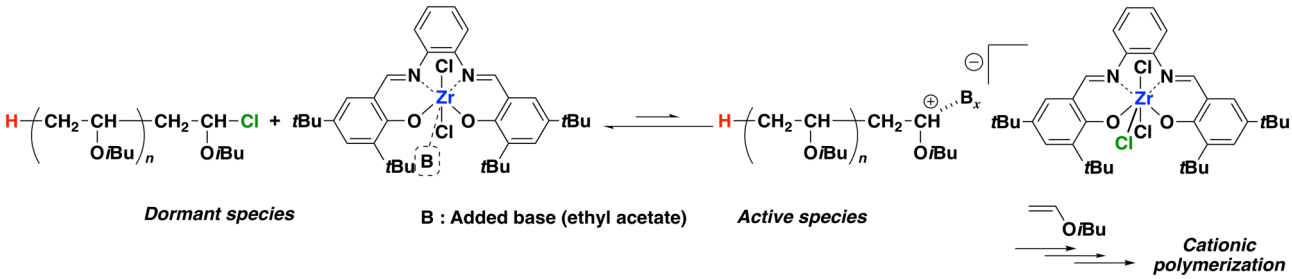

Scheme 2. Polymerization mechanism of IBVE using the **1**/$ZrCl_4$ initiating system.

To confirm the living nature of the polymerization with the **1**/$ZrCl_4$ initiating system, a monomer addition experiment was conducted under the optimized conditions. As shown in Figure 3, after the addition of a fresh feed of the monomer, the MWD of the products shifted toward the higher molecular weight region with no original polymer remaining. A linear increase in the M_n values against the monomer conversion was also confirmed. Moreover, the ^{1}H NMR spectra of these polymers showed the quantitative generation of the terminal acetal group[39] and undetectable undesired side reactions[32,33] (Figure 4) These results demonstrate the progression of living polymerization using the complex prepared *in situ* from **1** and $ZrCl_4$.

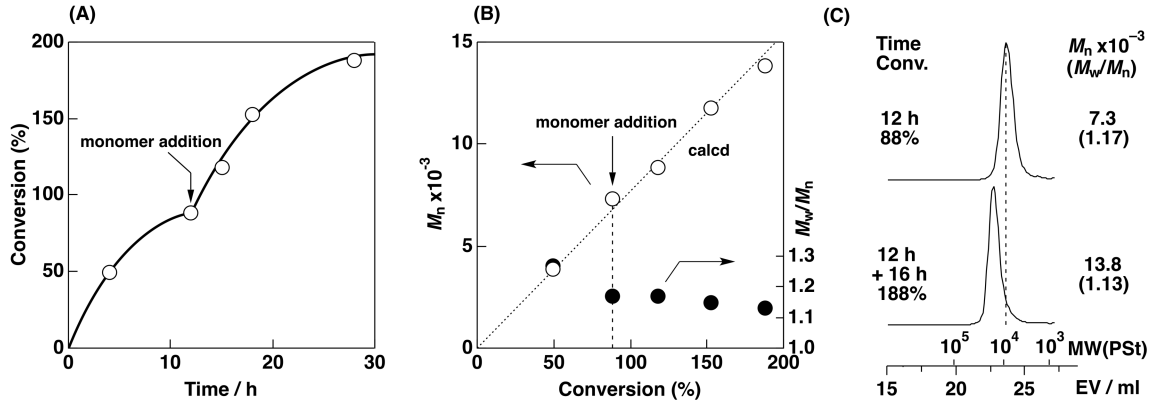

Figure. 3. (A) Time–conversion curves for the polymerization, (B) M_n (calculated M_n, dotted line) and M_w/M_n and (C) MWD curves for poly(IBVE)s obtained using the **1**/$ZrCl_4$ initiating system ($[IBVE]_0 = [IBVE]_{added}$ = 0.76 M, $[ZrCl_4]_0$ = 5.0 mM, $[\mathbf{1}]_0$ = 5.0 mM, [ethyl acetate] = 1.0 M, [heptane] = 5.0 vol% in toluene at 0 ºC).

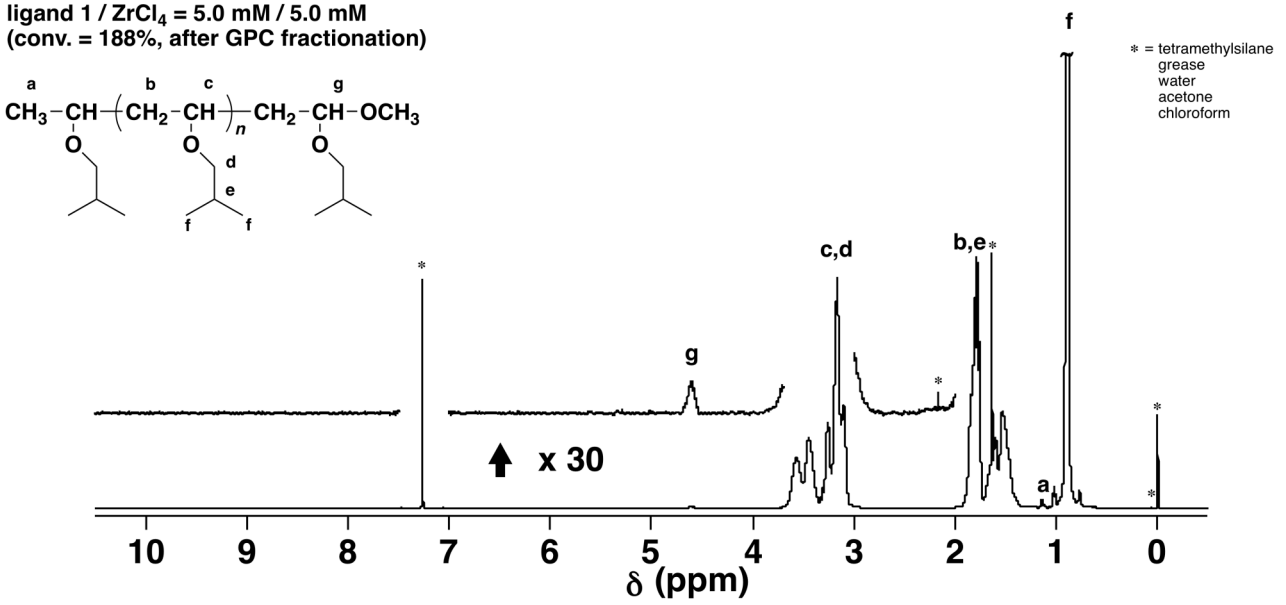

Figure 4. ^{1}H NMR spectrum of poly(IBVE) obtained using the **1**/$ZrCl_4$ initiating system ($[IBVE]_0 = [IBVE]_{added} = 0.76$ M, $[ZrCl_4]_0 = 5.0$ mM, $[\mathbf{1}]_0 = 5.0$ mM, [ethyl acetate] = 1.0 M, [heptane] = 5.0 vol% in toluene at 0 ºC; 500 MHz in $CDCl_3$ at 30 ºC; signal integral ratio: a/g = 3.00/1.03).

The stereoregularity of the product polymers was determined from the signals of the methylene carbons of the main chains in the ^{13}C NMR spectra recorded in $CDCl_3$ (Figure 5). The meso dyad values of the polymer prepared with the examined the **1**/MCl_n systems ranged from 60 to 66%, which is a range similar to the range obtained using simple metal halides as catalysts (61–67%).[14,40] These results indicate that the direction of the insertion of the monomer molecules to the propagating carbocation is not affected by the steric hindrance around the catalysts produced by the salphen framework employed in the present study.

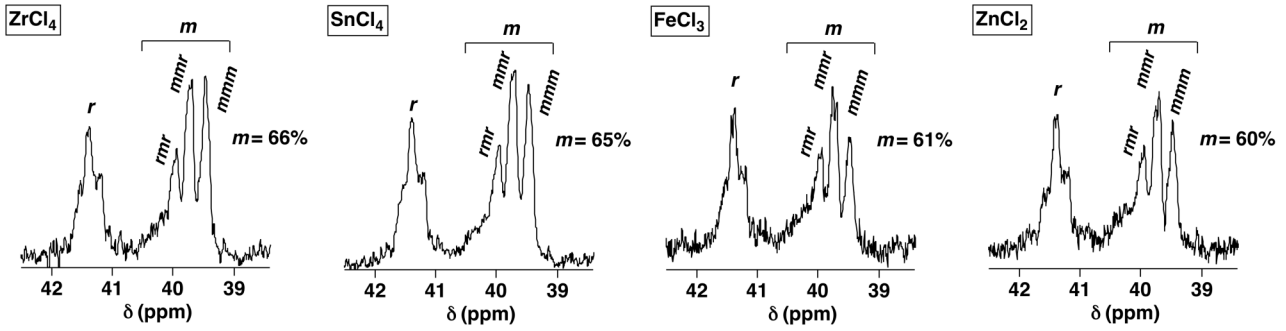

Figure 5. ^{13}C NMR spectra of poly(IBVE)s obtained using the **1**/MCl_n initiating systems ($[IBVE]_0 = 0.76$ M, $[MCl_n]_0 = 5.0$ mM, $[\mathbf{1}]_0 = 5.0$ mM, [ethyl acetate] = 1.0 M, [heptane] = 5.0 vol % in toluene at 0 ºC; 125 MHz for $ZrCl_4$, $FeCl_3$ and $ZnCl_2$ and 100 MHz for $SnCl_4$ in $CDCl_3$ at 30 ºC).

Table 2 summarizes the polymerization results under various conditions, demonstrating the importance of temperature and the polarity of the solvent. The polymerization using this initiating system in toluene was examined at various temperatures (Table 2, entries 1–5). The polymerizations proceeded successfully even at higher temperatures (entries 1–3, 0–60 ºC), producing polymers with relatively narrow MWDs. The M_n values of the polymers obtained at 0 and 30 °C were in agreement with the theoretical ones. In contrast, the polymers obtained at 60 °C had M_n values slightly lower than their calculated ones (Figure 6). The polymer obtained at high temperatures, particularly at 60 °C, had a small amount of irregular structures originating from an undesired reaction, i.e., the dealcoholization of the side chain, which was confirmed by ^{1}H NMR (Figure 7). The polymerization reactions at low temperatures (entries 4 and 5, –30 and –78 °C) yielded polymers with broad MWDs and M_n values that were higher than the theoretical ones. The linear first–order plots for the polymerization at –30 °C indicate that the reaction proceeded at a constant rate (Figure 8C). Thus, the broadening of the MWDs was not attributable to undesired side reactions, but instead, to slow initiation reaction kinetics. The polymerization in dichloromethane, a polar solvent,[41] at 0 °C proceeded at a much higher rate than in toluene, similar to polymerizations with other common catalysts. The reaction quantitatively yielded a polymer with a unimodal but slightly broader MWD (entry 6, Figure 9). The results obtained under various conditions demonstrate that the polymerization in toluene at 0 °C is the most suitable for the **1**/$ZrCl_4$ system.

Table 2. Cationic polymerization of IBVE using the **1**/$ZrCl_4$ initiating systems under various conditions[a]

entry	temp (ºC)	time (h)	conv (%)[c]	$M_n \times 10^{-3}$ (calcd)[d]	$M_n \times 10^{-3}$ (obs)[e]	M_w/M_n[e]	meso dyad (%)[f]
1	60	2.5	94	7.2	5.0	1.18	59
2	30	7	99	7.6	7.4	1.16	62
3	0	18.5	98	7.6	7.3	1.15	66
4	–30	98	96	7.4	8.9	1.37	70
5	–78	1410	59	1.5	3.2	1.49	75
6[b]	0	2	82	6.3	7.3	1.26	61

[a] $[IBVE]_0$ = 0.76 M, $[ZrCl_4]_0$ = 5.0 mM for entries 1–4 and 6, 15 mM for entry 5, $[\mathbf{1}]_0$ = 5.0 mM for entries 1–4 and 6, 15 mM for entry 5, [ethyl acetate] = 1.0 M, [heptane] = 5.0 vol% in toluene at 0 ºC. [b] In dichloromethane. [c] Determined by gas chromatography. [d] Based on the amounts of **1**.[30] [e] Determined by GPC (polystyrene standards). [f] Determined by ^{13}C NMR analysis (see Figure 10 for the spectra).

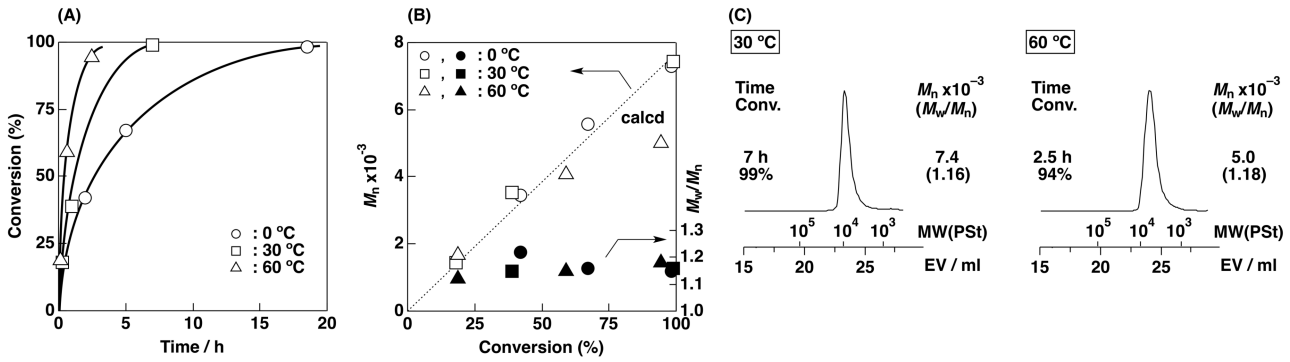

Figure 6. (A) Time–conversion curves for the polymerization, (B) M_n (dotted line: calculated M_n) and M_w/M_n and (C) MWD curves for poly(IBVE)s obtained using the **1**/$ZrCl_4$ initiating systems at 0, 30, or 60 ºC ($[IBVE]_0$ = 0.76 M, $[ZrCl_4]_0$ = 5.0 mM, $[\mathbf{1}]_0$ = 5.0 mM, [ethyl acetate] = 1.0 M, [heptane] = 5.0 vol% in toluene).

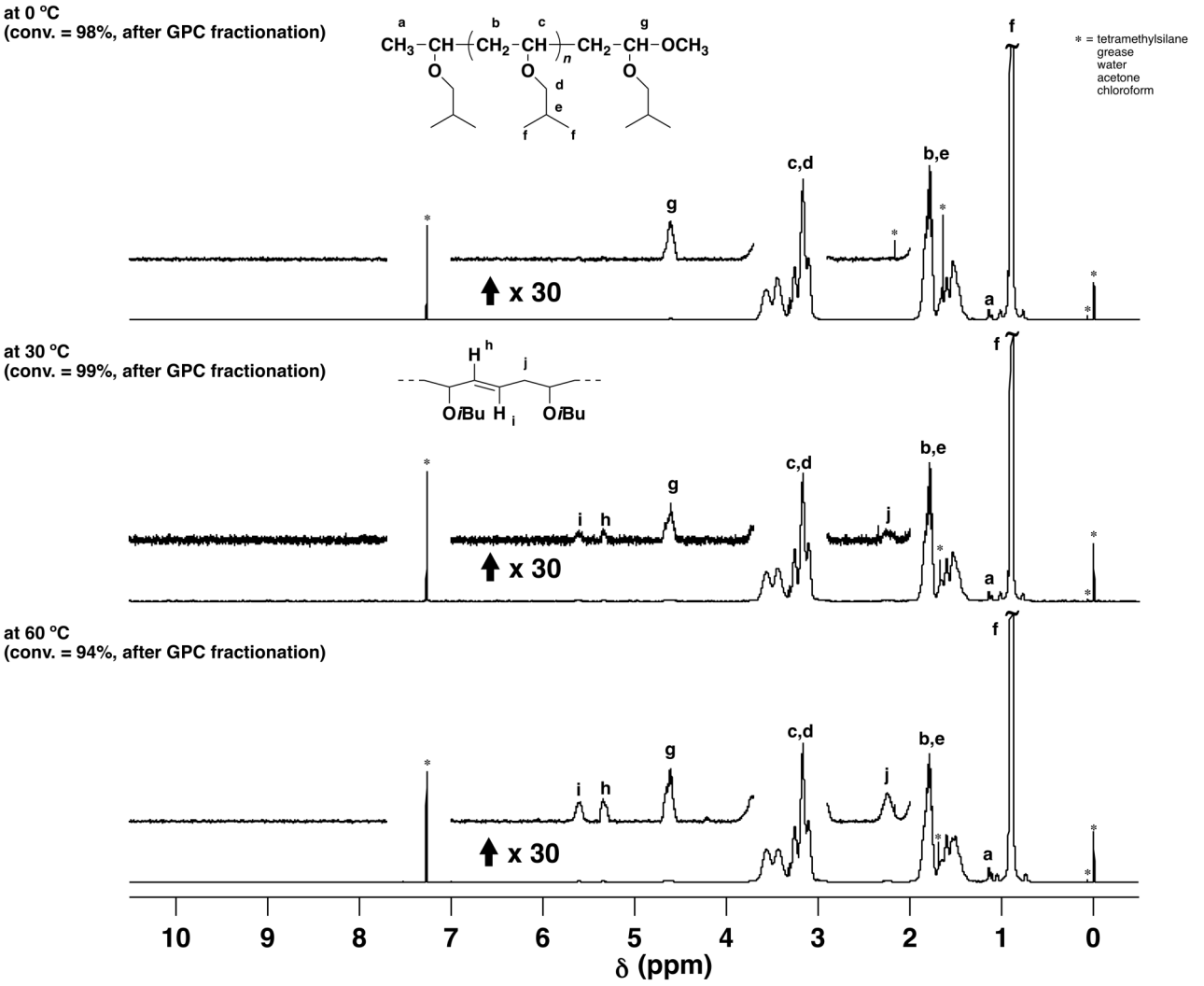

Figure 7. ^{1}H NMR spectra of poly(IBVE)s obtained using the **1**/$ZrCl_4$ initiating systems at 0, 30, or 60 ºC ($[IBVE]_0$ = 0.76 M, $[ZrCl_4]_0$ = 5.0 mM, $[\mathbf{1}]_0$ = 5.0 mM, [ethyl acetate] = 1.0 M, [heptane] = 5.0 vol % in toluene; 500 MHz in $CDCl_3$ at 30 ºC).

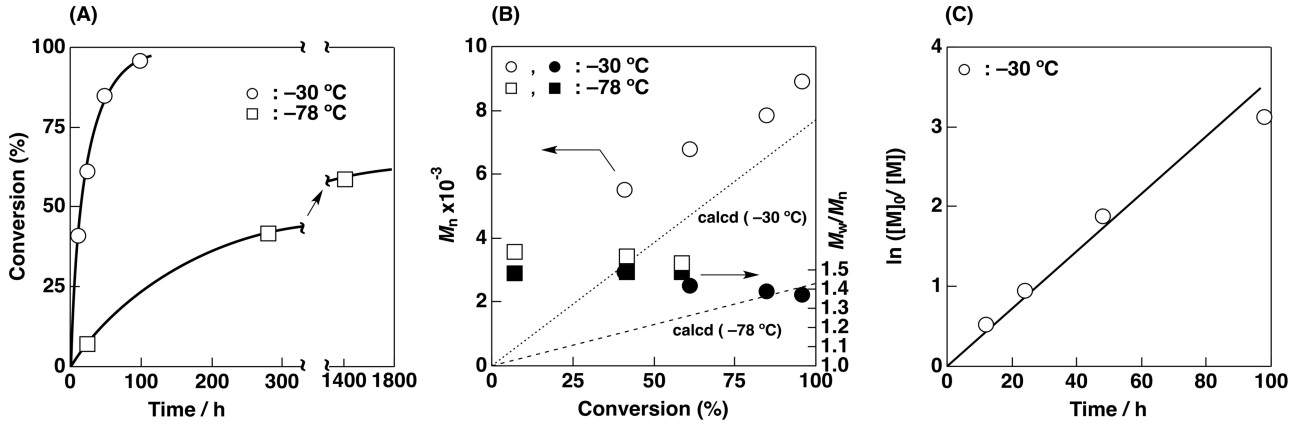

Figure 8. (A) Time–conversion curves, (B) M_n (dotted line: calculated line) and M_w/M_n for poly(IBVE)s, and (C) $\ln([M]_0/[M])$–time plots for the polymerization using the **1**/$ZrCl_4$ initiating systems at –30 or –78 ºC ($[IBVE]_0$ = 0.76 M, $[ZrCl_4]_0$ = 5.0 or 15 mM, $[\mathbf{1}]_0$ = 5.0 or 15 mM, [ethyl acetate] = 1.0 M, [heptane] = 5.0 vol% in toluene).

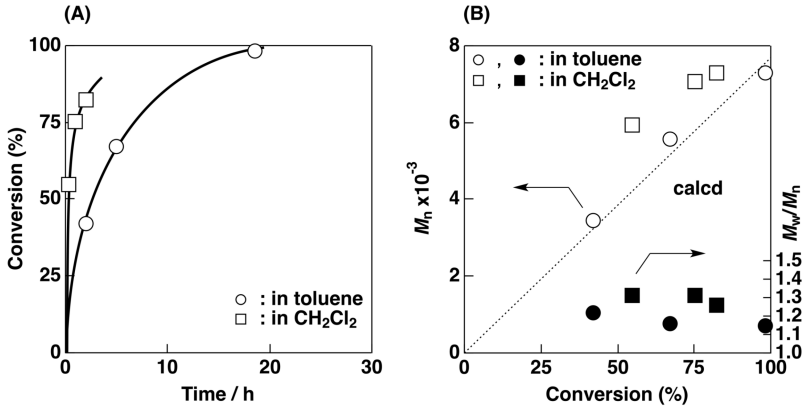

Figure 9. (A) Time–conversion curves for the polymerization and (B) M_n (dotted line: calculated line) and M_w/M_n for poly(IBVE)s obtained using the **1**/$ZrCl_4$ initiating system in toluene or dichloromethane ($[IBVE]_0$ = 0.76 M, $[ZrCl_4]_0$ = 5.0 mM, $[\mathbf{1}]_0$ = 5.0 mM, [ethyl acetate] = 1.0 M, [heptane] = 5.0 vol% at 0 ºC).

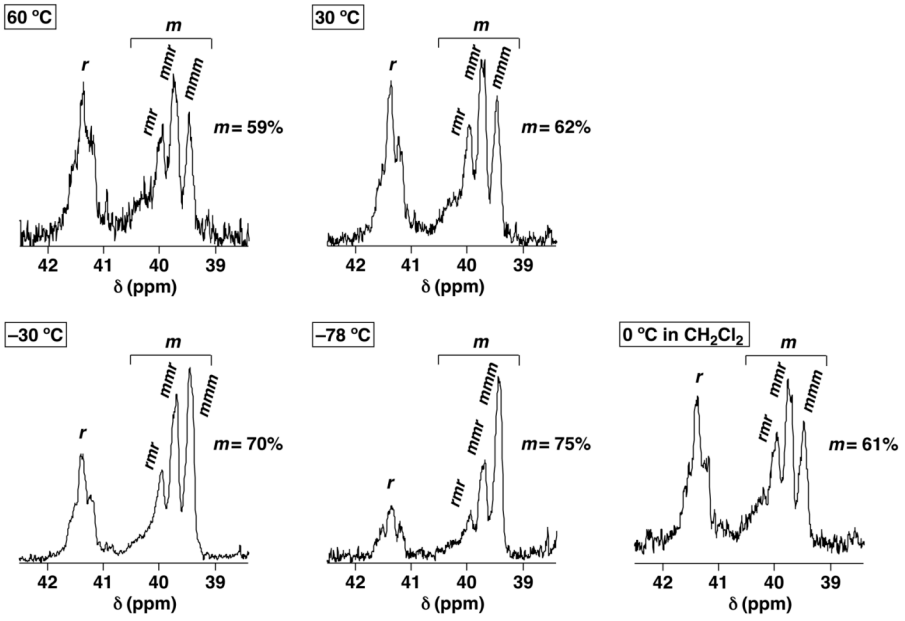

Figure 10. ^{13}C NMR spectra of poly(IBVE)s obtained using the **1**/$ZrCl_4$ initiating systems ($[IBVE]_0$ = 0.76 M, $[ZrCl_4]_0$ = 5.0 mM, $[\mathbf{1}]_0$ = 5.0 mM, [ethyl acetate] = 1.0 M, [heptane] = 5.0 vol % in toluene at various conditions; 125 MHz in $CDCl_3$ at 30 ºC).

The author examined the cationic polymerization of IBVE using an isolated salphen complex to confirm the occurrence of a quantitative and fast initiating reaction in the **1**/$ZrCl_4$ system (Figure 11). After the salphen complex was generated by mixing the **1** and $ZrCl_4$ in dichloromethane, similar to the method described above, the solvents were evaporated under reduced pressure (Figure 12). The dried salphen complex was used as a polymerization catalyst without further purification. Because the HCl generated during the complex formation was also removed during solvent evaporation, the adduct of IBVE with HCl (IBVE–HCl) was used as a cationogen for polymerization. The cationic polymerization of IBVE using the isolated catalyst proceeded in a controlled manner in the presence of ethyl acetate in toluene at 0 ºC (Figure 11). Although the polymerization rate with the isolated salphen complex system was slower than that with

the one prepared *in situ*,[42] the obtained polymers were similar in molecular weight and MWD to the products prepared with the *in situ* prepared salphen complex. In addition, the reaction without IBVE–HCl resulted in very slow polymerization (Figure 11), suggesting that HCl was removed during the catalyst isolation process. These results support the hypothesis that the **1**/$ZrCl_4$ initiating system, prepared *in situ*, led to quantitative complexation and a successive initiating reaction from the generated HCl.

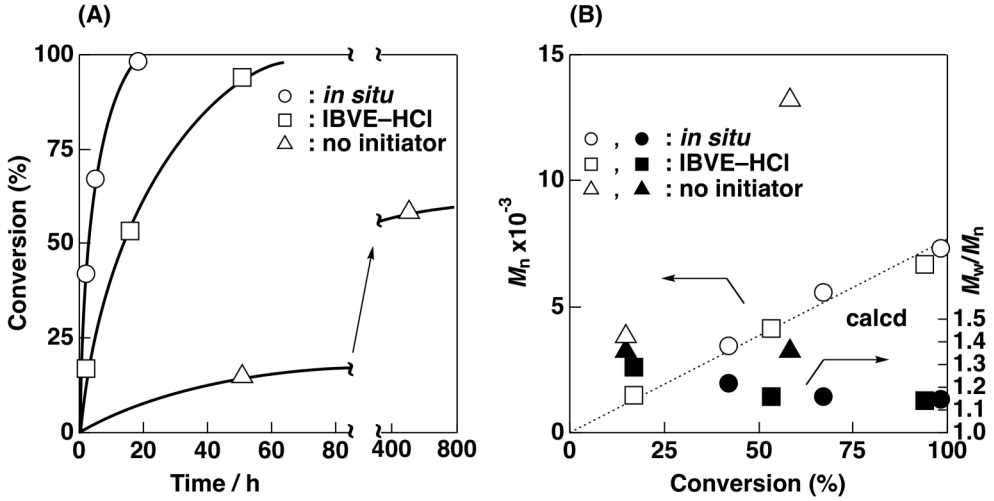

Figure 11. (A) Time–conversion curves for the polymerization and (B) M_n (dotted line: calculated M_n) and M_w/M_n for poly(IBVE)s obtained using the isolated **1**–$ZrCl_2$ complex (square and triangle) or the **1**/$ZrCl_4$ initiating system (circle) ([IBVE]$_0$ = 0.76 M, [**1**–$ZrCl_2$]$_0$ = 5.0 mM (square and triangle) or [$ZrCl_4$]$_0$ = [**1**]$_0$ = 5.0 mM (circle), [IBVE–HCl]$_0$ = 0 mM (circle and triangle) or 10 mM (square), [ethyl acetate] = 1.0 M, [heptane] = 5.0 vol % at 0 ºC).

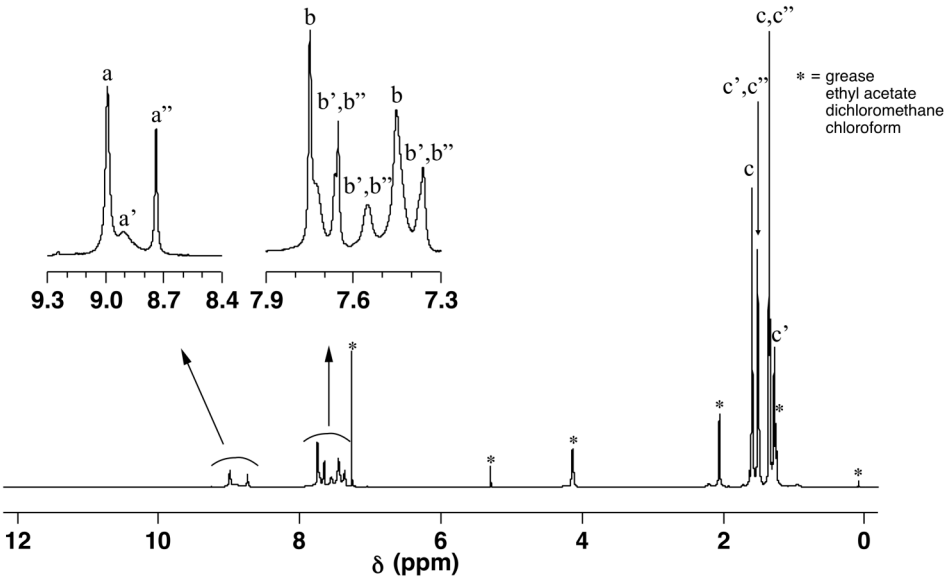

Figure 12. ^{1}H NMR spectrum of the isolated **1**–$ZrCl_2$ complex by evaporation {a, a’ and a” shows a signal of the methine proton of N=C*H*, b, b’ and b” shows a signal of the phenyl protons, and c, c’ and c” shows a signal of the protons of *t*Bu groups: signals of a, b and c are likely assigned to a *trans* isomer of **1**–$ZrCl_2$ complex, signals of a’, b’ and c’ are likely assigned to a α-*cis* isomer of **1**–$ZrCl_2$ complex, and signals of a”, b” and c” are likely assigned to an H_2O-coordinating **1**–$ZrCl_2$ complex[37,43] }.

Cationic polymerization of IBVE with substituted salphen ligands/$ZrCl_4$ systems

A precise design of catalysts through tuning of the electronic properties and the structure is expected to allow for elaborate control of polymerization reactions.[20,44] To examine the effects of the electronic properties on the polymerization behavior, salphen derivatives with different arylene groups were used for cationic polymerization by the *in situ* method (Table 3). The polymerizations of IBVE were conducted using ligands with 4-methyl (**2**) or 4,5-chloro (**3**) groups on the arylene group in conjunction with $ZrCl_4$ in the presence of ethyl acetate in toluene at 0 ºC. Both systems generated soluble catalysts upon mixing with $ZrCl_4$. The polymerizations proceeded smoothly to yield polymers with M_n values close to the theoretical ones. Thus, the substituted salphen ligands were also effective for the polymerization reaction via the *in situ* complexation method.

The observed polymerization rates for the three salphen ligands exhibited a trend different from that expected based on the electronic properties. The chloro-substituted ligand (**3**) was expected to result in an increase in the polymerization rate due to electron-withdrawing effects that could potentially decrease the electron density on the central metal. However, the polymerization rate with the **3**/$ZrCl_4$ system was slower than that for the systems with **1** or **2**. Zr–salphen complexes have six bonds, with two nitrogen and two oxygen atoms from the salphen ligand and two chlorine atoms. A seventh bond is formed through the coordination of a basic species to the labile coordination site, which is responsible for the Lewis acidic catalytic activity.[34–38] In the polymerization reaction, the association-dissociation equilibrium of ethyl acetate, used as a weak Lewis base, competes with the abstraction of the chloride anion from the growing chain end. The balance between the coordination of the two species is likely responsible for the difference in the experimental and expected trends of the polymerization rates. Another possible explanation is that the ratios of the two isomers (*trans* and α-*cis* types) of **1**–$ZrCl_2$ complexes made the difference in the polymerization rates.

Table 3. Cationic polymerization of IBVE using $ZrCl_4$ and the salphen ligands with substituted phenylene groups[a]

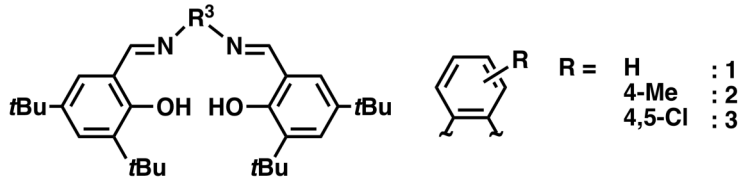

entry	ligand	time (h)	conv (%)[b]	$M_n \times 10^{-3}$ (calcd)[c]	$M_n \times 10^{-3}$ (obs)[d]	M_w/M_n[d]
1	**1**	18.5	98	7.6	7.3	1.15
2	**2**	18	99	7.6	7.3	1.23
3	**3**	48	92	7.1	5.9	1.31

[a] $[IBVE]_0$ = 0.76 M, $[ZrCl_4]_0$ = 5.0 mM, $[ligand]_0$ = 5.0 mM, [ethyl acetate] = 1.0 M, [heptane] = 5.0 vol% in toluene at 0 ºC. [b] Determined by gas chromatography. [c] Based on the amounts of ligands. [d] Determined by GPC (polystyrene standards).

The polymerization behavior when salphen complexes were used as catalysts was affected by the solubility of the complexes. The substituents at the R^1 and R^2 positions of the salphen ligands were found to be responsible for the solubility of the generated complexes. The polymerization proceeded in transparent solutions when **1** and **5** were used, whereas heterogeneous mixtures were generated from **4** and **6**. Interestingly, the polymerizations of IBVE still proceeded in the heterogeneous systems. However, quantitative comparison of the polymerization rates between the homogeneous and heterogeneous systems is difficult because of the difference in the effective concentrations of the catalysts. In the case of the **4**/$ZrCl_4$ initiating system, the polymerization solution gradually became homogeneous. This fact likely suggests that the **4**–Zr complex is soluble, but the intermediate state consisting of HCl and the complex possesses low solubility. ^{13}C NMR analysis of the polymers obtained using various ligands/$ZrCl_4$ initiating systems showed almost no relationship between the catalytic structure and tacticity (m ~ 64–66%).

Table 4. Cationic polymerization of IBVE using $ZrCl_4$ and the salphen ligands with substituted salicyl groups[a]

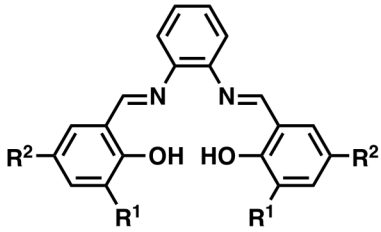

R^1 = *t*Bu, R^2 = *t*Bu : 1
R^1 = H, R^2 = *t*Bu : 4
R^1 = R^2 = cumyl : 5
R^1 = OMe, R^2 = H : 6

cumyl = 

entry	ligand	time (h)	conv (%)[b]	$M_n \times 10^{-3}$ (calcd)[c]	$M_n \times 10^{-3}$ (obs)[d]	M_w/M_n[d]	meso dyad (%)[e]	catalytic solution
1	**1**	18.5	98	7.6	7.3	1.15	66	transparent
2	**4**	117	98	7.5	7.6	1.39	64	heterogeneous
3	**5**	48	74	5.7	6.8	1.28	64	transparent
4	**6**	72	87	6.7	3.6	1.79	65	heterogeneous

[a] $[IBVE]_0$ = 0.76 M, $[ZrCl_4]_0$ = 5.0 mM, $[ligand]_0$ = 5.0 mM, [ethyl acetate] = 1.0 M, [heptane] = 5.0 vol% in toluene at 0 ºC. [b] Determined by gas chromatography. [c] Based on the amounts of ligands. [d] Determined by GPC (polystyrene standards). [e] Determined by ^{13}C NMR analysis.

Conclusion

A readily synthesized metal complex catalyst with a designed ligand was demonstrated to allow for the controlled cationic polymerization of IBVE. A salphen complex, synthesized *in situ* by mixing a ligand **1** with a metal chloride, was used for the polymerization. The difference in polymerization behaviour among metal chlorides correlated with the chemical affinity of the central metal, the existence of labile coordination sites, and the Lewis acidity. $ZrCl_4$ is the best choice as the catalyst precursor because of an appropriate oxophilicity and a vacant site for exhibition of Lewis acidity. The as-prepared **1**/$ZrCl_4$ complex induced the living cationic polymerization of IBVE in the presence of ethyl acetate as an added base in toluene at 0 °C. The use of tetradentate Schiff base ligands, which are easily tunable electronically and sterically, is expected to expand the available synthetic strategies for the precise control of cationic polymerization reactions, such as the adjustment of the catalytic activity and stereoselectivity of the catalyst. In addition, ligands with various substituents (ligands **2**–**6**) were also employed in the polymerization in conjunction with $ZrCl_4$. The electronic properties derived from the substituents likely affected the catalytic activity.

References

1. Bielawski, C. W.; Grubbs, R. H. *Prog. Polym. Sci.* **2007**, *32*, 1–29.
2. Schrock R. R. *Dalton Trans.* **2011**, *40*, 7484–7495.
3. (a) Kamigaito, M.; Ando, T.; Sawamoto, M. *Chem. Rev.* **2001**, *101*, 3689–3746. (b) Ouchi, M.; Terashima, T.; Sawamoto, M. *Chem. Rev.* **2009**, *109*, 4963–5050.
4. (a) Matyjaszewski, K.; Xia, J. *Chem. Rev.* **2001**, *101*, 2921–2990. (b) di Lena, F.; Matyjaszewski, K. *Prog. Polym. Sci.* **2010**, *35*, 959–1021.
5. Rosen B. M.; Percec, V. *Chem. Rev.* **2009**, *109*, 5069–5119.
6. Boffa, L. S.; Novak, B. M. *Chem. Rev.* **2000**, *100*, 1479–1494.
7. Chen, E. Y.-X. *Chem. Rev.* **2009**, *109*, 5157–5214.
8. Nakamura, A.; Ito, S.; Nozaki, K. *Chem. Rev.* **2009**, *109*, 5215–5244.
9. (a) Aoshima, S.; Yoshida, T.; Kanazawa, A.; Kanaoka, S. *J. Polym. Sci., Part A: Polym. Chem.* **2007**, *45*, 1801–1813. (b) Aoshima, S.; Kanaoka, S. *Chem. Rev.* **2009**, *109*, 5245–5287.
10. Kanazawa, A.; Kanaoka, S.; Aoshima, S. *J. Polym. Sci., Part A: Polym. Chem.* **2010**, *48*, 2509–2516.
11. Kanaoka, S.; Nakayama, S.; Aoshima, S. *Kobunshi Ronbunshu* **2011**, *68*, 349–351.
12. (a) Sawamoto, M. *Prog. Polym. Sci.* **1991**, *16*, 111–172. (b) Kennedy, J. P.; Ivan, B. *Designed Polymers by Carbocationic Macromolecular Engineering: Theory and Practice*; Hanser: New York, 1992. (c) Matyjaszewski, K.; Sawamoto, M. *Cationic Polymerizations*; Matyjaszewski, K., Ed.; Marcel Dekker: New York, 1996; Chapter 4. (d) Kennedy, J. P. *J. Polym. Sci., Part A: Polym. Chem.* **1999**, *37*, 2285–2293. (e) Puskas, J. E.; Kaszas, G. *Prog. Polym. Sci.* **2000**, *25*, 403–452. (f) De, P.; Faust, R. *Macromolecular Engineering. Precise Synthesis, Materials Properties, Applications*; Matyjaszewski, K.; Gnanou, Y.; Leibler, L., Eds.; Wiley-VCH GmbH & Co. KGaA: Weinheim, 2007; Chapter 3. (g) Goethals, E.; Prez, F. D. *Prog. Polym. Sci.* **2007**, *32*, 220–246.

13. (a) Baird, M. C. *Chem. Rev.* **2000**, *100*, 1471–1478. (b) Shaffer, T. D.; Ashbaugh, J. R. *J. Polym. Sci. Part A Polym. Chem.* **1997**, *35*, 329–344. (c) Bochmann, M. *Acc. Chem. Res.* **2010**, *43*, 1267–1278. (d) Jacob, S.; Pi, Z.; Kennedy, J. P. *Polym. Bull.* **1998**, *41*, 503–510. (e) Kostjuk, S. V.; Yeong, H. Y.; Voit, B. *J. Polym. Sci., Part A: Polym. Chem.* **2013**, *51*, 471–486. (f) Diebl, B. E.; Li, Y.; Cokoja, M.; Kühn, F. E.; Radhakrishnan, N.; Zschoche, S.; Komber, H.; Yeong, H. Y.; Voit, B.; Nuyken, O.; Hanefeld, P.; Walter, H.-M. *J. Polym. Sci., Part A: Polym. Chem.* **2010**, *48*, 3775–3786.
14. (a) Ouchi, M.; Kamigaito, M.; Sawamoto, M. *Macromolecules* **1999**, *32*, 6407–6411. (b) Ouchi, M.; Kamigaito, M.; Sawamoto, M. *J. Polym. Sci., Part A: Polym. Chem.* **2001**, *39*, 1060–1066.
15. Li, B.; Wu, Y.; Cheng, H.; Liu, W. *Polymer* **2012**, *53*, 3726–3734.
16. Banerjee, S.; Paira, T. K.; Mandal, T. K. *Macromol. Chem. Phys.* **2013**, *214*, 1332–1344.
17. Pernecker, T.; Kennedy, J. P.; Ivan, B. *Macromolecules* **1992**, *25*, 1642–1647.
18. Kamigaito, M.; Maeda, Y.; Sawamoto, M.; Higashimura, T. *Macromolecules* **1993**, *26*, 1643–1649.
19. Yonezumi, M.; Takano, N.; Kanaoka, S.; Aoshima, S. *J. Polym. Sci., Part A: Polym. Chem.* **2008**, *46*, 6746–6753.
20. Kamigaito, M.; Sawamoto, M.; Higashimura, T. *Macromolecules* **1995**, *28*, 5671–5675.
21. Hobday, M. D.; Smith, T. D. *Coord. Chem. Rev.* **1973**, *9*, 311–337.
22. Cozzi, P. G. *Chem. Soc. Rev.* **2004**, *33*, 410–421.
23. A polymerization using 2,6-diisopropylphenol and *o*-phenylenediamine with $ZrCl_4$ was conducted as a control experiment. The equimolar amounts of the three components were mixed to give a catalytic solution. The polymerization using the solution proceeded but the monomer conversion leveled off at around 30% (150 h, 31%). On the other hand, the reaction using 2,6-diisopropylphenol and $ZrCl_4$ without the diamine caused controlled polymerization in a manner similar to the polymerization using the alcohol/MCl_n initiating system[10]. Thus, the superiority of the salphen complex over the catalysts with these model compounds is that both the electronic and geometric characteristics can be readily tuned because of the versatility of the ligand design and the multidentate ligation.
24. (a) Palucki, M.; Finney, N. S.; Pospisil, P. J.; Güler, M. L.; Ishida, T.; Jacobsen, E. N. *J. Am. Chem. Soc.* **1998**, *120*, 948–954. (b) Ford, D. D.; Nielsen, L. P. C.; Zuend, S. J.; Musgrave, C. B.; Jacobsen, E. N. *J. Am. Chem. Soc.* **2013**, *135*, 15595–15608. (c) Katsuki, T. *Chem. Soc. Rev.* **2004**, *33*, 437–444. (d) McGarrigle, E. M.; Gilheany, D. G. *Chem. Rev.* **2005**, *105*, 1563–1602. (e) Iwasa, N.; Katao, S.; Liu, J.; Fujiki, M.; Furukawa, Y.; Nomura, K. *Organometallics* **2009**, *28*, 2179–2187. (f) Makio, H.; Terao, H.; Iwashita, A.; Fujita, T. *Chem. Rev.* **2011**, *111*, 2363–2449.
25. Higashimura, T.; Kamigaito, M.; Kato, M.; Hasebe, T.; Sawamoto, M. *Macromolecules* **1993**, *26*, 2670–2673.
26. Sanz, M.; Cuenca, T.; Galakhov, M.; Grassi, A.; Bott, R. K. J.; Hughes, D. L.; Lancaster, S. J.; Bochmann, M. *Organometallics* **2004**, *23*, 5324–5331.
27. Kochnev, A. I.; Oleynik, I. I.; Oleynik, I.V., Ivanchev, S. S.; Tolstikov, G. A. *Rus. Chem. Bull., Int. Ed.*, **2007**, *56*, 1125–1129.
28. In this system, it is difficult to tune polymerization rate without changing target molecular weights because the initiator and Lewis acid catalysts should be always mixed at the same concentrations.

29. An "added base" is a weak Lewis base that is used for living/controlled cationic polymerization. A weak Lewis base such as ethyl acetate, 1,4-dioxane, and THF controls the polymerization through its interaction with a Lewis acid catalyst, the propagating carbocation, and/or the counteranion.
30. The generated HCl during complex formation was employed as a protonogen, or an initiator, for the cationic polymerization of a vinyl ether. Hence, the theoretical M_n values were calculated based on the concentration of the generated HCl ($[HCl]_{theoretical} = 2 \times [\mathbf{1}]_0 = 10$ mM except for entry 5 or 30 mM for entry 5 in Table 2).
31. The polymerization using $ZrCl_4$ and 1.5 equimolar amounts of **1** (Figure 1, square) indicated that uncomplexed, free ligand molecules prevented the propagating reaction. The hydroxy group on the ligand possibly reacted with the propagating carbocation but the resulting structure, the acetal chain end having the ligand, was not detected on the ^{1}H NMR spectra of the products (Figure 2). In the reactions using $SnCl_4$ and $ZnCl_2$, ligand molecules that remained due to insufficient complex formation would have also reacted with the propagating chains, but a direct proof was not obtained similarly. The catalytic solutions for $SnCl_4$, $FeCl_3$, and $TiCl_4$ (entries 2, 3 and 5 in Table 1) afforded heterogeneous systems, and therefore, the polymerizations were conducted using partially soluble catalysts. The heterogeneity indicated that the complex formation was not quantitative or that several types of complexes were generated.
32. The product polymers had no irregular structures originating from undesired side reactions, such as β-proton elimination, dealcoholization, and the generation of aldehyde groups at chain ends[33], which was confirmed by ^{1}H NMR (Figures 2 and 4).
33. Kanazawa, A.; Kanaoka, S.; Aoshima, S. *J. Polym. Sci., Part A: Polym. Chem.* **2010**, *48*, 3702–3708.
34. Corazza, F.; Solari, E.; Floriani, C.; Chiesi-Villa, A.; Guastini, C. *J. Chem. Soc. Dalt. Trans.* **1990**, *4*, 1335–1344.
35. Repo, T.; Klinga, M.; Pietikäinen, P.; Leskelä, M.; Uusitalo, A.-M.; Pakkanen, T.; Hakala, K.; Aaltonen, P.; Löfgren, B. *Macromolecules* **1997**, *30*, 171–175.
36. Wang, M.; Zhu, H.; Jin, K.; Dai, D.; Sun, L. *J. Catal.* **2003**, *220*, 392–398.
37. Wang, M.; Zhu, H.; Huang, D.; Jin, K.; Chen, C.; Sun, L. *J. Organomet. Chem.* **2004**, *689*, 1212–1217.
38. Zhu, H.; Wang, M.; Ma, C.; Li, B.; Chen, C.; Sun, L.; *J. Organomet. Chem.* **2005**, *690*, 3929–3936.
39. The functionality of the terminal acetal group was determined from the signal integral ratio of the methyl proton of the initiating group (3H, signal a in Figure 2) and the methine proton of the end group (1H, signal g). The integral ratio a/g was 3.00/1.03, which indicates that quantitative functionality was achieved.
40. Kanazawa, A.; Kanaoka, S.; Aoshima, S. *Macromolecules* **2009**, *42*, 3965–3972.
41. Dean, J. A. *Lange's Handbook of Chemistry*, 15th ed.; Dean, J. A., Ed.; McGraw-Hill: New York, 1999; Section 5.
42. The ^{1}H NMR analysis of the isolated **1**–$ZrCl_2$ complex (Figure 12) indicated that this complex had several isomers[37,43]. The catalytic activities of these isomers likely differ from each other.
43. Sanz, M.; Cuenca, T.; Cuomo, C.; Grassi, A. *J. Organomet. Chem.* **2006**, *691*, 3816–3822.
44. (a) Zhou, Y.; Faust, R.; Chen, S.; Gido, S. P. *Macromolecules* **2004**, *37*, 6716–6725. (b) Zhou, Y.; Faust, R. *Polym. Bull.* **2004**, *52*, 421–428. (c) Hadjikyriacou, S.; Faust, R. *Macromolecules*, *29*, 5261–5267.

Chapter 3

Salen-Type Ligand/MCl_n Initiating Systems for the Controlled Cationic Polymerization of Isobutyl Vinyl Ether: Effects of the Ligand Framework

Introduction

The properties of a metal complex catalyst, which consists of a metal and a ligand, are determined by the metal–ligand bonding interactions, which allows for the modulation of the electronic properties of the metal and the influence of the steric environment. An appropriate combination of a metal with a ligand framework improves the catalytic properties, while an inappropriate metal-ligand combination induces undesired results, such as deactivation of the complex catalyst. Thus, tailoring the ligand framework to the metal species is highly important for the design of metal complex catalysts with sufficient stabilities and desirable catalytic properties.

Salen-type ligands have various advantages due to their easily tunable electronic and stereochemical properties, such as their coordination geometries and conformations. The ligand frameworks are obtained from the condensation of salicylaldehyde derivatives with diamines in high yield. The electronic and stereochemical properties of salen ligands can be easily and elaborately tuned because these starting materials are commercially available or can be obtained from simple synthetic procedures. Moreover, chiral salen complexes, which are categorized as privileged catalysts,[1] are widely used as catalysts in various enantioselective reactions.[2] The availability of chiral salen complexes as asymmetric catalysts was first reported by Jacobsen and Katsuki. These researchers independently developed chiral salen-Mn(III) complex catalysts for the enantioselective epoxidation of unfunctionalized olefins.[3,4]

In cationic polymerization, Lewis acid catalysts play a pivotal role in the precise synthesis of well-defined polymers with controlled molecular weights, narrow molecular weight distributions, end functionality, and controlled tacticity. Indeed, controlled/living cationic polymerization has been established with many initiating systems through the adjustment of the Lewis acidity of the catalysts by using additives such as weak Lewis bases and tetraalkylammonium halides.[5] Fine tuning of the electronic properties of the central Ti atom was proven to be effective for performing controlled/living cationic polymerization using $TiCl_n(OR)_{4-n}$ as the catalyst.[6] Furthermore, alcohol or acetylacetone efficiently react with appropriate metal halides to allow for *in situ* ligand exchange reactions, generating real catalytic species that induce living polymerization.[7] More interestingly, the ligand design of soluble complex catalysts, such as $TiCl_2(OAr)_2$ and transition metal complexes with tridentate ligands,[8,9] was demonstrated to be effective for stereospecific cationic polymerization.

As described in Chapter 2, the *in situ* complexation method was established in the cationic polymerization of isobutyl vinyl ether (IBVE) using salphen complex catalysts that were generated from

reactions between salphen ligands and $ZrCl_4$.[10] This method enables the facile preparation of metal complex catalysts without purification. In addition, since the initiation reaction occurs with the *in situ* generated hydrochloric acid, there is no need for the troublesome preparation of the conventional harmful initiators, such as vinyl ether-hydrogen halide adducts. The choice of metal chloride is also crucial in the controlled cationic polymerizations that use salphen/MCl_n initiating systems. Among the various metal chlorides (MCl_n; M = Zr, Sn, Fe, Zn, Ti, and Al), $ZrCl_4$ was superior to all the others. The type of MCl_n species that can be utilized in the *in situ* complexation method likely depends on the properties of the ligand framework, such as the electronic and steric features. Thus, the design of suitable ligand structures is expected to greatly contribute to the diversification of metal complex catalysts and impart a variety of characteristics in the controlled cationic polymerization.

In this chapter, several salen-type ligands are designed to widen the scope of applicable metal chlorides available for the *in situ* complexation method and to develop polymerization catalysts with discriminating features (Figure 1). First, a salen ligand possessing a cyclohexenyl group (**1**) is used in conjunction with various metal chlorides in the cationic polymerization of IBVE. Polymerization with the **1**/$ZrCl_4$ initiating system proceeds in a living manner, although the rate is slower than that when salphen ligand **2** is used. Interestingly, a wider variety of metal chlorides is applicable in the controlled polymerization when **1** is used as the ligand that when ligand **2** is used. Furthermore, salen derivatives with defferent substituents (ligands **3**, **4**) are used for the cationic polymerization using the ligand/$ZrCl_4$ initiating systems.

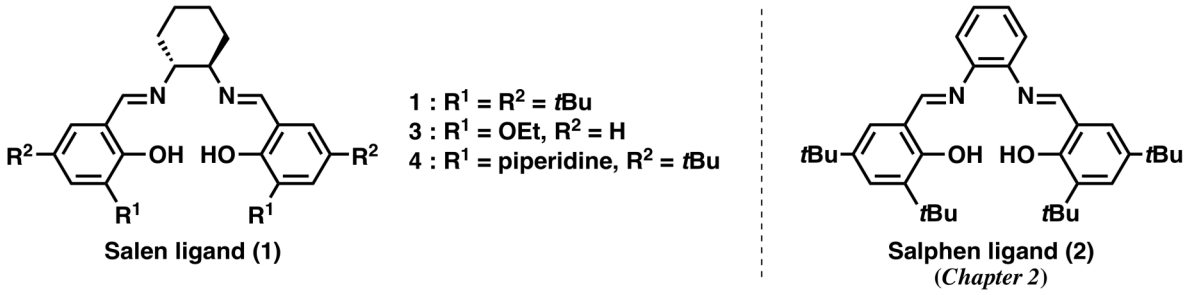

Figure 1. Structures of salen and salen-type ligands used in this chapter.

Experimental

Materials

Stock solutions of $GaCl_3$ in hexane and $HfCl_4$ in ethyl acetate were prepared from anhydrous $GaCl_3$ (Aldrich; >99.999%) and anhydrous $HfCl_4$ (Strem; >99.9%), respectively. Salen ligands [(*R*,*R*)-(–)-*N,N′*-bis(3,5-di-*tert*-butylsalicylidene)-1,2-cyclohexanediamine (**1**) (Aldrich; 98%) and (*R*,*R*)-(–)-*N,N′*-bis(3-(1-piperidinylmethyl)-5-*tert*-butylsalicylidene)-1,2-cyclohexanediamine (**4**) (Aldrich; 97%)] were used as received. Other materials were prepared and used as described in Chapter 2.

Synthesis of Ligands

(*R*,*R*)-(–)-*N,N′*-Bis(3-ethoxysalicylidene)-1,2-cyclohexanediamine (3)

A procedure similar to that described in Chapter 2 but with the use of (1*R*,2*R*)-(–)-1,2-diaminocyclohexane and two equivalents of 3-ethoxysalicylaldehyde gave the ligand. ^{1}H NMR (500 MHz, $CDCl_3$, 30 ºC): δ 8.23 (2H, s, N=C*H*), 6.85 (2H, m, C*H*-Ph), 6.77 (2H, m, C*H*-Ph), 6.70 (2H, m, C*H*-Ph), 4.07 (4H, m, O$CH_2$$CH_3$), 3.29 (2H, m, C*H*-N), 1.94 (2H, m, CH_2), 1.87 (2H, m, CH_2), 1.70 (2H, m, CH_2), 1.49 (2H, m, CH_2), 1.46 (6H, m, OCH_2CH_3).

Polymerization Procedure

Cationic polymerization reactions were conducted in a manner similar to that described in Chapter 2.

Characterization

The MWDs of the polymers were determined in a manner similar to that described in Chapter 2 with polystyrene gel columns [Tosoh; TSKgel G-4000H_{XL}, G-3000H_{XL}, and G-2000H_{XL} (exclusion limit molecular weight = 4×10^5, 6×10^4, and 1×10^4, respectively; bead size = 5 μm; column size = 7.8 mm i.d. × 300 mm), TSKgel MultiporeH_{XL}-M × 3 (exclusion limit molecular weight = 2×10^6; bead size = 5 μm; column size = 7.8 mm i.d. × 300 mm), or TSKgel GMH_{HR}-M × 3 or 2 (exclusion limit molecular weight = 4×10^6; bead size = 5 μm; column size = 7.8 mm i.d. × 300 mm); flow rate = 1.0 mL/min]. NMR spectra were measured as described in Chapter 2.

Results and Discussion

Cationic polymerization of IBVE with salen ligand (1)/MCl_n initiating systems

Cationic polymerization of IBVE was examined via the *in situ* complexation method using a salen ligand [(*R*,*R*)-(–)-*N*,*N'*-bis(3,5-di-*tert*-butylsalicylidene)-1,2-cyclohexanediamine, **1**] and $ZrCl_4$. Ligand **1** has a cyclohexenyl group in its backbone; hence, the corresponding salen complex is expected to have a catalytic environment different from that of a complex formed from salphen (**2**), which is the phenylene counterpart. The polymerization using the **1**/$ZrCl_4$ initiating system was conducted in the presence of ethyl acetate in toluene at 0 ºC. Ligand **1** and $ZrCl_4$ were first mixed in toluene, generating a transparent yellow solution. The catalyst solution was added to a solution containing monomer, which triggered the polymerization reaction. As shown in Figure 2A (open symbols), the polymerization proceeded smoothly, reaching approximately 90% conversion of IBVE in 150 h. The M_n values of the obtained polymers increased linearly with the monomer conversion (Figure 2B), indicating that the polymerization proceeded in a controlled manner. The M_n values of the polymers were slightly larger than the values calculated based on the concentration of the phenoxy group in the salen ligand. In addition, ^{1}H NMR analysis of the obtained polymer revealed that the signals assigned to the structures derived from side reactions were negligible (Figure 3).[12]

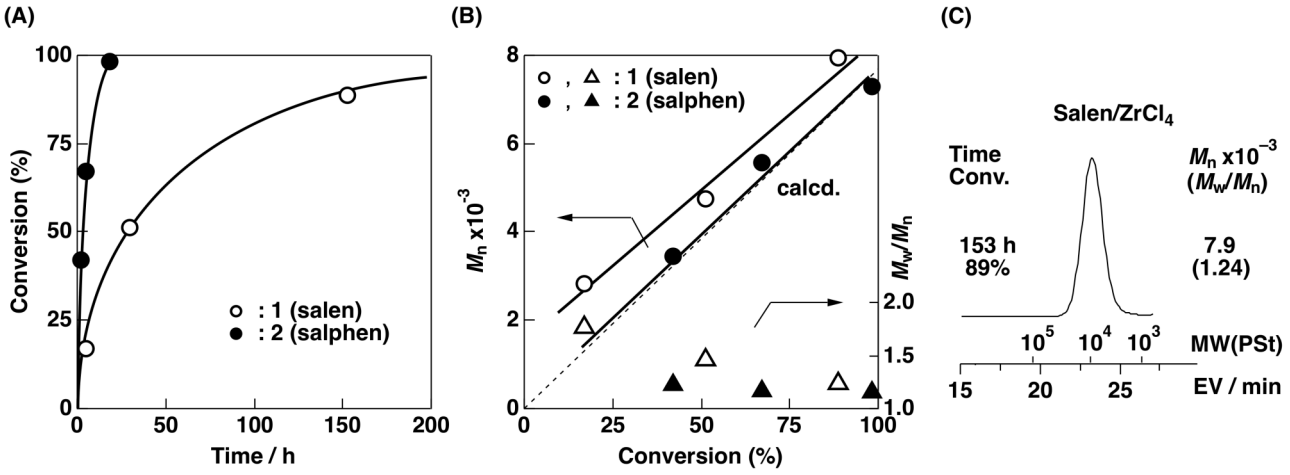

Figure 2. (A) Time–conversion curves of the polymerization, (B) M_n (dotted line: calculated line) and M_w/M_n values of obtained polymers, and (C) the MWD curve of the poly(IBVE) obtained using the **1** or **2**/$ZrCl_4$ initiating system ($[IBVE]_0$ = 0.76 M, $[ZrCl_4]_0$ = 5.0 mM, $[ligand]_0$ = 5.0 mM, [ethyl acetate] = 1.0 M, [heptane] = 5.0 vol% in toluene at 0 ºC).

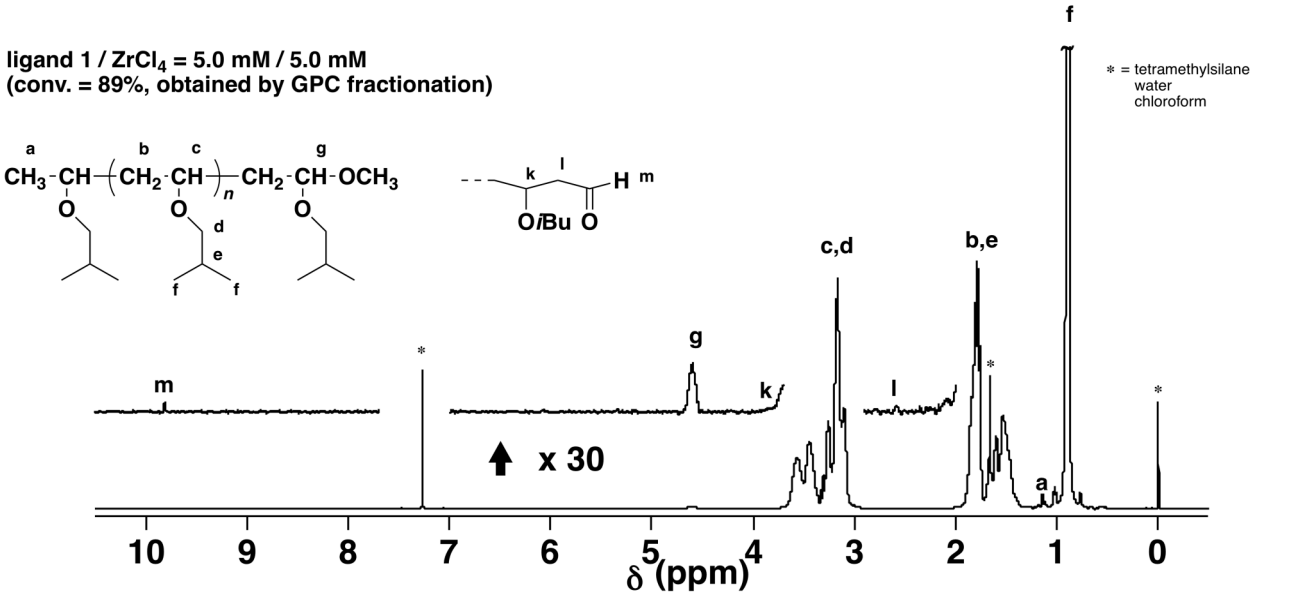

Figure 3. ^{1}H NMR spectrum of the poly(IBVE) obtained using the **1**/$ZrCl_4$ initiating system ($[IBVE]_0$ = 0.76 M, $[ZrCl_4]_0$ = 5.0 mM, $[\mathbf{1}]_0$ = 5.0 mM, [ethyl acetate] = 1.0 M, [heptane] = 5.0 vol% in toluene at 0 ºC; 500 MHz in $CDCl_3$ at 30 ºC; signal integral ratio: a/g = 3.00/0.98).

The livingness of the polymerization performed with the **1**/$ZrCl_4$ initiating system was confirmed through a monomer addition experiment. The first stage of polymerization was conducted under the same conditions as those demonstrated above. When the monomer conversion reached 84%, a fresh feed of IBVE was added to the polymerization solution. As shown in Figure 4C, the signal in the MWD curve shifted toward the higher MW regime after the addition while maintaining a relatively narrow MWD. In addition, the M_n values of the products obtained increased linearly with the conversion (Figure 4B). These results indicate that the polymerization proceeded in a living manner.

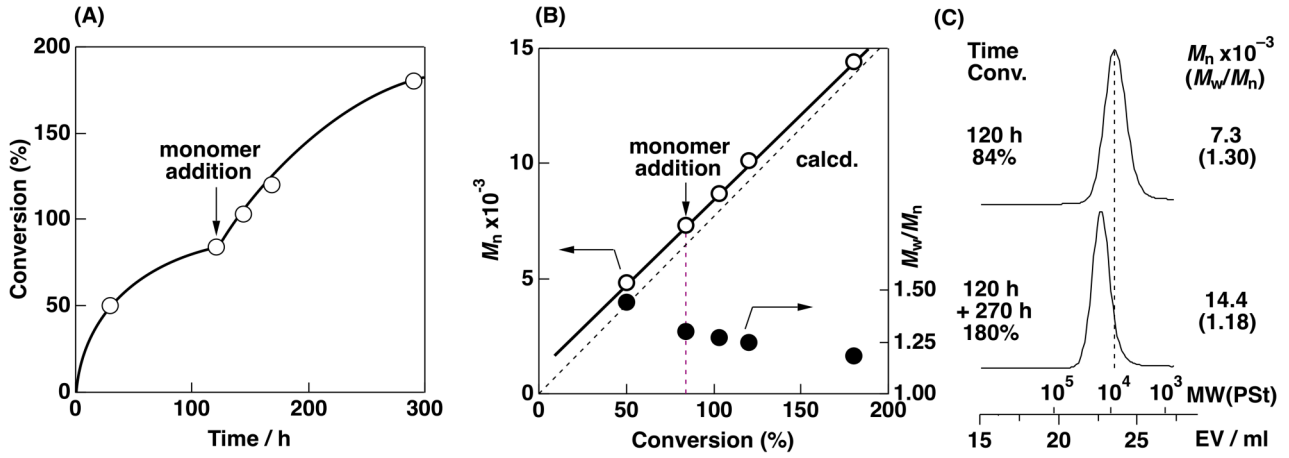

Figure 4. (A) Time–conversion curve of the polymerization, (B) M_n (dotted line: calculated line) and M_w/M_n values, and (C) MWD curves of poly(IBVE)s obtained in the monomer addition experiment using the **1**/$ZrCl_4$ initiating system ($[IBVE]_0 = [IBVE]_{added}$ = 0.76 M, $[ZrCl_4]_0$ = 5.0 mM, $[\mathbf{1}]_0$ = 5.0 mM, [ethyl acetate] = 1.0 M, [heptane] = 5.0 vol% in toluene at 0 ºC).

The polymerization results obtained above indicate that the introduction of a cyclohexenyl group into the ligand instead of a phenylene group resulted in the deceleration of the polymerization reaction (Figure 2; Table 1, entries 1 and 2). The polymerization rate observed with the salen complex was approximately 10 times slower than that with the salphen complex (Figure 2A). An enhancement of the electron-donating character of the central metal of a catalyst typically decreases the Lewis acidity and decelerates the cationic polymerization rate. On the basis of the Hammett substituent constants,[13] an alkyl substituent possesses a stronger electron-donating ability than a phenyl group. Therefore, the lower Lewis acidity of the salen complex (**1**–$ZrCl_2$) compared to that of the salphen complex (**2**–$ZrCl_2$) most likely resulted from the electron-donating effect of the cyclohexenyl group. On the other hand, the difference between the possible isomers of **1**–$ZrCl_2$ and **2**–$ZrCl_2$ complexes may also affect the polymerization rate.[14,15]

The *in situ* complexation method with ligand **1** was effective for the controlled polymerization of IBVE when $FeCl_3$ was employed as the metal chloride instead of $ZrCl_4$ (entry 3 in Table 1). The polymerization with the **1**/$FeCl_3$ system proceeded at a very fast rate, reaching quantitative conversion in 30 min, although an induction period was observed. The induction period possibly stemmed from the slow initiation reaction of a species generated from **1** and $FeCl_3$. The M_n values of the product polymers were close to the calculated values, and the MWDs were very narrow. These results indicate the occurrence of controlled cationic polymerization with the **1**/$FeCl_3$ system, which is in sharp contrast to the uncontrolled reaction with the salphen counterpart (entry 4). The electron-donating ability of the cyclohexenyl group and/or the structure of the complex generated from **1** was likely responsible for the controlled reaction when $FeCl_3$ was used.

The polymerizations performed with other metal chlorides (MCl_n: M = Ti, Hf, Sn, Al, Ga, or Zn) were obviously different from those with $ZrCl_4$ and $FeCl_3$. The polymerization behavior of the *in situ* complexation method with the salen ligand was classified into the following four groups: controlled polymerization ($ZrCl_4$ and $FeCl_3$); partly controlled polymerization ($ZnCl_2$ and $HfCl_4$); uncontrolled polymerization ($SnCl_4$ and $GaCl_3$); and no reaction ($TiCl_4$ and $AlCl_3$) (Table 1, Figure 5). The polymerization of IBVE with the **1**/$ZnCl_2$ system produced polymers with M_n values close to the calculated values. However, the MWDs of the polymers were broad, indicating the occurrence of a slow initiation reaction. Comparison of the M_n values of the polymers obtained using the **1**/$ZnCl_2$ and **2**/$ZnCl_2$ systems showed that the salen system exhibited a higher initiation efficiency than did the salphen system. Slow initiation also occurred in the **1**/$HfCl_4$ system, resulting in broad MWDs and M_n values that was close to the theoretical values. On the other hand, polymerization using the **1**/$SnCl_4$ and $GaCl_3$ systems generated polymers with M_n values higher than the theoretical values. In the **1**/$GaCl_3$ system, the MWDs of the obtained polymers shifted to the higher MW region, which indicates the production of long-lived species. Unlike the above cases, no polymerization occurred for the combination of **1** with $TiCl_4$ or $AlCl_3$.

Table 1. Cationic polymerization of IBVE using MCl_n with **1** and **2**[a]

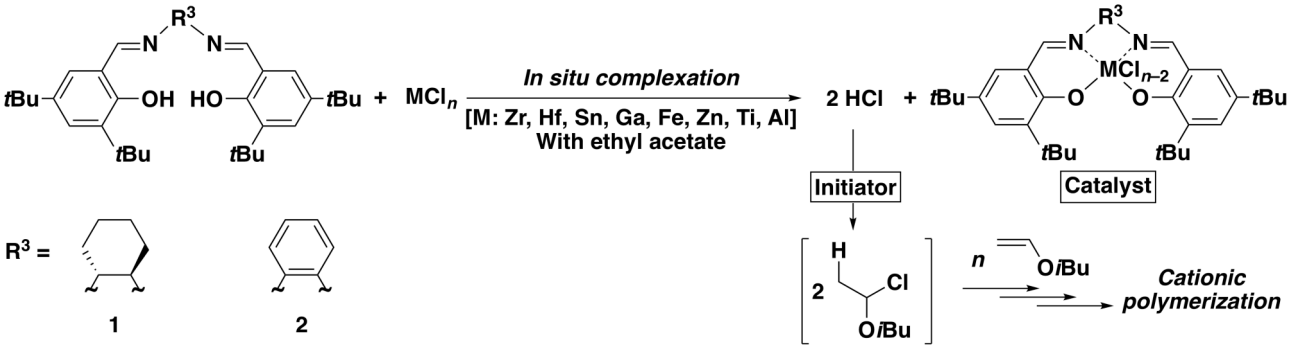

entry	MCl_n	ligand	time	conv (%)[b]	$M_n \times 10^{-3}$ (calcd)[c]	$M_n \times 10^{-3}$ (obs)[d]	M_w/M_n[d]	meso dyad (%)[e]
1	$ZrCl_4$	**1**	153 h	89	6.8	7.9	1.24	65
2		**2**	18.5 h	98	7.6	7.3	1.15	66
3	$FeCl_3$	**1**	30 min	99	7.6	8.3	1.11	62
4		**2**	5 s	90	7.0	11.5	1.57	61
5	$HfCl_4$	**1**	240 h	89	6.8	7.0	1.88	64
6	$ZnCl_2$	**1**	2 h	94	7.3	8.8	1.61	62
7		**2**	6 h	97	7.5	17.3	1.94	60
8	$SnCl_4$	**1**	6 h	96	7.4	12.8	1.51	65
9		**2**	20 min	94	7.3	10.5	1.37	65
10	$GaCl_3$	**1**	0.5 h	80	6.2	13.2	1.62	62
11	$TiCl_4$	**1**	504 h	8	0.6	n.d.	n.d.	n.d.
12		**2**	168 h	12	0.9	n.d.	n.d.	n.d.
13	$AlCl_3$	**1**	360 h	7	0.5	n.d.	n.d.	n.d.
14		**2**	430 h	2	0.2	n.d.	n.d.	n.d.

[a] $[IBVE]_0 = 0.76$ M, $[MCl_n]_0 = 5.0$ mM, $[ligand]_0 = 5.0$ mM, [ethyl acetate] = 1.0 M, [heptane] = 5.0 vol% in toluene at 0 ºC. [b] Determined by gas chromatography. [c] Based on the amounts of **1** or **2**. [d] Determined by GPC (polystyrene standards). [e] Determined by ^{13}C NMR analysis.

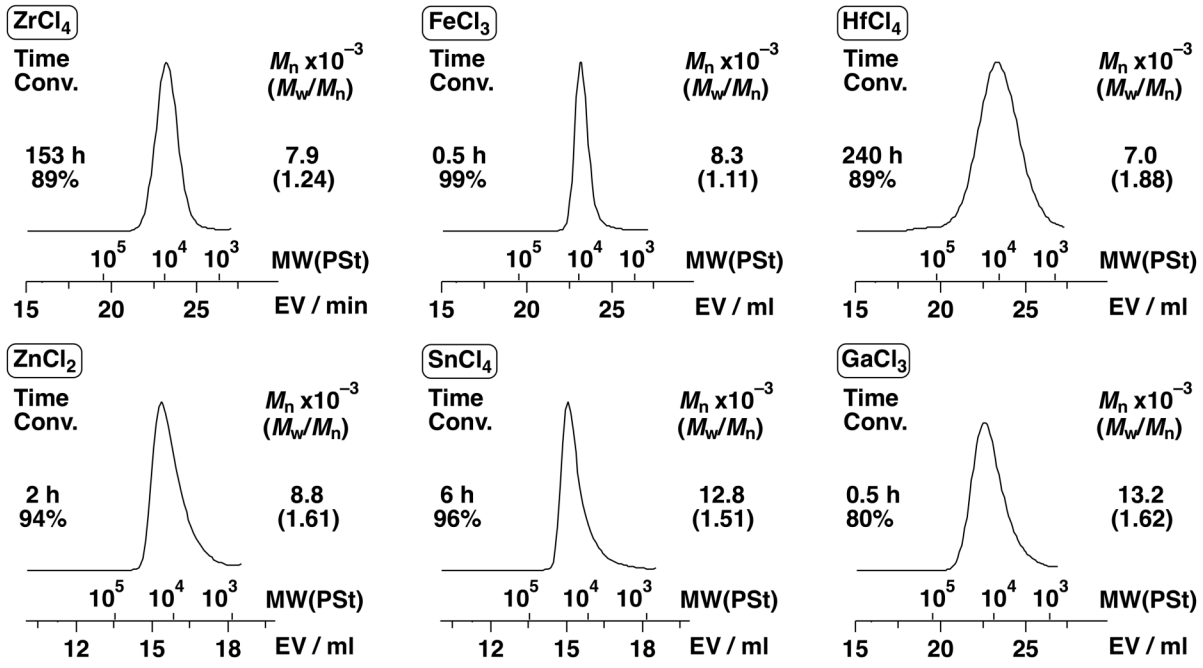

Figure 5. MWD curves of poly(IBVE)s obtained using the **1**/$ZrCl_4$ initiating system ($[IBVE]_0 = 0.76$ M, $[MCl_n]_0 = 5.0$ mM, $[\mathbf{1}]_0 = 5.0$ mM, [ethyl acetate] = 1.0 M, [heptane] = 5.0 vol% in toluene at 0 ºC).

^{1}H NMR analysis of complexation and polymerization by the isolated complex

^{1}H NMR analyses of the ligand alone, a mixture of the ligand and $ZrCl_4$, and a polymerization solution indicated the progress of complex formation, initiation, and polymerization (Figure 6). The spectrum of the solution containing **1** and ethyl acetate (Figure 6A) had signals corresponding to the imino (8.2 ppm) and aryl (7.2 and 6.9 ppm) protons at low magnetic fields. The addition of $ZrCl_4$ to **1** resulted in the appearance of complicated signals, indicating the occurrence of a reaction between **1** and $ZrCl_4$. In particular, several signals, which are likely assignable to the imino protons of the protonated nitrogen atom species (-C*H*=N(H)-), appeared at 8–12 ppm.[16] The complicated spectrum suggests that the salen framework was in several conformational states at this stage.[14] The addition of IBVE to the **1**/$ZrCl_4$ solution resulted in the disappearance of several signals (Figure 6C) likely because the consumption of HCl in the initiation reaction transformed several states of the salen framework in the equilibrium to the rigid complex state. The signal assigned to the methine proton at the propagating C–Cl ends (5.8ppm) also indicates that the polymerization began via the mechanism involving HCl formation in the exchange reaction between the chloride anion and phenoxy group of the metal chloride and ligand **1**, respectively.

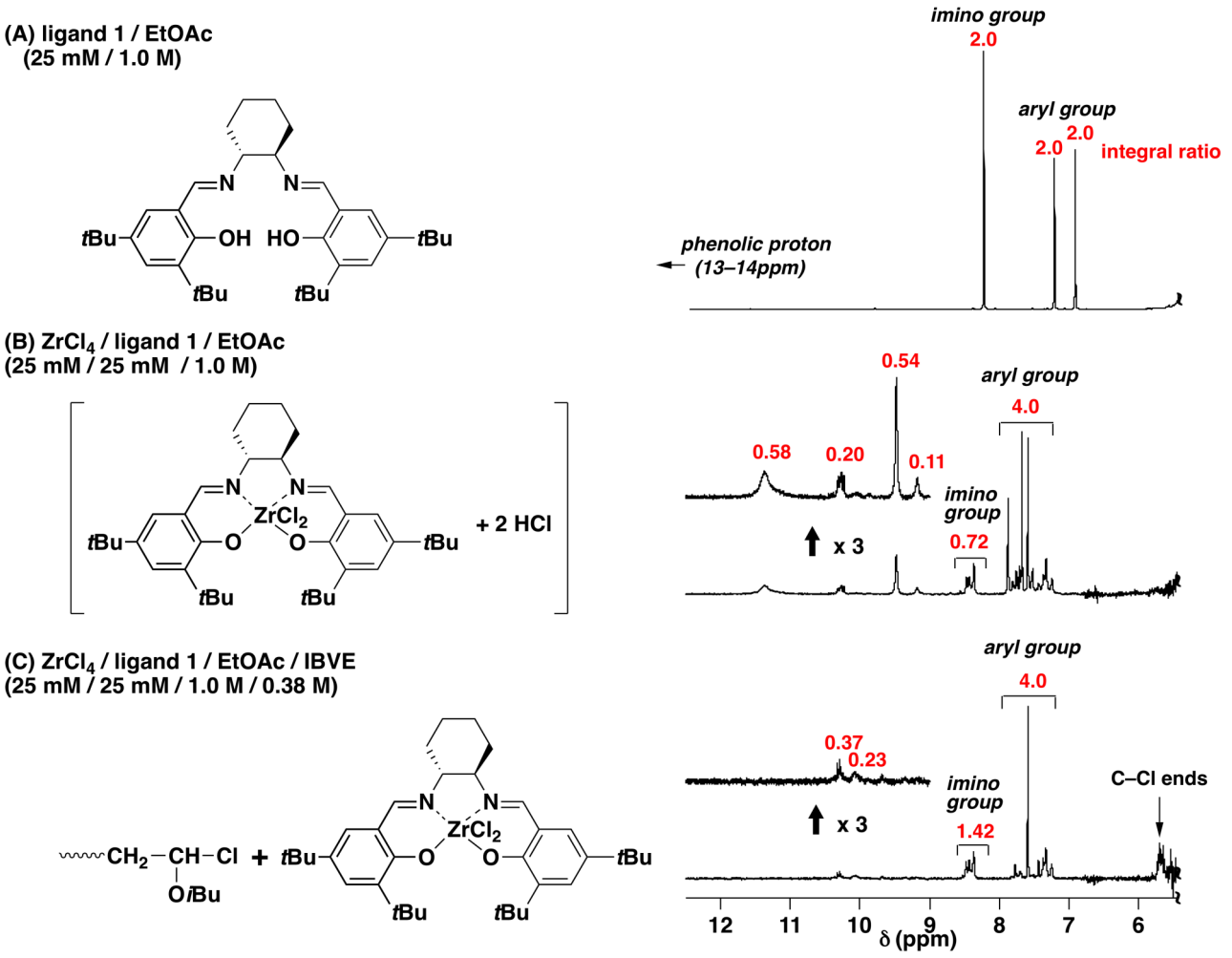

Figure 6. ^{1}H NMR spectra of (A) a ligand 1, (B) the mixture of **1** and $ZrCl_4$ and (C) polymerization solutions using the **1**/$ZrCl_4$ initiating system ($[IBVE]_0$ = 0 or 0.38 M, $[ZrCl_4]_0$ = 0 or 25 mM, $[\mathbf{1}]_0$ = 0 or 25 mM, [ethyl acetate] = 1.0 M; 500 MHz in CD_2Cl_2 at 30 ºC).

A **1**–$ZrCl_2$ complex isolated by recrystallization exhibited a catalytic activity similar to that of the complex generated *in situ* in the **1**/$ZrCl_4$ system in the polymerization of IBVE. The salen complex was prepared by the reaction of **1** and $ZrCl_4$ in a manner similar to the *in situ* method and subsequently recrystallized from the solution by the addition of hexane as a poor solvent. The crystalline products were isolated by filtration, washed, and then dried under reduced pressure. The isolated **1**–$ZrCl_2$ complex was used for the cationic polymerization of IBVE in conjunction with IBVE–HCl as a cationogen under the same conditions as those used for the polymerization by the *in situ* method. The polymerization proceeded at the same rate as that of the *in situ* generated system (Figure 7). In addition, the M_n values of the product polymers increased linearly with the conversion, although the values were slightly smaller than the theoretical values. Residual HCl in the isolated complex may be responsible for the lower values. The results obtained by using the isolated complex suggests that the **1**–$ZrCl_2$ complex is generated, even by the *in situ* generated method.

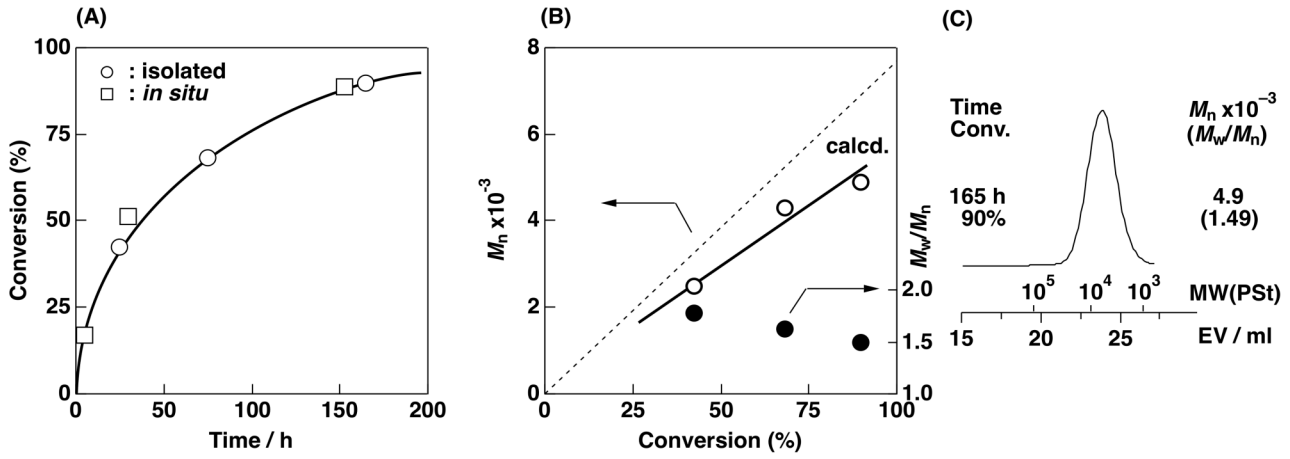

Figure 7. (A) Time–conversion curve of the polymerization, (B) M_n (dotted line: calculated line) and M_w/M_n values, and (C) MWD curves of poly(IBVE) obtained using the **1**–$ZrCl_2$ complex ($[IBVE]_0$ = 0.76 M, $[IBVE\text{-}HCl]_0$ = 10 mM, $[\mathbf{1}\text{–}ZrCl_2]_0$ = 5.0 mM, [ethyl acetate] = 1.0 M, [heptane] = 5.0 vol% in toluene at 0 ºC).

Cationic polymerization of IBVE with substituted salen ligands/$ZrCl_4$ systems

Salen derivatives with different substituents on the phenoxy groups were investigated in polymerization by the *in situ* method. Dichloromethane was used as the solvent instead of toluene because of the low solubility of the derivatives in toluene and/or the low catalytic activity of the complexes formed (Table 2). The polymerizations of IBVE were conducted using the substituted salen ligand/$ZrCl_4$ systems in the presence of ethyl acetate at 0 ºC. Even in the polar solvent, the **3**/$ZrCl_4$ system generated precipitates. The polymerization proceeded slowly, reaching quantitative conversion in 99 h (entry 2). The rate was much slower than that with the **1**/$ZrCl_4$ system (entry 1). In addition, no polymerization occurred for the combination of $ZrCl_4$ and **4**, a salen possessing a piperidinyl group. The strong nucleophilic group likely suppressed the polymerization reaction through deactivation of the catalyst, reaction with the propagating carbocation, or inhibition of the initiation reaction.

Table 2. Cationic polymerization of IBVE using $ZrCl_4$ and salen ligands with substituted salicyl groups[a]

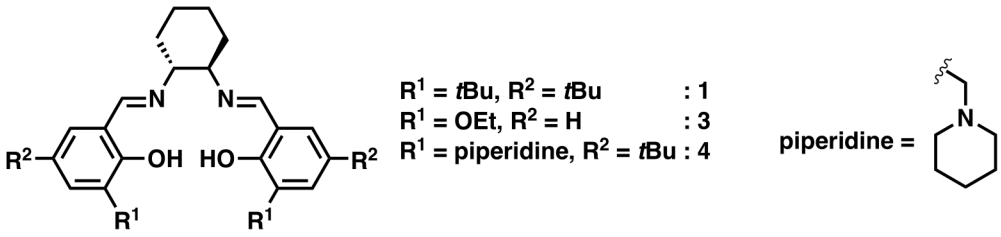

entry	ligand	time (h)	conv (%)[b]	$M_n \times 10^{-3}$ (calcd)[c]	$M_n \times 10^{-3}$ (obs)[d]	M_w/M_n[d]	catalytic solution
1	**1**	1.5	78	6.0	5.7	1.73	transparent
2	**3**	99	100	7.6	5.1	1.38	heterogeneous
3	**4**	216	0	-	-	-	transparent

[a] $[IBVE]_0$ = 0.76 M, $[ZrCl_4]_0$ = 5.0 mM, $[ligand]_0$ = 5.0 mM, [ethyl acetate] = 0.10 M, [heptane] = 5.0 vol% in dichloromethane at 0 ºC. [b] Determined by gas chromatography. [c] Based on the amounts of ligands. [d] Determined by GPC (polystyrene standards).

Conclusion

The controlled cationic polymerization of IBVE was achieved by using the **1**/$ZrCl_4$ initiating system in the presence of ethyl acetate in toluene at 0 ºC. Comparison of the **1**/$ZrCl_4$ and **2**/$ZrCl_4$ systems indicated that the complex structure was crucial for the catalytic activity. The polymerization performed with the salen system proceeded at an approximately ten times slower rate than that of the salphen system. However, ligand **1** provided an appropriate catalytic environment for Fe species and catalyzed the controlled polymerization of IBVE, which is in contrast to the **2**/$FeCl_3$ initiating system. In addition, salen-type ligands with different substituents were also employed in the polymerization in conjunction with $ZrCl_4$.

References

1. Yoon, T. P.; Jacobsen, E. N. *Science* **2003**, *299*, 1691-1693.
2. (a) Atwood, D. A.; Harvey, M. J. *Chem. Rev.* **2001**, *101*, 37–52. (b) Katsuki, T. *Synlett* **2003**, *3*, 281–297. (c) Cozzi, P.G. *Chem. Soc. Rev.* **2004**, *33*, 410–421. (d) Katsuki, T. *Chem. Soc. Rev.* **2004**, *33*, 437–444. (e) Darensbourg, D. J.; Mackiewicz, R. M.; Phelps, A. L.; Billodeaux, D. R. *Acc. Chem. Res.* **2004**, *37,* 836–844. (f) Venkataramanan, N. S.; Kuppuraj, G.; Rajagopal, S. *Coord. Chem. Rev.* **2005**, *249*, 1249–1268. (g) McGarrigle, E. M.; Gilheany, D. G. *Chem. Rev.* **2005**, *105*, 1563–1602. (h) Baleizao, C.; Garcia, H. *Chem. Rev.* **2006**, *106*, 3987–4043. (i) Matsumoto, K.; Saito, B.; Katsuki, T. *Chem. Commun.* **2007**, *35*, 3619–3627. (j) Darensbourg, D. J. *Chem. Rev.* **2007**, *107*, 2388–2410.
3. Zhang, W.; Loebach, J. L.; Wilson, S. R.; Jacobsen, E. N. *J. Am. Chem. Soc.* **1990**, *112*, 2801–2803.
4. Irie, R.; Noda, K.; Ito, Y.; Matsumoto, N.; Katsuki, T. *Tetrahedron Lett.* **1990**, *31*, 7345–7348.
5. (a) Sawamoto, M. *Prog. Polym. Sci.* **1991**, *16,* 111–172. (b) Aoshima, S.; Kanaoka, S. *Chem. Rev.* **2009**, *109*, 5245–5287.
6. (a) Kamigaito, M.; Sawamoto, M.; Higashimura, T. *Macromolecules* **1995**, *28*, 5671–5675. (b) Zhou, Y.; Faust, R.; Chen, S.; Gido, S. P. *Macromolecules* **2004**, *37*, 6716–6725. (c) Zhou, Y.; Faust, R. *Polym. Bull.* **2004**, *52*, 421–428. (d) Hadjikyriacou, S.; Faust, R. *Macromolecules* **1996**, *29*, 5261–5267.
7. (a) Kanazawa, A.; Kanaoka, S.; Aoshima, S. *Macromolecules* **2010**, *43*, 2739–2747. (b) Kanazawa, A.; Kanaoka, S.; Aoshima, S. *J. Polym. Sci., Part A: Polym. Chem.* **2010**, *48*, 2509–2516. (c) Kanaoka, S.; Nakayama, S.; Aoshima, S. *Kobunshi Ronbunshu* **2011,** *68,* 349–351.
8. (a) Ouchi, M.; Kamigaito, M.; Sawamoto, M. *Macromolecules* **1999**, *32*, 6407–6411. (b) Ouchi, M.; Kamigaito, M.; Sawamoto, M. *J. Polym. Sci., Part A: Polym. Chem.* **2001**, *39*, 1060–1066.
9. Sudhakar, P.; Vijayakrishna, K. *ChemCatChem* **2010**, *2*, 649–652.
10. Kigoshi, S.; Kanazawa, A.; Kanaoka, S.; Aoshima, S. *Polym. Chem.* **2015**, *6*, 30–34.
11. Kochnev, A. I.; Oleynik, I. I.; Oleynik, I.V.; Ivanchev, S. S.; Tolstikov, G. A. *Rus. Chem. Bull., Int. Ed.* **2007**, *56*, 1125–1129.
12. Kanazawa, A.; Kanaoka, S.; Aoshima, S. *J. Polym. Sci., Part A: Polym. Chem.* **2010**, *48*, 3702–3708.
13. Hansch, C.; Leo, A.; Taft, R. W. *Chem. Rev.* **1991**, *91*, 165–195.
14. Cuomo, C.; Strianese, M.; Cuenca, T.; Sanz, M.; Grassi, A. *Macromolecules* **2004**, *37*, 7469–7476.
15. Sanz, M.; Cuenca, T.; Cuomo, C.; Grassi, A. *J. Organomet. Chem.* **2006**, *691*, 3816–3822.
16. Strauch, J.; Warren, T. H.; Erker, G.; Frohlich, R.; Saarenketo, P. *Inorg. Chim. Acta* **2000**, *300–302*, 810–821.

Part II

Catalytic Structure–Property Relationship of Complex Catalysts in Cationic Polymerization Using Initiating Systems Consisting of Bidentate Schiff Base Ligands and Metal Chlorides

Chapter 4

Appropriate Ligand Frameworks for Various Polymerization Systems

Introduction

The construction of metal complexes that provide effective catalytic environments through the design of ligands has contributed to the development of catalysts with various activities, the precise control of polymer structures, and the expansion of the monomer scope. In particular, the electronic features of the central metal and the steric demands of the metal coordination sphere can be carefully tuned using ligands with suitable electronic and steric properties. Indeed, extensive studies of ligand design for olefin polymerizations have allowed the precise synthesis of polymers with controlled molecular weights, degrees of branching, and tacticity; resulting in a remarkable improvement in the catalytic activity and broadening the scope of polymerizable monomers such as polar monomers.[1–3] Transition metal-catalyzed living radical polymerizations or ATRP using metal complexes with suitable redox potentials are excellent examples of reactions achieved through careful ligand design.[4–7]

In cationic polymerizations, the screening of ligand frameworks is expected to be helpful not only for elucidating the relationship between the structures and catalytic properties of metal complex catalysts but also for the development of new catalysts with attractive properties such as remarkably high reactivity and stereoselectivity. General criteria for ligand design are needed to achieve desirable catalytic activities. A few successful examples of ligand design in cationic polymerization include $Ti(OR)_nCl_{4-n}$ for living polymerizations in the absence of additives;[8,9] alcohols and acac/MCl_n initiating system for living polymerizations;[10,11] and $TiCl_2(OAr)_2$ catalysts and aminodiolate-based titanium catalysts for stereoselective polymerizations.[12,13] However, the relationship between ligand structures and catalytic properties has not been sufficiently elucidated in the field of cationic polymerization. The limitations of ligand designs, which stem from the deactivation of catalysts or propagating carbocations by strong electron-donating ligands,[14–16] has prevented the development of criteria for ligand design in cationic polymerization. A methodical approach to catalyst design is expected to help elucidate the structure–reactivity relationship in cationic polymerization catalysts.

In this chapter, the author aims to conduct ligand screening for the design of catalysts that exhibit characteristic cationic polymerization activities. Salphen- and salen-type ligands are demonstrated to be effective for living cationic polymerization of vinyl ethers (VEs) in Chapters 2 and 3. Thus, bidentate [*N*,*O*]-type phenoxyimine ligands (**1**, **9**–**16**), which have similar structures to salphen- or salen-type tetradentate [*O*,*N*,*N*,*O*] chelating ligands, are examined as a ligand framework for catalyst modifications. Moreover, [*O*,*O*]-type salicylate derivatives (**2**, **3**) and [*N*,*N*]-type pyridineimine ligands (**7**) are designed based on phenoxyimine ligands. Diacetamide derivatives (**4**–**6**), which have structures similar to

acetylacetone,[11] are also employed as [*O*,*O*]-type ligands. In addition, a bidentate [*N*,*N*]-type α-diimine (**8**) is used as a typical pyridineimine ligand for comparison. These ligand frameworks with oxygen and/or nitrogen atoms as coordination sites are screened in combination with $ZrCl_4$ via *in situ* complexation for cationic polymerization of IBVE.

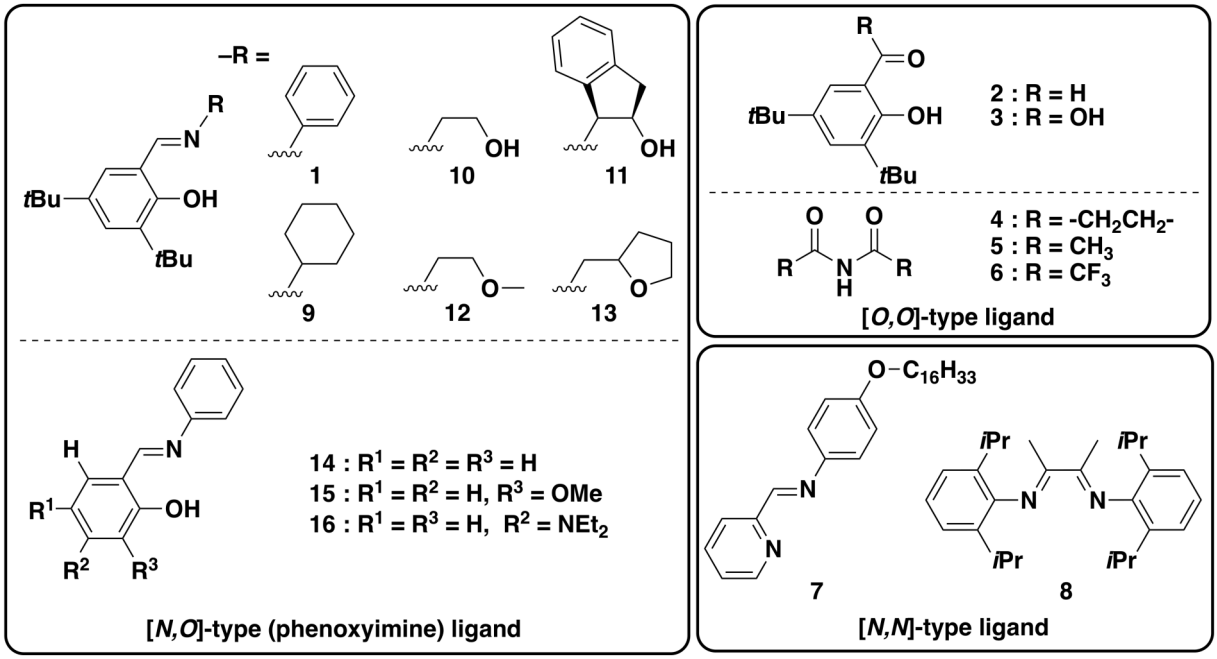

Figure 1. Structures of various ligand frameworks related to this chapter.

Experimental

Materials

Isopropyl VE (IPVE; Wako; 97.0+%) and ethyl VE (EVE; TCI; >98.0%) were washed with 10% aqueous sodium hydroxide solution, followed by water, and then distilled twice over calcium hydride. *p*-Methoxystyrene (pMOS; Wako; >97.0%) was dried over sodium sulfate overnight and distilled twice over calcium hydride under reduced pressure. Succinimide (TCI; >98.0%), diacetamide (TCI; >98.0%), bistrifluoroacetamide (TCI; >98.0%), (1*R*,2*S*)-1-(3,5-di-*tert*-butylsalicylideneamino)-2-indanol (Aldrich; 97%) and 3,5-di-*tert*-butylsalicylaldehyde (Aldrich; 99%) were used as received. 3,5-Di-*tert*-butyl-salicylicacid (Aldrich; 97%), and salicylideneaniline (Aldrich; 97%) were recrystallized from hexane. Other materials were prepared and used as described in Chapters 2 and 3.

Synthesis

N-Phenyl-3,5-di-*tert*-butylsalicylideneamine (1)

Aniline (0.94g, 101 mmol) was added to a methanol solution of 3,5-di-*tert*-butylsalicylaldehyde (2.37 g, 101 mmol) while stirring under a nitrogen atmosphere at room temperature. The mixed solution was

refluxed for 6 h, and the reaction mixture was then cooled to room temperature. After filtration, the solid fraction was washed with cold methanol and dried under reduced pressure. Furthermore, the obtained solid was purified by recrystallization from hexane to mainly remove residual methanol. The crystalline orange solid was filtered and then dried under reduced pressure (2.25 g, 72.7 mmol, 72% yield). ^{1}H NMR (500 MHz, $CDCl_3$, 30 °C): δ 13.68 (1H, s, O*H*), 8.63 (1H, s, N=C*H*), 7.46 (1H, d, *J* = 2.9 Hz, C*H*-phenol), 7.42–7.38 (2H, m, C*H*-aniline), 7.30–7.23 (3H, m, C*H*-aniline), 7.22 (1H, d, *J* = 2.4 Hz, C*H*-phenol), 1.48, 1.33 (9H each, s, C(CH_3)$_3$). ^{13}C NMR (100 MHz, $CDCl_3$, 30 °C): δ 163.8 (N=*C*H), 158.3 (*C*-OH), 148.8 (*ipso*-aniline), 140.6, 137.0, 118.3 (*ipso*-phenol), 128.0, 126.8 (phenol), 129.3, 126.5, 121.2 (aniline), 35.1, 34.2 (*C*(CH_3)$_3$), 31.5, 29.5 (C(*C*H_3)$_3$).

***N*-(4-Hydroxyphenyl)-pyridineamine**

A procedure similar to that described for ligand **1** but with the use of 4-hydroxyaniline (0.80 g, 49.9 mmol) and 3,5-di-*tert*-butylsalicylaldehyde (1.17 g, 49.9 mmol) gave a yellow solid. (1.11 g, 29.4 mmol, 59% yield). ^{1}H NMR (500 MHz, DMSO-d_6, 30 °C): δ 9.61 (1H, s, O*H*), 8.69 (1H, m, C*H*-pyridine), 8.60 (1H, s, N=C*H*), 8.12 (1H, m, C*H*-pyridine), 7.92 (1H, m, C*H*-pyridine), 7.48 (1H, m, C*H*-pyridine), 7.30 (2H, m, C*H*-phenol), 6.83 (2H, m, C*H*-phenol).

***N*-(4-Hexadecanoxyphenyl)-pyridineamine (7)**

N-(4-Hydroxyphenyl)-pyridineamine (0.92 g, 4.63 mmol), 1-bromohexadecane (1.42 g, 4.64 mmol), KOH (0.31 g, 5.47 mmol) and NaI (about 10 mg) were mixed in DMF (20 ml). The mixture was stirred at 70 ºC overnight. After solvent was evaporated, the obtained black oil was dissolved in CH_2Cl_2 and then washed several times with 0.10 M NaOH aq. and water. The organic layer was dried over magnesium sulfate. After filtration, the solvent was evaporated. The product was recrystallized from hexane (1.14 g, 2.70 mmol, 58%yield). ^{1}H NMR (500 MHz, $CDCl_3$, 30 °C): δ 8.70 (1H, m, C*H*-pyridine), 8.63 (1H, s, N=C*H*), 8.19 (1H, m, C*H*-pyridine), 7.80 (1H, m, C*H*-pyridine), 7.36–7.30 (3H, m, C*H*-pyridine and C*H*-phenol), 6.94 (2H, m, C*H*-phenol), 3.98 (2H, t, OCH_2), 1.80 (2H, m, OCH_2CH_2), 1.50–1.20 (26H, m, CH_2), 0.88 (3H, t, CH_3). ^{13}C NMR (100 MHz, $CDCl_3$, 30 °C): δ 158.1 (N=*C*H), 158.6, 143.5 (*ipso*-aniline), 155.0 (*ipso*-pyridine), 149.6, 121.6, 124.7, 136.6 (pyridine), 115.1, 122.7 (aniline), 68.3 (O*C*H_2), 31.9 (OCH_2CH_2), 29.7, 29.6, 29.4, 29.3, 26.1 (*C*H_2), 22.7 (*C*H_2CH_3), 14.1 (CH_2CH_3).

***N*, *N*′-Bis-(2,6-diisopropylphenyl)-2,3-butanediimine (8)**

A procedure similar to that described for ligand **1** but with the use of diacetyl (0.41 g, 4.79 mmol) and 2,6-di-isopropylaniline (1.70 g, 9.60 mmol) gave a yellow solid (0.68 g, 1.69 mmol, 35% yield). ^{1}H NMR (400 MHz, $CDCl_3$, 30 °C): δ 6.20–6.07 (6H, m, C*H*-aryl), 1.73 (4H, m, C*H*(CH_3)$_2$), 1.08 (6H, s, CCH_3), 0.20 (24H, m, CH(CH_3)$_2$). ^{13}C NMR (100 MHz, $CDCl_3$, 30 °C): ^{13}C NMR (100 MHz, $CDCl_3$, 30 °C): δ 168.2 (N=*C*H), 146.2, 135.1 (*ipso*-aniline), 123.0, 123.7 (aniline), 28.5 (*C*H(CH_3)$_2$), 23.0, 22.7 (CH(*C*H_3)$_2$), 16.6 (C*C*H_3).

_N_-Cyclohexyl-3,5-di-*tert*-butylsalicylideneamine (9)

A procedure similar to that described for ligand **1** but with the use of cyclohexylamine (0.50 g, 5.04 mmol) and 3,5-di-*tert*-butylsalicylaldehyde (1.18 g, 5.03 mmol) gave a yellow solid (1.32 g, 4.18 mmol, 83% yield). ^{1}H NMR (500 MHz, $CDCl_3$, 30 °C): δ 14.02 (1H, s, O*H*), 8.37 (1H, s, N=C*H*), 7.36 (1H, d, *J* = 2.5 Hz, C*H*-phenol), 7.07 (1H, d, *J* = 2.5 Hz, C*H*-phenol), 2.00–1.25 (10H, m, CH_2-cyclohexane), 1.45, 1.30 (9H each, s, C(CH_3)$_3$). ^{13}C NMR (100 MHz, $CDCl_3$, 30 °C): δ 163.3 (N=*C*H), 158.3 (*C*-OH), 139.8, 136.7, 118.0 (*ipso*-phenol), 126.5, 125.7 (phenol), 67.6, 34.4, 25.6, 24.5 (cyclohexane), 35.0, 34.1 (*C*(CH$_3$)$_3$), 31.5, 29.5 (C(*C*H$_3$)$_3$).

_N_-Hydroxyethyl-3,5-di-*tert*-butylsalicylideneamine (10)

A procedure similar to that described for ligand **1** but with the use of ethanolamine (0.31 g, 4.99 mmol) and 3,5-di-*tert*-butylsalicylaldehyde (1.19 g, 5.08 mmol) gave a yellow solid (0.78 g, 2.82 mmol, 57% yield). ^{1}H NMR (500 MHz, $CDCl_3$, 30 °C): δ 13.53 (1H, s, O*H*), 8.42 (1H, s, N=C*H*), 7.39 (1H, d, *J* = 3.0 Hz, C*H*-phenol), 7.11 (1H, d, *J* = 3.0 Hz, C*H*-phenol), 3.93 (2H, q, OCH_2), 3.75 (2H, t, NCH_2), 1.44, 1.31 (9H each, s, C(CH_3)$_3$). ^{13}C NMR (100 MHz, $CDCl_3$, 30 °C): δ 168.1 (N=*C*H), 158.0 (*C*-OH), 140.2, 136.7, 117.8 (*ipso*-phenol), 127.1, 126.1 (phenol), 61.8 (N*C*H$_2$), 62.3 (*C*H$_2$-OH), 35.0, 34.1 (*C*(CH$_3$)$_3$), 31.5, 29.4 (C(*C*H$_3$)$_3$).

_N_-Methoxyethyl-3,5-di-*tert*-butylsalicylideneamine (12)

A procedure similar to that described for ligand **1** but with the use of 2-methoxyethylamine (0.38 g, 5.06 mmol) and 3,5-di-*tert*-butylsalicylaldehyde (1.18 g, 5.02 mmol) gave a yellow solid (1.36 g, 4.66 mmol, 93% yield). ^{1}H NMR (400 MHz, $CDCl_3$, 30 °C): δ 13.70 (1H, s, O*H*), 8.37 (1H, s, N=C*H*), 7.37 (1H, d, *J* = 2.8 Hz, C*H*-phenol), 7.08 (1H, d, *J* = 2.4 Hz, C*H*-phenol), 3.75 (2H, t, CH_2), 3.67 (2H, t, CH_2), 3.31 (3H, s, OCH_3) 1.44, 1.30 (9H each, s, C(CH_3)$_3$). ^{13}C NMR (100 MHz, $CDCl_3$, 30 °C): δ 167.4 (N=*C*H), 158.1 (*C*-OH), 140.0, 136.6, 117.9 (*ipso*-phenol), 126.9, 126.0 (phenol), 72.0 (O*C*H$_2$), 59.0, 59.1 (N*C*H$_2$ and O*C*H$_3$), 35.0, 34.1 (*C*(CH$_3$)$_3$), 31.5, 29.5 (C(*C*H$_3$)$_3$).

_N_-Tetrahydrofurfuryl-3,5-di-*tert*-butylsalicylideneamine (13)

A procedure similar to that described for ligand **1** but with the use of tetrahydrofurfurylamine (0.51 g, 5.04 mmol) and 3,5-di-*tert*-butylsalicylaldehyde (1.18 g, 5.04 mmol) gave an oil. After filtration, the oil was dried under reduced pressure (0.84 g, 2.65 mmol, 53% yield). ^{1}H NMR (400 MHz, $CDCl_3$, 30 °C): δ 13.71 (1H, s, O*H*), 8.37 (1H, s, N=C*H*), 7.37 (1H, d, *J* = 2.4 Hz, C*H*-phenol), 7.09 (1H, d, *J* = 2.4 Hz, C*H*-phenol), 3.75 (1H, m, OC*H*), 3.90–3.72 (2H, m, OCH_2), 3.68 (2H, m, NCH_2) 2.11–1.70 (4H, m, CH_2-furfulyl), 1.44, 1.30 (9H each, s, C(CH_3)$_3$). ^{13}C NMR (100 MHz, $CDCl_3$, 30 °C): δ 167.4 (N=*C*H), 158.2 (*C*-OH), 139.9, 136.6, 117.9 (*ipso*-phenol), 126.9, 126.0 (phenol), 78.2 (O*C*H), 68.4 (O*C*H$_2$), 63.6 (N*C*H$_2$), 35.0, 34.1 (*C*(CH$_3$)$_3$), 31.5, 29.4 (C(*C*H$_3$)$_3$), 29.3, 25.8 (*C*H$_2$-furfuryl).

_N_-Phenyl-3-methoxysalicylideneamine (15)

A procedure similar to that described for ligand **1** but with the use of aniline (0.47 g, 5.05 mmol)

and 3-methoxysalicylaldehyde (0.77 g, 5.04 mmol) gave an orange crystal (0.54 g, 2.36 mmol, 47% yield). ^{1}H NMR (400 MHz, $CDCl_3$, 30 °C): δ 13.66 (1H, s, O*H*), 8.63 (1H, s, N=C*H*), 7.42 (1H, m, C*H*-aryl), 7.31–7.26 (3H, m, C*H*-aryl), 7.04–6.97 (2H, m, C*H*-aryl), 6.88 (1H, t, C*H*-phenol), 3.94 (3H, s, OCH_3). ^{13}C NMR (100 MHz, $CDCl_3$, 30 °C): δ 162.6 (N=*C*H), 151.5 (*C*-OH), 148.6 (*ipso*-aniline), 148.2, 119.2 (*ipso*-phenol), 129.4, 121.2 (aniline), 127.0, 125.5, 103.8, 97.9 (aniline and phenol), 56.2 (O*C*H_3).

***N*-Phenyl-4-diethylaminosalicylideneamine (16)**

A procedure similar to that described for ligand **1** but with the use of aniline (0.47 g, 5.05 mmol) and 4-(diethylamino)salicylaldehyde (0.97 g, 5.03 mmol) gave an orange solid (0.99 g, 3.71 mmol, 74% yield). ^{1}H NMR (500 MHz, $CDCl_3$, 30 °C): δ 13.79 (1H, s, O*H*), 8.42 (1H, s, N=C*H*), 7.37 (2H, m, C*H*-aryl), 7.25–7.12 (4H, m, C*H*-aryl), 6.25 (1H, dd, *J* = 2.0, 8.5 Hz, C*H*-phenol), 6.19 (1H, d, *J* = 2.0 Hz, C*H*-phenol), 3.41 (4H, q, CH_2CH$_3$), 1.21 (6H, t, CH$_2$CH_3). ^{13}C NMR (100 MHz, $CDCl_3$, 30 °C): δ 160.5 (N=*C*H), 164.3 (*C*-OH), 148.9 (*ipso*-aniline), 151.9, 109.2 (*ipso*-phenol), 129.3, 120.8 (aniline), 133.7, 125.5, 103.8, 97.9 (aniline and phenol), 44.6 (*C*H$_2$CH$_3$), 12.7 (CH$_2$*C*H$_3$).

***N*-(2,6-Di-methylphenyl)- 3,5-di-*tert*-butylsalicylidene-amine (17)**

A procedure similar to that described for ligand **1** but with the use of 2,6-di-methylaniline (0.61 g, 5.06 mmol) and 3,5-di-*tert*-butylsalicylaldehyde (1.18 g, 5.05 mmol) gave a yellow solid (0.36 g, 1.08 mmol, 21% yield). ^{1}H NMR (500 MHz, $CDCl_3$, 30 °C): δ 13.43 (1H, s, O*H*), 8.33 (1H, s, N=C*H*), 7.48 (1H, d, *J* = 2.4 Hz, C*H*-phenol), 7.14 (1H, d, *J* = 2.4 Hz, C*H*-phenol), 7.08 (2H, m, C*H*-aniline), 7.00 (1H, m, C*H*-aniline), 2.21 (6H, s, Ar-CH_3), 1.49, 1.33 (9H each, s, C(CH_3)$_3$). ^{13}C NMR (100 MHz, $CDCl_3$, 30 °C): δ 167.7 (N=*C*H), 158.4 (*C*-OH), 148.4 (*ipso*-aniline), 140.4, 128.5, 137.2, 117.8 (*ipso*-phenol), 128.0, 126.6 (phenol), 128.3, 124.7 (aniline), 35.2, 34.2 (*C*(CH$_3$)$_3$), 31.5, 29.5 (C(*C*H$_3$)$_3$), 18.6 (Ar-*C*H$_3$).

***N*-(4-Trifluoromethylphenyl)-3,5-di-*tert*-butylsalicylideneamine (19)**

A procedure similar to that described for ligand **1** but with the use of 4-trifluoromethylaniline (0.80 g, 49.9 mmol) and 3,5-di-*tert*-butylsalicylaldehyde (1.17 g, 49.9 mmol) gave a yellow solid (1.11 g, 29.4 mmol, 59% yield). ^{1}H NMR (500 MHz, $CDCl_3$, 30 °C): δ 13.30 (1H, s, O*H*), 8.63 (1H, s, N=C*H*), 7.66 (2H, d, *J* = 8.6 Hz, C*H*-aniline), 7.50 (1H, d, *J* = 2.6 Hz, C*H*-phenol), 7.34 (2H, d, *J* = 8.3 Hz, C*H*-aniline), 7.24 (1H, d, *J* = 2.4 Hz, C*H*-phenol), 1.48, 1.34 (9H each, s, C(CH_3)$_3$). ^{13}C NMR (100 MHz, $CDCl_3$, 30 °C): δ 165.5 (N=*C*H), 158.4 (*C*-OH), 151.8 (*ipso*-aniline), 140.9, 137.2, 118.0 (*ipso*-phenol), 128.9, 127.2 (phenol), 128.3 (q, *J* = 32.4 Hz*, ipso*-aniline), 126.6 (q, *J* = 3.8 Hz, aniline), 121.5 (aniline), 124.2 (q, *J* = 270.3 Hz, *C*F$_3$) 35.1, 34.2 (*C*(CH$_3$)$_3$),, 31.4, 29.4 (C(*C*H$_3$)$_3$).

***N*-(Pentafluorophenyl)- 3,5-di-*tert*-butylsalicylideneamine (20)**

A procedure similar to that described for ligand **1** but with the use of pentafluoroaniline (0.85 g, 4.63 mmol) and 3,5-di-*tert*-butylsalicylaldehyde (1.18 g, 5.04 mmol) gave a solid (0.15 g, 0.37 mmol, 8% yield). ^{1}H NMR (500 MHz, $CDCl_3$, 30 °C): δ 12.70 (1H, s, O*H*), 8.81 (1H, s, N=C*H*), 7.54 (1H, d, *J* = 2.3 Hz, C*H*-phenol), 7.19 (1H, d, *J* = 2.4 Hz, C*H*-phenol), 1.47, 1.33 (9H each, s, C(CH_3)$_3$).

_N_-(4-Methoxyphenyl)-3,5-di-*tert*-butylsalicylideneamine (21)

A procedure similar to that described for ligand **1** but with the use of 4-methoxyaniline (0.62 g, 50.2 mmol) and 3,5-di-*tert*-butylsalicylaldehyde (1.18 g, 50.2 mmol) gave a yellow solid (1.17 g, 34.5 mmol, 69% yield). ^{1}H NMR (500 MHz, $CDCl_3$, 30 °C): δ 13.82 (1H, s, O*H*), 8.61 (1H, s, N=C*H*), 7.43 (1H, d, *J* = 2.1 Hz, C*H*-phenol), 7.26 (2H, d, *J* = 8.9 Hz, C*H*-aniline), 7.20 (1H, d, *J* = 2.7 Hz, C*H*-phenol), 6.93 (2H, d, *J* = 8.9 Hz, C*H*-aniline), 3.82 (3H, s, OCH_3), 1.48, 1.33 (9H each, s, C(CH_3)$_3$). ^{13}C NMR (100 MHz, $CDCl_3$, 30 °C): δ 161.8 (N=*C*H), 158.1 (*C*-OH), 158.6, 141.7 (*ipso*-aniline), 140.5, 136.9, 118.5 (*ipso*-phenol), 127.5, 126.5 (phenol), 114.6, 122.2 (aniline), 55.5 (O*C*H$_3$), 35.1, 34.2 (*C*(CH$_3$)$_3$), 31.5, 29.5 (C(*C*H$_3$)$_3$).

Polymerization Procedure

Cationic polymerization reactions were conducted in a similar manner to that described in Chapter 2.

Bulk polymerization of IBVE

A $ZrCl_4$ solution in dichloromethane was added to a ligand in dichloromethane, and the solution was then kept at 0 °C for at least 30 min to achieve quantitative complexation. The solvent of the resulting solution was evaporated under reduced pressure and then dried for 3 h. The polymerization was started by the addition of a monomer into a tube containing the solid catalyst without any solvents. The reaction was terminated by the addition of methanol containing a small amount of aqueous ammonia solution. The quenched reaction mixture was diluted with hexane and then washed with water. The volatile materials were then removed under reduced pressure.

Characterization

The MWD and NMR spectra of the polymers were determined as described in Chapters 2 and 3.

Results and Discussion

Cationic polymerization of IBVE using various ligand frameworks/$ZrCl_4$ initiating systems

Cationic polymerization of IBVE was examined via *in situ* complexation using $ZrCl_4$ and an *N*-phenyl phenoxyimine ligand (**1**), which is an [*N*,*O*]-type chelating ligand, in the presence of ethyl acetate in toluene at 0 °C (Table 1, entry 1). The catalyst was prepared *in situ* by adding $ZrCl_4$ to a solution of **1** in the presence of ethyl acetate in toluene/CH_2Cl_2 (4/5 v/v). To start the polymerization, the resulting transparent yellow solution was injected to a solution containing the monomer. The polymerization using the **1**/$ZrCl_4$ initiating system proceeded smoothly and reached a high conversion of IBVE (Figure 2A). The M_n values of the obtained polymers increased linearly with increasing monomer conversion. The polymers had relatively narrow molecular weight distributions (Figure 2B). Moreover, the first-order plot exhibited a linear increase (Figure 2A), indicating that the concentration of the propagating species was constant during polymerization. These results indicate that the polymerization proceeded in a highly controlled manner. However, the M_n values were lower than the calculated values (Table 1, entry 1), which indicates that excess amounts of initiation reactions occurred from protic impurities such as adventitious water.

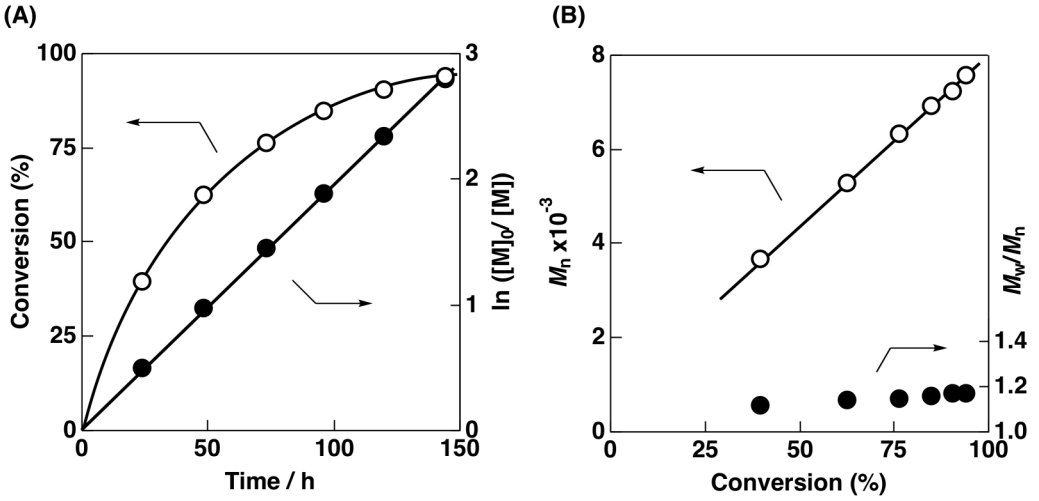

Figure 2. (A) Time–conversion curves and ln([M]$_0$/[M])–time plots of the polymerization, and (B) M_n and M_w/M_n values of poly(IBVE)s obtained using the **1**/$ZrCl_4$ initiating system ([IBVE]$_0$ = 0.76 M, [$ZrCl_4$]$_0$ = 5.0 mM, [**1**]$_0$ = 5.0 mM, [ethyl acetate] = 1.0 M, [heptane] = 5.0 vol% in toluene at 0 ºC).

Cationic polymerizations of IBVE using [*O*,*O*]-type ligands (**2**–**6**) and $ZrCl_4$ were conducted under similar conditions to those used for the polymerization using the [*N*,*O*]-type ligands. The results were categorized into the following two groups: ligands that functioned as proton donors (**2**, **3**, and **6**) and aprotic (**4** and **5**) (Table 1, entries 2–6). The **2** or **3**/$ZrCl_4$ systems initiated the reaction via the *in situ*-generated HCl. The cationic polymerizations then proceeded in a controlled manner and yielded polymers with M_n values corresponding to the amounts of hydroxy groups (including both the phenol moiety and the carboxylic group) (Table 1, entries 2 and 3). In the case of the diacetamide derivatives (**4**–**6**), the acidity of the N–H

Table 1. Cationic polymerization of IBVE using $ZrCl_4$ and various ligand frameworks[a]

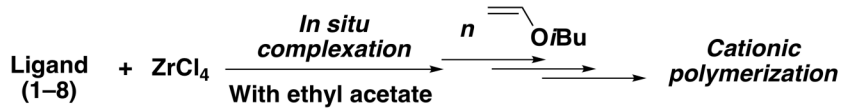

entry	ligand	[ethyl acetate] (M)	time (h)	conv (%)[b]	$M_n \times 10^{-3}$ (calcd)[c]	$M_n \times 10^{-3}$ (obs)[d]	M_w/M_n[d]	meso dyad (%)[e]	catalytic solution
1	**1**	1.0	144	94	14.5	7.6	1.17	63	transparent
2	**2**	1.0	47	98	15.0	9.8	1.26	65	transparent
3	**3**	1.0	22	96	7.4[g]	5.0	1.70	64	transparent
4	**4**	1.0	8	84	12.9	23.7	1.13	–	transparent
5	**5**	0.1	6	89	13.7	30.4	1.13	–	heterogeneous
6	**6**	1.0	22	96	14.6	9.7	1.18	65[h]	transparent
7[f]	**7**	0.1	144	98	15.1	7.3	1.38	65	heterogeneous
8[f]	**8**	1.0	7	97	14.9	7.2	1.14	66	transparent
9	–	1.0	22	98	–	20.6	1.13	66	transparent

[a] $[IBVE]_0$ = 0.76 M, $[ZrCl_4]_0$ = 5.0 mM, $[ligand]_0$ = 5.0 mM, [heptane] = 5.0 vol% in toluene at 0 ºC. [b] Determined by gas chromatography. [c] Based on the amounts of ligands or IBVE–HCl. [d] Determined by GPC (polystyrene standards). [e] Determined by ^{13}C NMR analysis. [f] $[IBVE–HCl]_0$ = 5.0 mM. [g] Based on the amounts of hydroxy groups ($[HCl]_{theoretical} = 2 \times [\mathbf{3}]_0$ = 10 mM). [h] The value of the polymer obtained at a different polymerization time: time = 4 h, conv. = 44%, $M_n = 3.8 \times 10^3$.

bond was a key factor for initiating the reaction through the *in situ*-generated HCl.[18] In comparison with the polymerization using $ZrCl_4$ without a cation donor (Table 1, entry 9), ligand **6**, which has an electron-withdrawing group (CF_3), was found to function as a cation donor, while ligands **4** and **5**, which do not have electron-withdrawing groups, were completely ineffective as a proton source (Table 1, entries 4–6). Thus, a phenol-type ligand framework, such as those of **1**–**3** and relatively acidic diacetamide compounds such as **6**, were served as proton sources in the *in situ* complexation method.

Bidentate [*N,N*]–type ligands (**7** and **8**) were also found to function efficiently, although the use of a protic ligand was required for the controlled cationic polymerization of IBVE (Table 1, entries 7 and 8). Ligands **7** and **8** did not possess protons that can be liberated through complexation with a metal chloride; hence, IBVE–HCl was used as the proton source in the polymerization. The mixture of $ZrCl_4$ and **7** became a heterogeneous system and induced an IBVE polymerization reaction that proceeded slowly. The combination of $ZrCl_4$ and **8** generated a transparent deep red solution. The red color gradually disappeared after the addition of the complex solution to a solution containing IBVE and ethyl acetate, which indicates that the state of the complex derived from $ZrCl_4$ and **8** changed when it initiated the reaction. Moreover, the polymerization using **8** proceeded at a relatively high rate. The neutral ligand and metal chloride form an association-dissociation equilibrium; hence, free $ZrCl_4$ likely catalyzed the polymerization instead of the poorly soluble catalyst complex generated from $ZrCl_4$ and **7** or the low-activity catalyst complex generated from $ZrCl_4$ and **8**. The selection of a metal with a high affinity for a nitrogen is likely important for using [*N,N*]-type ligand frameworks.

Cationic polymerization of IBVE using [*N*,*O*]-type phenoxyimine ligands/$ZrCl_4$ initiating systems

Polymerization behavior using [*N*,*O*]-type phenoxyimine ligands (**9**–**16**) was found to depend on the substituents attached to the phenol moiety. The mixtures of $ZrCl_4$ and [*N,O*]-type phenoxyimine ligands possessing *t*Bu groups on the phenol moiety (**9**–**13**) in toluene were transparent, while ligands with no substituent (**14**) or methoxy (**15**) or NEt_2 groups (**16**) generated precipitates in the presence of $ZrCl_4$. Controlled cationic polymerizations proceeded when **9**–**13**, phenoxyimines possessing *t*Bu groups on the phenol moiety, were used in conjunction with $ZrCl_4$ as the metal chloride (entries 1–5 in Table 2). In contrast, the use of phenoxyimine ligands with other substituents on the phenol moiety (**14**–**16**) resulted in uncontrolled polymerizations (entries 6–8). The solubility of the generated complexes was most likely responsible for the differences in their ability to control the reaction.

The substituents on the N atom also affected the polymerization reactions. The polymerization using an *N*-alkyl substituted ligand, **9**, instead of the *N*-aryl analog, **1**, is also effective for the polymerization via *in situ* complexation. In contrast, polymerizations using tridentate dianionic ligands, namely, **10** and **11**, produced polymers with M_n values lower than those of the polymers obtained using the **1**/$ZrCl_4$ system (Table 2, entries 2 and 3). The results indicate that the hydroxy groups of **10** and **11** most likely functioned as proton donors. In addition, tridentate monoanionic ligands with an ether pendant, namely, **12** and **13**, exerted significant deceleration effects (Table 2, entries 4 and 5). The polymerizations using these ligands proceeded at rates that were less than one sixth that of using **9**, which was likely due to the hemilability of the ether pendant of the ligands. Thus, [*N*,*O*]-type ligands with substituents that enhance solubility, reactivity, and quantitative initiation efficiency (Figure 3) were demonstrated to be useful for the controlled cationic polymerization using *in situ* complexation. ^{13}C NMR analysis of the obtained polymers, however, indicated a negligible difference in stereoselectivity.

Table 2. Cationic polymerization of IBVE using $ZrCl_4$ and various [*N,O*]-type ligands[a]

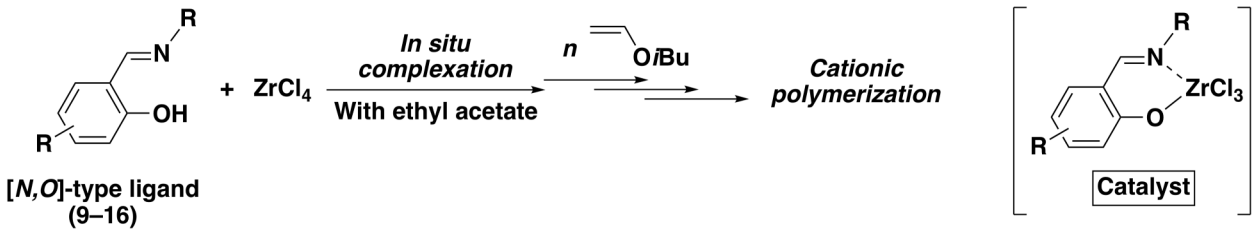

entry	ligand	time (h)	conv (%)[b]	$M_n \times 10^{-3}$ (calcd)[c]	$M_n \times 10^{-3}$ (obs)[d]	M_w/M_n[d]	meso dyad (%)[e]	catalytic solution
1	**9**	48	96	14.7	8.4	1.12	62	transparent
2	**10**	70	96	7.4[f]	5.5	1.20	65	transparent
3	**11**	144	94	7.2[f]	3.8	1.39	61	transparent
4	**12**	220	91	13.9	9.4	1.15	64	transparent
5	**13**	648	97	14.9	8.5	1.25	65	transparent
6	**14**	120	90	13.8	7.2	1.58	65	heterogeneous
7	**15**	72	94	14.5	4.6	1.55	65	heterogeneous
8	**16**	480	91	14.0	14.0	1.52	66	heterogeneous

[a] $[IBVE]_0 = 0.76$ M, $[ZrCl_4]_0 = 5.0$ mM, $[ligand]_0 = 5.0$ mM, [ethyl acetate] = 1.0 M, [heptane] = 5.0 vol% in toluene at 0 °C. [b] Determined by gas chromatography. [c] Based on the amounts of phenoxyimine ligands. [d] Determined by GPC (polystyrene standards). [e] Determined by ^{13}C NMR analysis. [f] Based on the amounts of hydroxy groups ($[HCl]_{theoretical} = 2 \times [ligand]_0 = 10$ mM).

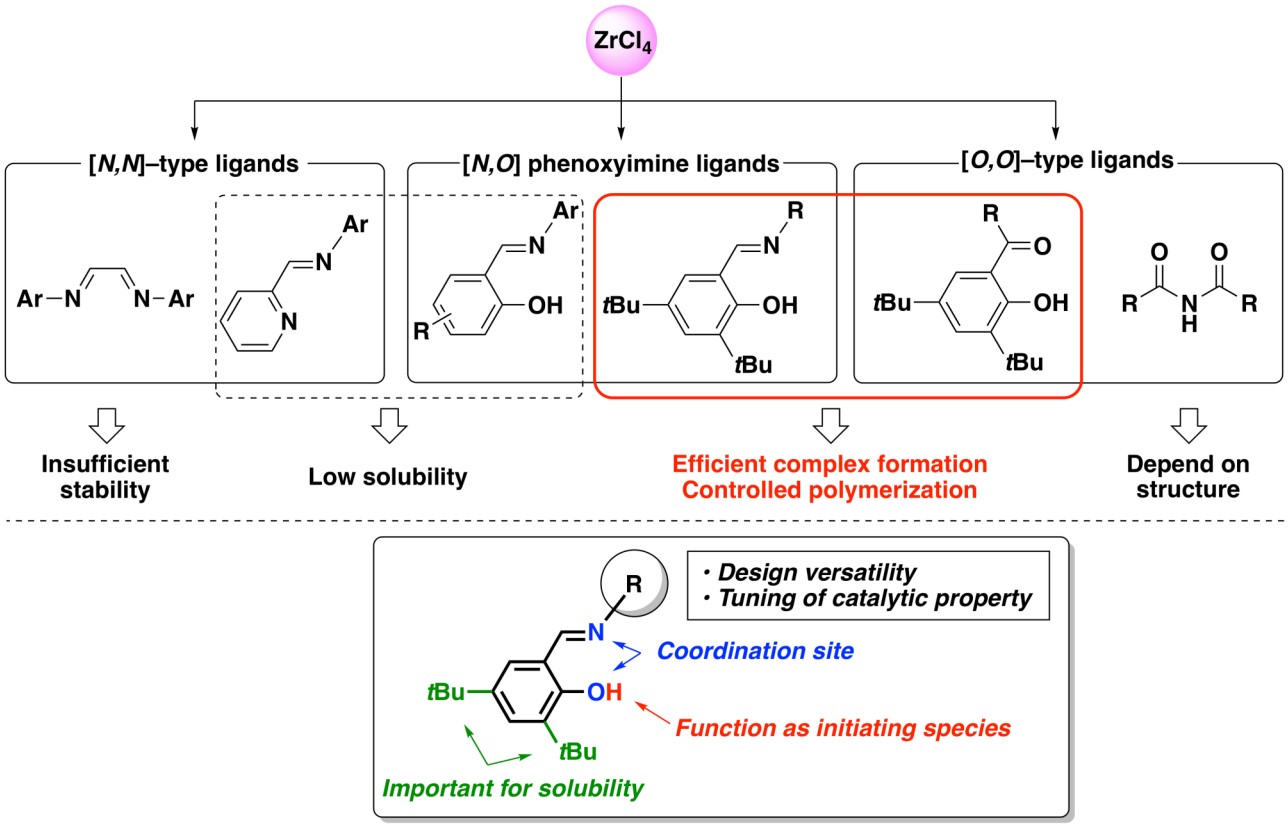

Figure 3. Summary of the polymerizations of IBVE using various ligand frameworks/$ZrCl_4$ initiating systems.

Investigation of appropriate combinations of *N*-phenyl phenoxyimine ligand and metal chlorides for controlled cationic polymerizations of IBVE

The use of $ZrCl_4$ as a metal chloride was indispensable for the controlled polymerization using *N*-phenyl phenoxyimine ligand in the presence of ethyl acetate, which was confirmed by the reactions using other metal chlorides (MCl_n: M = Ga, Zn, Ti, or Al). Transparent catalytic solutions were obtained from the combinations of **1** and various metal chlorides. Polymerization proceeded with the **1**/$GaCl_3$ and $ZnCl_2$ systems in the presence of ethyl acetate in toluene at 0 °C; however, the obtained polymers had broad MWDs (Table 3, entries 2 and 3). In addition, the M_n values of the polymers obtained from the **1**/$ZnCl_2$ systems were higher than the calculated values. The higher M_n values were likely the result of a lower proton source concentration (HCl) due to insufficient complex formation. Moreover, polymerization was extremely slow when $TiCl_4$ or $AlCl_3$ were used as the metal chlorides (Table 3, entries 4 and 6), indicating that complexes generated from **1** and $TiCl_4$ or $AlCl_3$ likely have very low catalytic activities. The large amount of ethyl acetate present in the mixture likely suppressed the activity of these Lewis acids. Indeed, the **1**/$TiCl_4$ system in the absence of ethyl acetate induced fast polymerization of IBVE although the polymerization proceeded in an uncontrolled manner (Table 5, entry 5). The polymerization using the **1**/$TiCl_4$ system is described below.

To examine the livingness of the polymerization, a monomer addition experiment was conducted using the **1**/$ZrCl_4$ initiating system. A fresh batch of IBVE was added into the polymerization solution when the monomer conversion reached 84%. The freshly added IBVE was smoothly polymerized to produce polymers with molecular weights that increased linearly with increasing monomer conversion (Figure 4). However, the MWD curves became broader slightly as the polymerization proceeded. These results indicate that the polymerization proceeded in a controlled manner.

Table 3. Cationic polymerization of IBVE using MCl_n and **1**[a]

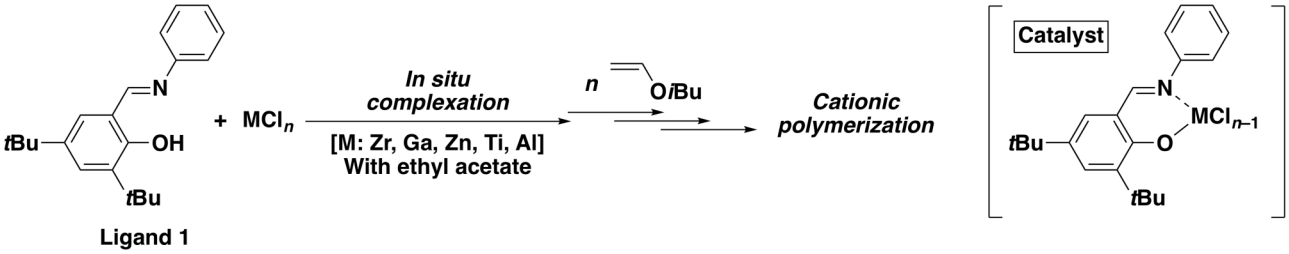

entry	MCl_n	time	conv (%)[b]	$M_n \times 10^{-3}$ (calcd)[c]	$M_n \times 10^{-3}$ (obs)[d]	M_w/M_n[d]	meso dyad (%)[e]
1	$ZrCl_4$	144 h	94	14.5	7.6	1.17	63
2	$GaCl_3$	5 min	98	15.0	14.5	2.47	62
3	$ZnCl_2$	25 h	96	14.7	33.6	2.10	62
4	$TiCl_4$	360 h	14	2.2	1.4	2.28	–
5[f]		3 h	100	15.3	9.0	5.16	65
6	$AlCl_3$	408 h	17	2.7	1.8	2.87	59

[a] $[IBVE]_0$ = 0.76 M, $[MCl_n]_0$ = 5.0 mM, $[\mathbf{1}]_0$ = 5.0 mM, [ethyl acetate] = 1.0 M, [heptane] = 5.0 vol% in toluene at 0 ºC. [b] Determined by gas chromatography. [c] Based on the amounts of **1**. [d] Determined by GPC (polystyrene standards). [e] Determined by ^{13}C NMR analysis. [f] Without ethyl acetate.

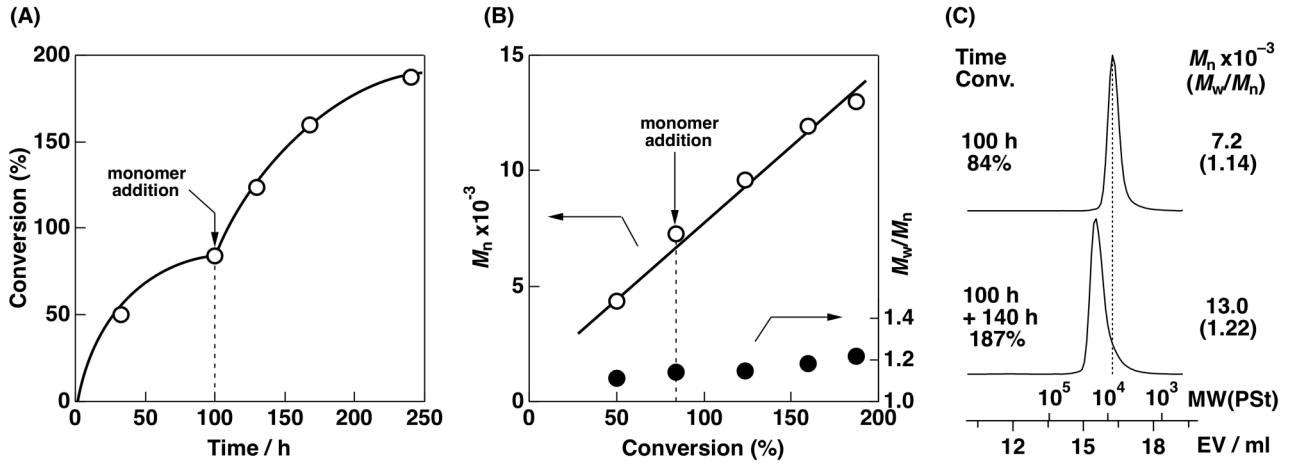

Figure 4. (A) Time–conversion curves for the polymerization, (B) M_n and M_w/M_n values, and (C) MWD curves for poly(IBVE)s obtained in the monomer-addition experiment using the **1**/$ZrCl_4$ initiating system ($[IBVE]_0$ = $[IBVE]_{added}$ = 0.76 M, $[ZrCl_4]_0$ = 5.0 mM, $[\mathbf{1}]_0$ = 5.0 mM, [ethyl acetate] = 1.0 M, [heptane] = 5.0 vol.% in toluene at 0 ºC).

The complex formation, initiation, and polymerization reaction using the **1**/$ZrCl_4$ system was examined by ^{1}H NMR spectroscopy (Figure 5). The spectrum of the solution containing **1** and ethyl acetate (Figure 5A) had signals attributable to the phenolic (13.9 ppm), imino (8.2 ppm), and aryl (7.5 and 6.9–7.2 ppm) protons. The addition of $ZrCl_4$ to **1** resulted in the appearance of two signals at approximately 11.7 and 10.3 ppm and a change in the chemical shifts of the signals of the aromatic region, indicating the occurrence of a reaction between **1** and $ZrCl_4$. The newly generated signals can likely be assigned to the imino protons (-C*H*=N(H)-, 10.3 ppm) and the protic species associated with the nitrogen atom (-CH=N(*H*)-, 11.7 ppm),[19] which indicates that an intermediate complex was generated in the mixture of **1** and $ZrCl_4$. The subsequent addition of IBVE to the **1**/$ZrCl_4$ solution resulted in the disappearance of these two signals (Figure 5C) probably because of the consumption of HCl in the initiation reaction pushed the complex formation to completion (Scheme 1A). The presence of the signal from the methine proton of the propagating -C*H*(OR)–Cl ends (5.8 ppm) also indicates that the polymerization started via an *in situ* complexation mechanism.

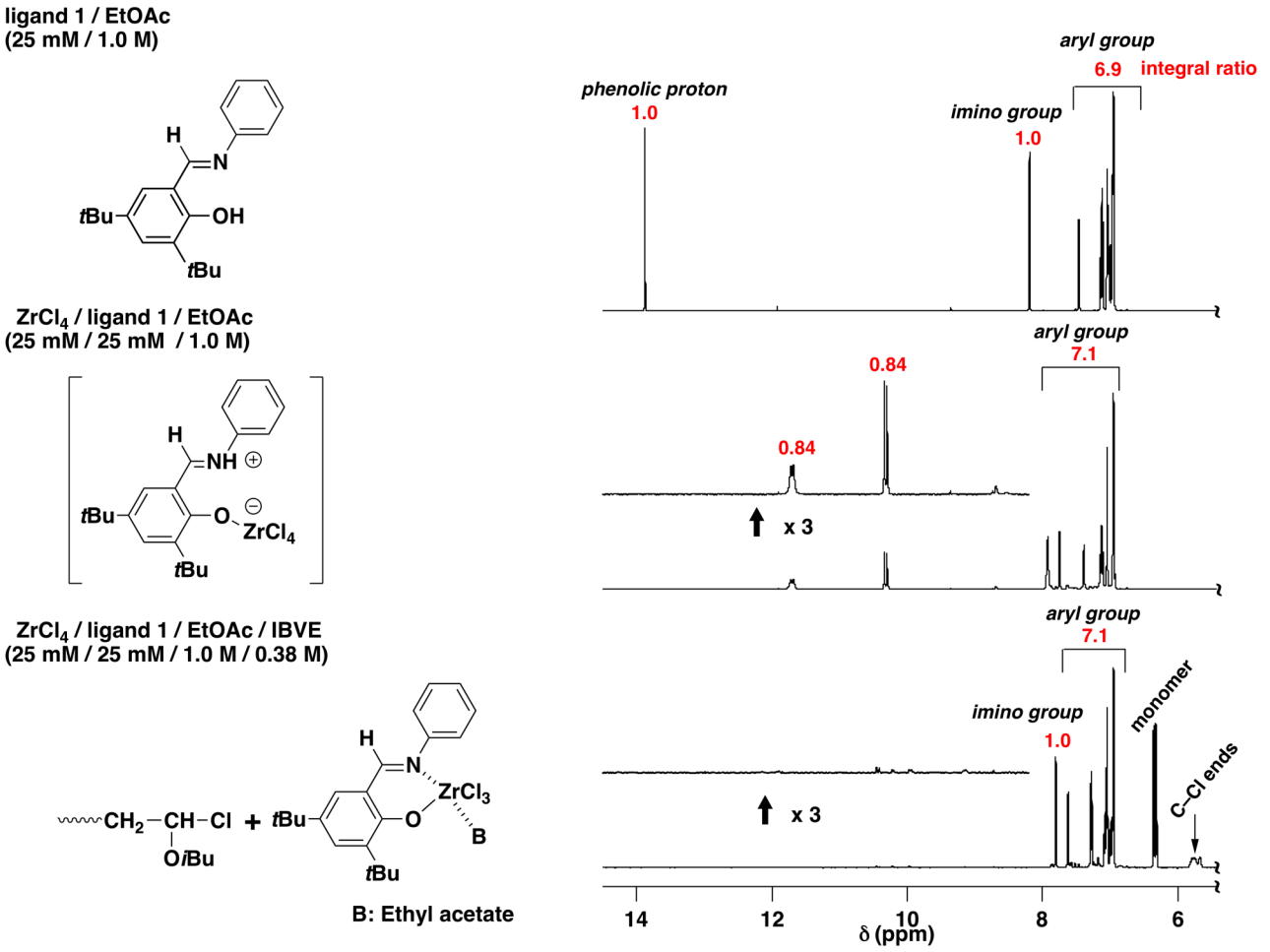

Figure 5. ^{1}H NMR spectra (signals of the protons of the imino and aryl groups) of (A) ligand **1**, (B) the mixture of **1** and $ZrCl_4$ and (C) a polymerization solution using the **1**/$ZrCl_4$ initiating system (in toluene-d_8 at 0 ºC, 500 MHz; $[\mathbf{1}]_0$ = 25 mM, [ethyl acetate] = 1.0 M, $[ZrCl_4]_0$ = 0 or 25 mM, $[IBVE]_0$ = 0 or 0.38 M).

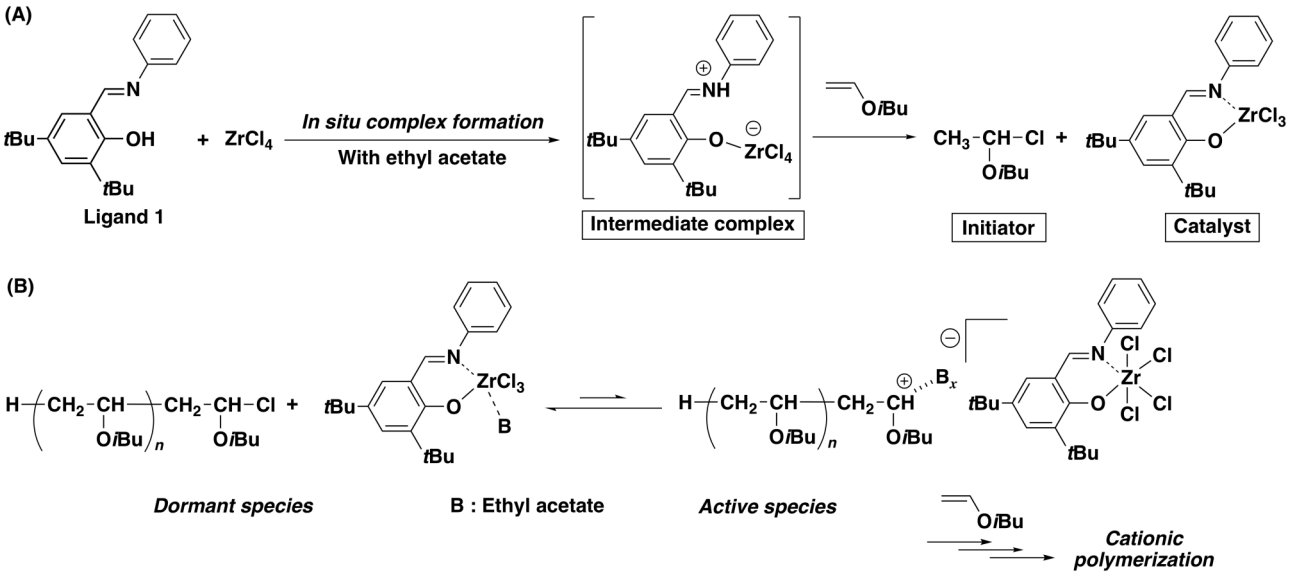

Scheme 1. (A) *In situ* complexation between **1** and $ZrCl_4$ and initiation reaction with IBVE and (B) the polymerization mechanism of IBVE using the **1**/$ZrCl_4$ initiating system.

N-Phenyl phenoxyimine ligand/MCl_n systems in the absence of ethyl acetate

To expand the scope of applicable metal species for controlled cationic polymerization using *in situ* complexation, polymerizations using the **1**/MCl_n systems were examined in the absence of ethyl acetate. The polymerizations of IBVE were conducted in the absence of Lewis basic additives at –78 °C because the activities of the catalysts were suppressed in the presence of ethyl acetate. The polymerization using the **1**/$TiCl_4$ initiating system proceeded smoothly and reached more than 90% conversion of IBVE (Figure 6A). The M_n values of the obtained polymers increased linearly with increasing monomer conversion, indicating that the polymerization proceeded in a controlled manner (Figure 6B). The M_n values of the polymers were approximately twice the values calculated based on the concentration of the phenolic hydrogen atoms of the ligand (Table 4, entry 1). In addition, the change in the **1**/$TiCl_4$ concentration corresponded to a change in the M_n values of the obtained polymers, indicating that the protic species generated *in situ* from **1**/$TiCl_4$ initiated the reaction (Table 4, entry 2, Figure 6B). The **1**/$TiCl_4$ initiating system produced a polymer with a very narrow MWD, while the IBVE–HCl/$TiCl_4$ system gave a polymer with a broad MWD (Table 4, entry 3, Figure 6C) under the similar conditions. Thus, the coordination of the ligand on the Ti species suitably moderated the Lewis acidity of the central metal, causing the well-controlled cationic polymerization.

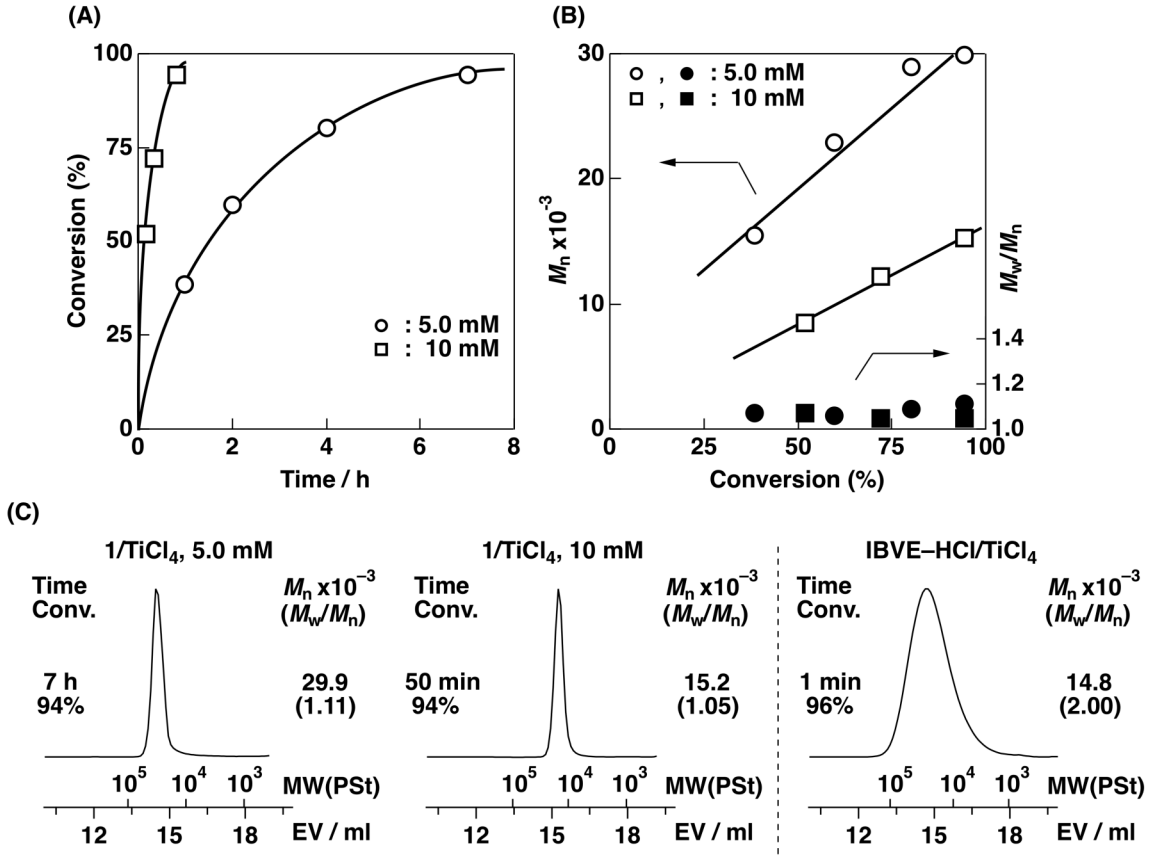

Figure 6. (A) Time–conversion curves of the polymerization, (B) M_n and M_w/M_n values, and (C) MWD curves of poly(IBVE)s obtained using the **1**/$TiCl_4$ initiating system or the IBVE–HCl/$TiCl_4$ system ($[IBVE]_0$ = 0.76 M, $[\mathbf{1}]_0$ = $[TiCl_4]_0$ = 5.0 or 10 mM or $[IBVE–HCl]_0$ = $[TiCl_4]_0$ = 5.0 mM, [heptane] = 5.0 vol% in toluene at –78 ºC).

In contrast to the **1**/$TiCl_4$ initiating system, in the absence of ethyl acetate, the **1**/MCl_n initiating systems with various metal chlorides (MCl_n: M = Zr, Hf, Sn, Ga, Zn) induced uncontrolled polymerization of IBVE (Table 4, entries 4–8). In the cases of $ZrCl_4$ and $HfCl_4$, their complexations with **1** in the absence of ethyl acetate in toluene generated yellow suspensions. Thus, ethyl acetate most likely functions not only as a reagent that moderates the Lewis acidity of the catalyst but also as a regent that assists the solubility of the catalyst. The polymerization of IBVE using the suspensions proceeded in an uncontrolled manner and produced polymers with M_n values much larger than the calculated values and broad MWDs. A **1**/$SnCl_4$ mixture also generated a slightly turbid catalytic solution. The M_n values of the obtained polymers using the **1**/$SnCl_4$ system increased linearly with increasing the monomer conversion. However, the M_n values were much larger than the values calculated based on the amount of **1**, indicating that the polymerization occurred with a very low initiation efficiency. Unlike the above cases, the **1**/$GaCl_3$ and $ZnCl_2$ mixtures became transparent catalytic solutions. The **1**/$GaCl_3$ system led to uncontrolled polymerization and produced a polymer with a considerably high peak molecular weight ($M_{pt} = 2.0 \times 10^5$). The polymerization using the **1**/$ZnCl_2$ system proceeded very slowly. No significant change was observed in shapes of the MWD curves of the polymers obtained at different conversions.

The complex generated from $TiCl_4$ exhibited different stereoselectivity compared to those of other metal chlorides. ^{13}C NMR analyses of the polymers obtained using the **1**/MCl_n systems, except for the **1**/$TiCl_4$, system exhibited almost the same meso dyad values (Table 4, entries 4–8, m = 68–74%). In contrast, the **1**/$TiCl_4$ initiating system produced polymers with low meso dyad values (m = 59%). The results indicate that the complex derived from **1**/$TiCl_4$ generated a propagating carbocation–counteranion pair that form preferably racemo dyads.

Table 4. Cationic polymerization of IBVE using MCl_n and **1** in the absence of ethyl acetate[a]

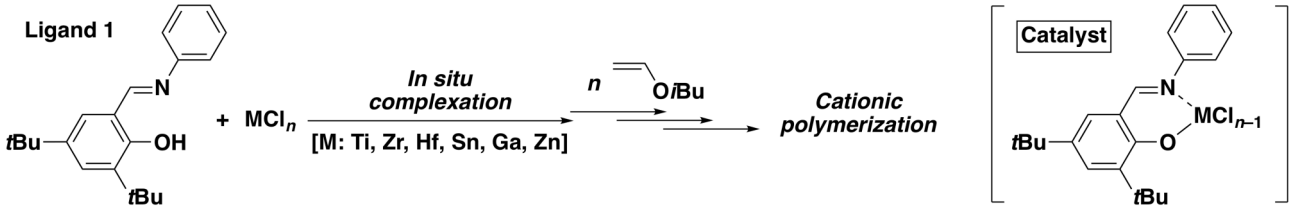

entry	MCl_n	time	conv (%)[b]	$M_n \times 10^{-3}$ (calcd)[c]	$M_n \times 10^{-3}$ (obs)[d]	M_w/M_n[d]	meso dyad (%)[e]	catalytic solution
1	$TiCl_4$	7 h	94	14.5	29.9	1.11	59	transparent
2		50 min	94	7.3	15.2	1.05	62	transparent
3[f]		1 min	96	14.8	14.8	2.00	72	transparent
4	$ZrCl_4$[g]	72 h	44	6.7	39.7	2.21	74	suspension
5	$HfCl_4$[g]	29 h	78	11.9	37.9	2.15	74	suspension
6	$SnCl_4$	20 min	90	13.9	55.7	1.24	74	thin turbidity
7	$GaCl_3$	24 h	92	14.1	27.4	9.16	72	transparent
8	$ZnCl_2$	360 h	37	5.7	28.5	1.88	68	transparent

[a] $[IBVE]_0$ = 0.76 M, $[MCl_n]_0$ = 5.0 mM for entries 1 and 3–8 or 10 mM for entry 2, $[\mathbf{1}]_0$ = 5.0 mM for entries 1 and 4–8 or 10 mM for entry 2, [heptane] = 5.0 vol% in toluene at –78 ºC. [b] Determined by gas chromatography. [c] Based on the amounts of **1**. [d] Determined by GPC (polystyrene standards). [e] Determined by ^{13}C NMR analysis. [f] $[IBVE–HCl]_0$ = 5.0 mM. [g] Solid metal chloride was directly mixed with a ligand.

Cationic polymerization of various monomers using *N*-aryl phenoxyimine ligands/$ZrCl_4$ systems

To confirm the monomer versatility of the **1**/$ZrCl_4$ initiating system, polymerizations of EVE and IPVE were conducted in the presence of ethyl acetate in toluene at 0 °C. The polymerizations of EVE and IPVE using the **1**/$ZrCl_4$ initiating system proceeded smoothly in similar manners to that of the polymerization of IBVE, indicating the occurrence of efficient initiation reactions via *in situ* complexation. These results indicated that the **1**/$ZrCl_4$ initiating system is effective for the controlled polymerization of various VE derivatives.

The polymerization behavior of pMOS using the ligand/$ZrCl_4$ initiating system was significantly affected by the ligand structure (Table 5, entries 4–7). The polymerization of pMOS using the **1**/$ZrCl_4$ system proceeded smoothly, however, a polymer with a bimodal MWD was obtained (Figure 7). The main peak, in the lower MW region, was sharp and shifted to a higher MW as the reaction proceeded, which indicates that living propagation species were somehow generated. The higher MW portion, which had a broader MWD, was likely generated at an earlier stage of the polymerization, suggesting the occurrence of undesired initiation reactions. Therefore, a small portion of IBVE, a monomer more reactive than pMOS, was used for the polymerization of pMOS using the **1**/$ZrCl_4$ system to promote smooth initiation reactions. As expected, the formation of the high-MW portion was significantly suppressed, resulting in a polymer with a narrow MWD. Unlike in the reaction using **1**, a negligible amount of uncontrolled portion with a large MW was generated in the polymerization using the **17**/$ZrCl_4$ system even in the absence of IBVE. This result indicates that the occurrence of the undesired reaction in the initiation step is affected by the ligand structure. The polymerization using the salphen (**18**)/$ZrCl_4$ initiating system did not reach high monomer conversion in 168 h, confirming that a low-activity and/or bulky catalyst complex is detrimental for the polymerization of pMOS.

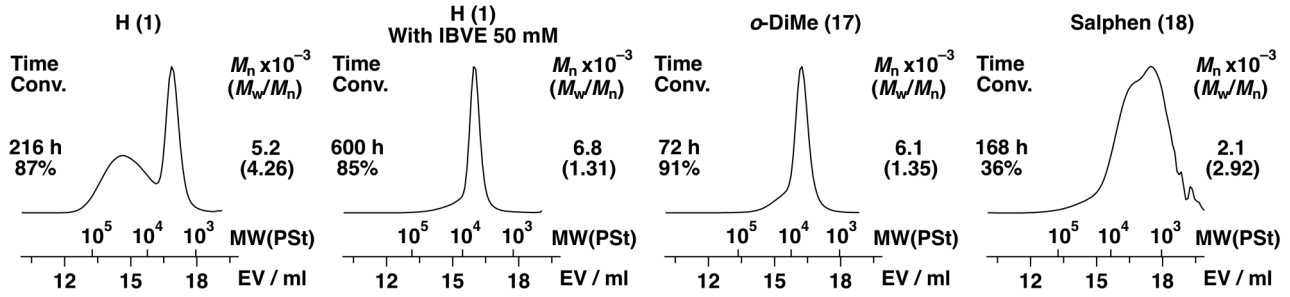

Figure 7. MWD curves for poly(pMOS)s obtained with various ligands/$ZrCl_4$ initiating systems ($[pMOS]_0$ = 0.38 M, $[ZrCl_4]_0$ = 5.0 mM, $[ligand]_0$ = 5.0 mM, [ethyl acetate] = 0.10 M, [heptane] = 5.0 vol% in toluene at 0 ºC).

Table 5. Cationic polymerization of IBVE using $ZrCl_4$ and various ligands[a]

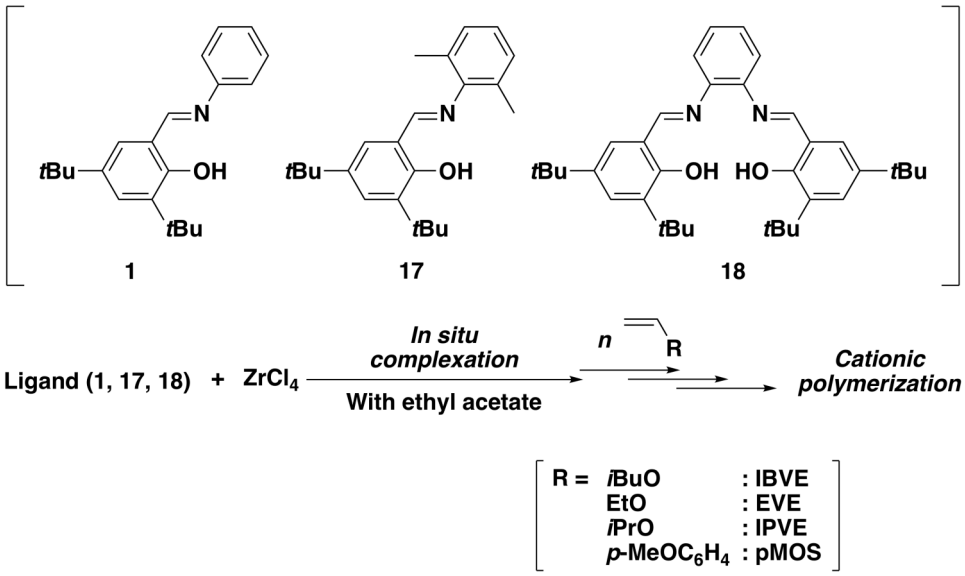

entry	monomer	ligand	[ethyl acetate] (M)	time (h)	conv (%)[b]	$M_n \times 10^{-3}$ (calcd)[c]	$M_n \times 10^{-3}$ (obs)[d]	M_w/M_n[d]
1	IBVE	**1**	1.0	144	92	14.1	7.2	1.13
2	EVE	**1**	1.0	52	93	10.5	6.7	1.30
3	IPVE	**1**	1.0	9	94	12.4	8.3	1.34
4	pMOS	**1**	0.10	216	87	8.8	5.2	4.26
5[e]		**1**	0.10	600	85	8.6	6.8	1.31
6		**17**	0.10	72	91	9.2	6.1	1.35
7		**18**	0.10	168	36	1.8	2.1	2.92

[a] $[Monomer]_0$ = 0.76–0.79 M for VE or 0.38 M for pMOS, $[ZrCl_4]_0$ = 5.0 mM, $[ligand]_0$ = 5.0 mM, [heptane] = 5.0 vol% in toluene at 0 ºC. [b] Determined by gas chromatography. [c] Based on the amounts of ligands. [d] Determined by GPC (polystyrene standards). [e] $[IBVE]_0$ = 50 mM.

Copolymerization of IBVE and pMOS proceeded successfully using the phenoxyimine/$ZrCl_4$ initiating system in a controlled, domino-type manner (Figure 8).[20] The copolymerization reactions were conducted using the substituted phenoxyimines (**1**, **17**, **19**, and **20**)/$ZrCl_4$ initiating systems in the presence of ethyl acetate in toluene at 0 °C. The MWDs of the obtained polymers were monomodal but relatively broad (M_w/M_n = 1.36–1.63). The relationship between the content of pMOS in the copolymer and the conversion of IBVE is shown in Figure 8. In all case, the pMOS contents were relatively low until the conversion of IBVE reached over 70–80%, indicating the occurrence of a domino-type reaction. The plots of **1** and **17** exhibited similar trends to those of the IBVE–HCl/$ZrCl_4$ system, which suggests that these ligands had a negligible effect on the monomer selectivity of the copolymerization. In contrast, the IBVE selectivities achieved using **19** and **20** were slightly lower than those of the above cases. The environment around the propagating carbocation and the counteranion generated from these ligands may be responsible for the decreased IBVE selectivity, although the details are unclear.

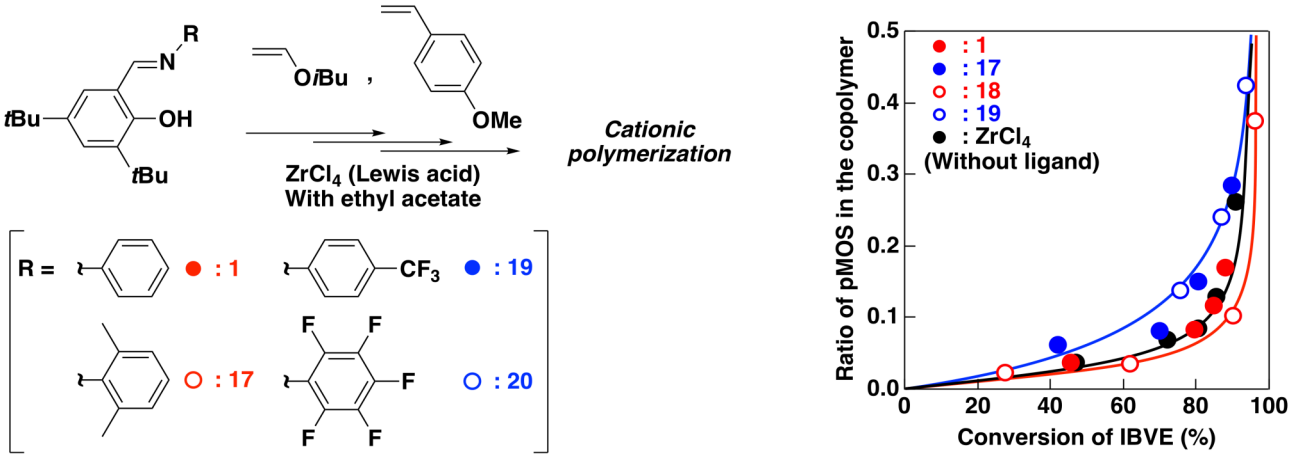

Figure 8. The ratio of pMOS units in the products obtained in the copolymerization of IBVE and pMOS using the phenoxyimine ligands/$ZrCl_4$ initiating systems ($[IBVE]_0$ = $[pMOS]_0$ = 0.50 M, $[ZrCl_4]_0$ = 5.0 mM, $[ligand]_0$ = 0 or 5.0 mM, $[IBVE–HCl]_0$ = 0 or 5.0 mM, [ethyl acetate] = 0.10 M, [heptane] = 5.0 vol% in toluene at 0 ºC).

Bulk polymerization of IBVE using *N*-aryl phenoxyimine ligands/$ZrCl_4$ systems

A metal–ligand bonding interaction, which directly tunes a Lewis acidity of a central metal, can be effective for a controlled bulk polymerization. Bulk polymerization of IBVE using an isolated **1**/$ZrCl_4$ catalyst was demonstrated to proceed in a controlled manner (Table 6). The isolated complex was synthesized from **1** and $ZrCl_4$ by an *in situ* complexation and subsequent evaporation of the solvents under reduced pressure. The polymerization was conducted by the addition of a monomer into a tube containing the solid catalyst in the absence of solvent. The bulk polymerization using the catalyst generated from **1**/$ZrCl_4$ proceeded smoothly and reached quantitative conversion in 15 h. The obtained polymer had a very large MW and a relatively narrow MWD (Figure 9A; M_w/M_n ~ 1.26 for a main peak). In sharp contrast, negligible polymerization occurred with the isolated catalyst generated from salphen-type **18** and $ZrCl_4$ by a method similar to that used with **1**. The difference likely comes from the presence of HCl in the isolated catalysts. The dried catalyst from **1**/$ZrCl_4$ may be isolated as the protonated species (Figure 5B), whereas the *in situ*-generated HCl in **18**/$ZrCl_4$ was almost completely removed by drying under reduced pressure. The advantage of the complex generated from **1** was demonstrated by a reference experiment using the IBVE–HCl/$ZrCl_4$ system under similar conditions. The reaction generated a polymer with a broad MWD (Figure 9D; M_w/M_n = 1.92). The moderation of the Lewis acidity of the metal species via the metal–ligand bonding interaction is likely responsible for the controlled polymerization achieved using **1**.

The electronic properties of the complex can be tuned through the introduction of substituents, which is useful for adjusting the catalytic activity in bulk polymerizations. The polymerization using the catalyst generated from the *p*-MeO-substituted ligand/$ZrCl_4$ system, which had relatively moderate Lewis acidity due to the electron-donating effect of the MeO group, proceeded at a moderate rate and generated a well-defined polymer (Table 6, Figure 9C). In contrast, the introduction of an electron-withdrawing group to the ligand led to uncontrolled polymerization. A catalyst generated from CF_3 group-substituted ligand **19**

exhibited very high catalytic activity. The conversion reached approximately 90% in 5 min. The obtained polymer contained a high-MW portion as a leading peak (Figure 9B). The uncontrolled composition was likely due to uncontrolled reactions that resulted from the heat of the reaction from a very high polymerization rate under bulk conditions. Indeed, the generation of bubbles, which were likely from partial evaporation of the monomer due to the rapid temperature increase, was visually confirmed. Thus, the appropriate moderation of the catalytic activity was effective for controlled bulk polymerizations.

Table 6. Cationic polymerization of IBVE using various ligands/$ZrCl_4$ systems under bulk conditions[a]

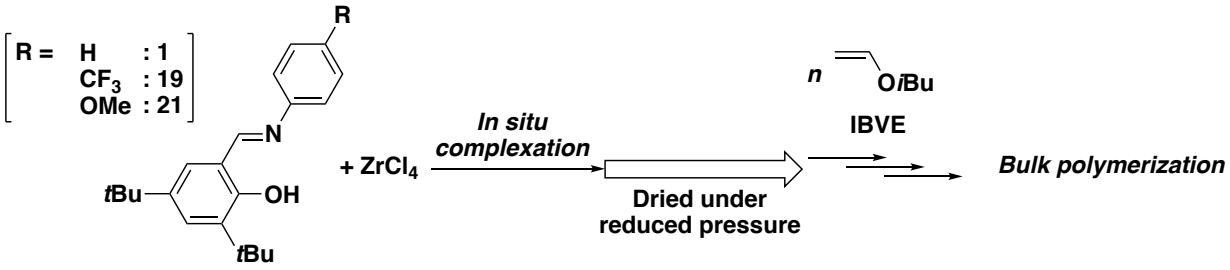

entry	ligand (initiator)	time	conv (%)[b]	$M_n \times 10^{-4}$ (calcd)[c]	$M_n \times 10^{-4}$ (obs)[d]	M_w/M_n [d]	$M_n \times 10^{-4}$ (main)[d]	M_w/M_n (main)[d]
1	**1**	15 h	99	15.2	6.4	1.65	6.5	1.26
2	**18**	528 h	10	0.8	0.4	8.30	-	-
3	**19**	5 min	88	13.6	3.3	4.36	2.8	2.16
4	**21**	12 h	95	14.6	7.7	1.20	-	-
5[e]	IBVE–HCl	2.5 min	74	5.1	3.0	1.92	-	-

[a] $[IBVE]_0/[complex]_0$ = 7.6 M/0.005 M at 0 ºC. [b] Determined by gas chromatography. [c] Based on the amounts of ligands. [d] Determined by GPC (polystyrene standards). [e] $[IBVE]_0$ = 6.9 M, $[IBVE–HCl]_0$ = 10 mM, $[ZrCl_4]_0$ = 5.0 mM, [ethyl acetate] = 100 mM, CH_2Cl_2: 10 vol% at 0 ºC.

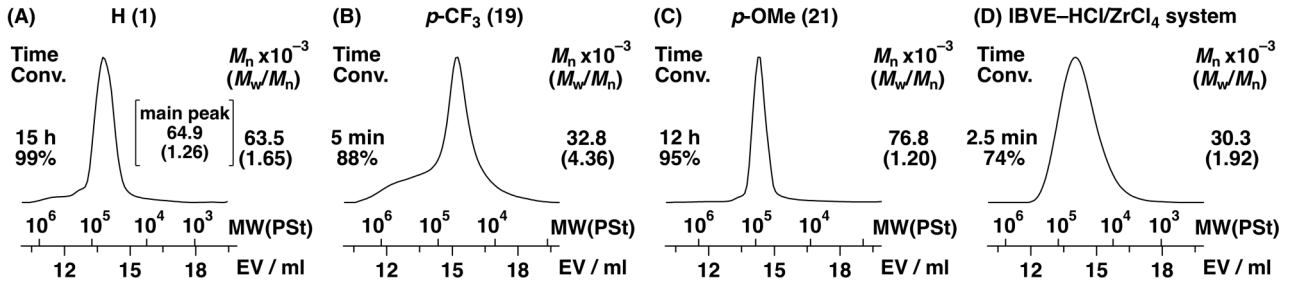

Figure 9. MWD curves for poly(IBVE)s obtained using the ligands/$ZrCl_4$ initiating systems (A–C: $[IBVE]_0/[complex]_0$ = 7.6 M/0.005 M at 0 ºC. D: $[IBVE]_0$ = 6.9 M, $[IBVE–HCl]_0$ = 10 mM, $[ZrCl_4]_0$ = 5.0 mM, [ethyl acetate] = 100 mM, CH_2Cl_2: 10 vol% at 0 ºC).

Conclusion

Various ligand frameworks were screened to identify an appropriate ligand scaffold for cationic polymerizations. The [*N*,*O*]-type phenoxyimine ligands were useful for modifying metal chloride catalysts. Notably, *t*Bu group-substituted phenoxyimine ligand/$ZrCl_4$ initiating systems induced well-controlled cationic polymerizations of IBVE in the presence of ethyl acetate in toluene at 0 °C. ^{1}H NMR analysis indicated that the mixture of ligand **1** and $ZrCl_4$ formed a protonated intermediate species. The completion of complex formation and initiation of the reaction was achieved by the consumption of HCl through the addition of a monomer to the reaction mixture. The **1**/$TiCl_4$ initiating system was also effective for the polymerization of IBVE in the absence of ethyl acetate in toluene at –78 °C. Polymerization results using **1** and various metal chlorides indicated that $ZrCl_4$ and $TiCl_4$ were appropriate for the controlled cationic polymerization of IBVE. In addition, the phenoxyimine ligands/$ZrCl_4$ initiating systems were also effective for controlled polymerization of pMOS, a styrene derivative less reactive than alkyl VEs. The reaction proceeded in a controlled manner when a ligand with an appropriate structure was used. The bulk polymerization using isolated catalysts also produced polymers with narrow MWDs, particularly with the use of a ligand with an electron-donating group.

References

1. Domski, G. J.; Rose, J. M.; Coates, G. W.; Boling, A. D.; Brookhart, M. *Prog. Polym. Sci.* **2007**, *32*, 30–92.
2. (a) Matsugi, T.; Fujita, T. *Chem. Soc. Rev.* **2008**, *37*, 1264–1277. (b) Maiko, H.; Terao, H.; Iwashita, A.; Fujita, T. *Chem. Rev.* **2011**, *111*, 2363–2449.
3. (a) Nakamura, A.; Ito, S.; Nozaki, K. *Chem. Rev.* **2009**, *109*, 5215–5244. (b) Nakamura, A.; Anselment, T. M. J.; Claverie, J.; Goodall, B.; Jordan, R. F.; Mecking, S.; Rieger, B.; Sen, A.; van Leeuwen, P. W. N. M.; Nozaki, K. *Acc. Chem. Res.* **2013**, *46*, 1438–1449. (c) Chen, E. Y.-X. *Chem. Rev.* **2009**, *109*, 5157–5214.
4. Kamigaito, M.; Ando, T.; Sawamoto, M. *Chem. Rev.* **2001**, *101*, 3689–3745.
5. (a) Ouchi, M.; Terashima, T.; Sawamoto, M. *Chem. Rev.* **2009**, *109*, 4963–5050. (b) Ouchi, M.; Sawamoto, M. *Macromolecules* **2017**, *50*, 2603–2614.
6. Matyjaszewski, K. *Macromolecules* **2012,** *45,* 4015–4039.
7. Rosen, B. M.; Percec, V. *Chem. Rev.* **2009**, *109*, 5069–5119.
8. Kamigaito, M.; Sawamoto, M.; Higashimura, T. *Macromolecules* **1995**, *28*, 5671–5675.
9. (a) Hadjikyriacou, S.; Faust, R. *Macromolecules* **1996**, *29*, 5261–5267. (b) Zhou, Y.; Faust, R.; Chen, S.; Gido, S. P. *Macromolecules* **2004**, *37*, 6716–6725. (c) Zhou, Y.; Faust, R. *Polym. Bull.* **2004**, *52*, 421–428.
10. (a) Kanazawa, A.; Kanaoka, S.; Aoshima, S. *Macromolecules* **2010**, *43*, 2739–2747. (b) Kanazawa, A.; Kanaoka, S.; Aoshima, S. *J. Polym. Sci., Part A: Polym. Chem.* **2010**, *48*, 2509–2516.
11. Kanaoka, S.; Nakayama, S.; Aoshima, S. *Kobunshi Ronbunshu* **2011,** *68,* 349–351.
12. (a) Ouchi, M.; Kamigaito, M.; Sawamoto, M. *Macromolecules* **1999**, *32*, 6407–6411. (b) Ouchi, M.; Kamigaito, M.; Sawamoto, M. *J. Polym. Sci., Part A: Polym. Chem.* **2001**, *39*, 1060–1066.

13. Sudhakar, P.; Vijayakrishna, K. *ChemCatChem* **2010**, *2*, 649–652.
14. (a) Pernecker, T.; Kennedy, J. P.; Ivan, B. *Macromolecules* **1992**, *25*, 1642–1647. (b) Pernecker, T.; Kennedy, J. P. *Polym. Bull.* **1992**, *29*, 27–33.
15. Kamigaito, M.; Maeda, Y.; Sawamoto, M.; Higashimura, T. *Macromolecules* **1993**, *26*, 1643–1649.
16. Yonezumi, M.; Takano, N.; Kanaoka, S.; Aoshima, S. *J. Polym. Sci., Part A: Polym. Chem.* **2008**, *46*, 6746–6753.
17. Kigoshi, S.; Kanazawa, A.; Kanaoka, S.; Aoshima, S. *Polym. Chem.*, **2015**, *6*, 30–34.
18. Koppel, I.; Koppel, J.; Maria, P.-C.; Gal, J.-F.; Notario, R.; Vlasov, V. M.; Taft, R. W. *Int. J. Mass Spectrom. Ion Processes* **1998**, *175*, 61-69.
19. Strauch, J.; Warren, T. H.; Erker, G.; Frohlich, R.; Saarenketo, P. *Inorg. Chim. Acta* **2000**, *300–302*, 810–821.
20. Kanaoka, S.; Yamada, M.; Ashida, J.; Kanazawa, A.; Aoshima, S. *J. Polym. Sci., Part A: Polym. Chem.* **2012**, *50*, 4594–4598.

Chapter 5

Structure–Property Relationship of Phenoxyimine Ligands/MCl_n Initiating Systems for Cationic Polymerizations of Vinyl Ether

Introduction

Correlation analyses such as linear free energy relationship (LFER)[1] and quantitative structure–activity relationship (QSAR)[2] studies have been widely used for predicting the properties of substrates and quantitatively estimating their various parameters, including their reactivities, physical (spectroscopic) properties, reaction constants, and biological activities, in fields such as organic chemistry, physical chemistry, and biochemistry. In organic chemistry, LFERs describe the relationships between resultant data, such as equilibrium data, rate constants, or excitation energies, and a variety of perturbations, such as the presence of substituents on a substrate, reaction solvents, and reaction species. LFERs are very useful for systematically understanding and quantitatively evaluating a chemical reaction and have been extensively employed to elucidate reaction mechanisms.[3–5]

The Hammett equation, which is an example of an LFER, gives the relationship between the chemical structure and the reactivity of the aromatic rings. [1a,6] The Hammett substituent constant σ, which is established based on the ionization constants of substituted benzoic acids, quantifies the electron-donating/withdrawing ability of a substituent.[1a] The substituent constant is composed of both inductive and resonance effects. The contribution from the inductive effect depends on the electronegativity difference regardless of the nature of the reaction, while the contribution from the resonance effect depends on the type of reaction. Thus, σ^+ and σ^- values were proposed to account for the enhanced resonance effects of *p*-positioned electron-donating and electron-withdrawing substituents, which stabilize positive and negative charges, respectively, on an aromatic ring. Hammett-type analyses using these substituent constants are highly effective for both elucidating reaction mechanisms and predicting reaction rates and equilibria.

A phenoxyimine ligand, which has advantages due to its easily tunable electronic and stereochemical properties, has been extensively investigated for olefin polymerization catalysts.[7] Phenoxyimine ligands are obtained from the condensation of salicylaldehyde derivatives with amines in high yield. The starting materials for preparing these ligands are commercially available or can be obtained from simple synthetic procedures. As olefin polymerization catalysts, phenoxyimine complexes have practical ligand frameworks. The accessibility of various structures in phenoxyimine complexes results in several advantages, including good stability of complexes, catalytic activity, and stereoregularity of the obtained polymers.

In Chapter 4, the *N*-phenyl phenoxyimine ligand/$ZrCl_4$ or $TiCl_4$ initiating systems were shown to induce the controlled cationic polymerization of isobutyl vinyl ether (IBVE) under appropriate conditions. In

this chapter, the substituent effects of phenoxyimine ligands on cationic polymerization behaviors are investigated using the *N*-aryl phenoxyimine ligands with various substituents on the aniline moiety. Accordingly, the author aims to examine the relationship between the electronic properties and the catalytic activities in cationic polymerizations of various phenoxyimine ligands (Figure 1). In cationic polymerizations, a complex catalyst catalyzes the cleavage of the carbon–halogen bonds (a C–Cl bond in this study) at the initiating and propagating ends to generate a carbocationic species and a counteranion. Hammett analysis is expected to provide information on the electronic effects of the ligands on the polymerization behavior. Specifically, a complex catalyst is converted to a negatively charged counteranion through the abstraction of a heteroatom from the propagating chain ends. Thus, analysis using ligands with a series of substituents will likely result in a Hammett plot with a positive slope. In addition, the *o*-substituents on the phenoxyimine ligands are expected to provide catalytic environments that are different from those of *p*- and *m*-substituted analogs in terms of their electronic and steric features due to the steric repulsion around the imino moiety.

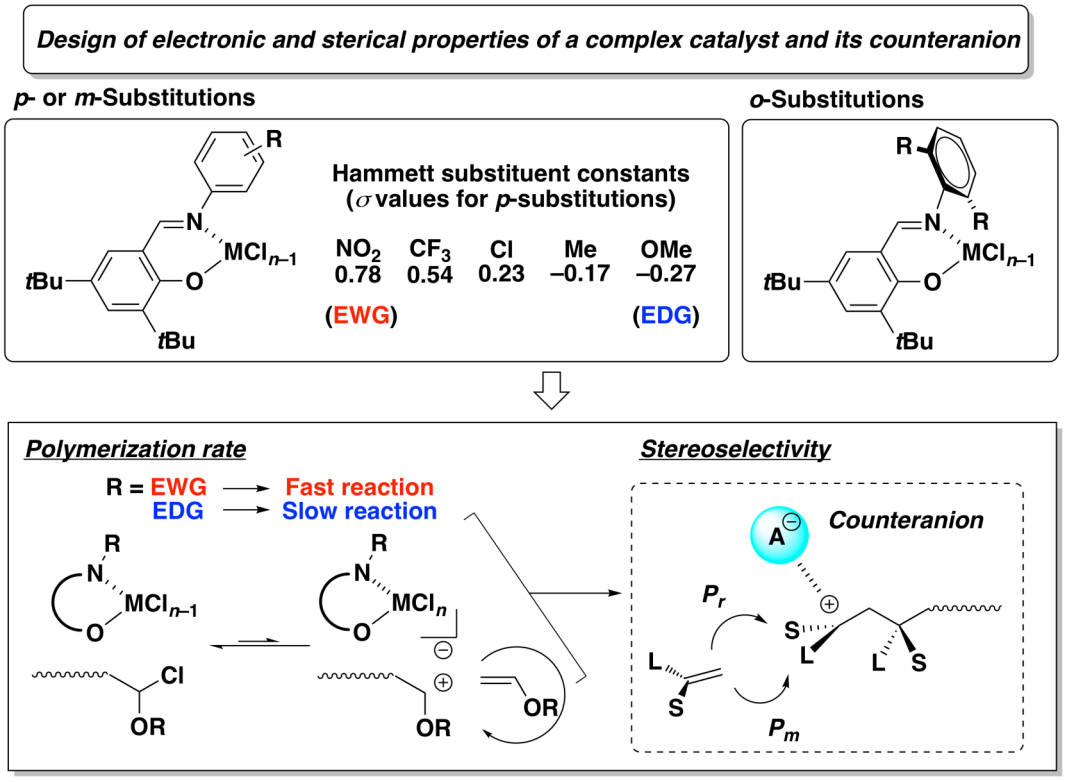

Figure 1. Structure–property relationship of cationic polymerization catalysts.

Experimental

Materials

Materials were prepared and used as described in Chapters 2–4.

Synthesis

General procedure

All materials were prepared using the following procedure. An aniline derivative was added to a methanol solution with an equivalent amount of 3,5-di-*tert*-butylsalicylaldehyde and a few drops of formic acid while stirring under a nitrogen atmosphere at room temperature. The solution was heated under reflux for at least 6 h, and the reaction mixture was then cooled to room temperature. After filtration, the solid was washed with cold methanol and dried under reduced pressure. The product was then purified by recrystallization from hexane or dichloromethane. The solid was filtered and washed and then dried under reduced pressure.

***N*-(4-Nitrophenyl)-3,5-di-*tert*-butylsalicylideneamine**

^{1}H NMR (500 MHz, $CDCl_3$, 30 °C): δ 13.07 (1H, s, O*H*), 8.65 (1H, s, N=C*H*), 8.29 (2H, d, *J* = 9.0 Hz, C*H*-aniline), 7.53 (1H, d, *J* = 2.4 Hz, C*H*-phenol), 7.37 (2H, d, *J* = 9.0 Hz, C*H*-aniline), 7.26 (1H, d, *J* = 2.3 Hz, C*H*-phenol), 1.48, 1.34 (9H each, s, C(CH_3)$_3$). ^{13}C NMR (100 MHz, $CDCl_3$, 30 °C): δ 166.4 (N=*C*H), 158.6 (*C*-OH), 154.4, 145.9 (*ipso*-aniline), 141.2, 137.4, 117.9 (*ipso*-phenol), 129.5, 127.4 (phenol), 125.2, 121.8 (aniline), 35.1, 34.2 (*C*(CH_3)$_3$), 31.4, 29.4 (C(*C*H_3)$_3$).

Mehyl-4-[(3,5-di-*tert*-butylsalicylidene)amino]benzoate

^{1}H NMR (500 MHz, $CDCl_3$, 30 °C): δ 13.39 (1H, s, O*H*), 8.65 (1H, s, N=C*H*), 8.09 (2H, d, *J* = 8.2 Hz, C*H*-aniline), 7.49 (1H, d, *J* = 2.7 Hz, C*H*-phenol), 7.30 (2H, d, *J* = 8.6 Hz, C*H*-aniline), 7.24 (1H, d, *J* = 2.6 Hz, C*H*-phenol), 3.92 (3H, s, CO_2CH_3) 1.48, 1.33 (9H each, s, C(CH_3)$_3$). ^{13}C NMR (100 MHz, $CDCl_3$, 30 °C): 166.6 (*C*$O_2$$CH_3$), 165.2 (N=*C*H), 158.5 (*C*-OH), 152.5, 128.0 (*ipso*-aniline), 140.7, 137.2, 118.1 (*ipso*-phenol), 128.8, 127.1 (phenol), 131.0, 121.1 (aniline), 52.1 (CO_2*C*H_3) 35.1, 34.2 (*C*(CH_3)$_3$), 31.4, 29.4 (C(*C*H_3)$_3$).

***N*-(4-Chlorophenyl)-3,5-di-*tert*-butylsalicylideneamine**

^{1}H NMR (500 MHz, $CDCl_3$, 30 °C): δ 13.46 (1H, s, O*H*), 8.60 (1H, s, N=C*H*), 7.47 (1H, d, *J* = 2.7 Hz, C*H*-phenol), 7.36 (2H, d, *J* = 8.7 Hz, C*H*-aniline), 7.23–7.19 (3H, m, C*H*-aryl), 1.48, 1.33 (9H each, s, C(CH_3)$_3$). ^{13}C NMR (100 MHz, $CDCl_3$, 30 °C): δ 164.1 (N=*C*H), 158.3 (*C*-OH), 147.3, 132.1 (*ipso*-aniline), 140.8, 137.1, 118.2 (*ipso*-phenol), 128.4, 126.9 (phenol), 129.5, 122.4 (aniline), 35.1, 34.2 (*C*(CH_3)$_3$), 31.5, 29.4 (C(*C*H_3)$_3$).

***N*-(4-Mehylphenyl)-3,5-di-*tert*-butylsalicylideneamine**

^{1}H NMR (500 MHz, $CDCl_3$, 30 °C): δ 13.79 (1H, s, O*H*), 8.63 (1H, s, N=C*H*), 7.44 (1H, d, *J* = 2.4 Hz, C*H*-phenol), 7.22–7.18 (5H, m, C*H*-aryl), 2.37 (3H, s, Ar-CH_3), 1.48, 1.33 (9H each, s, *t*Bu). ^{13}C NMR (100 MHz, $CDCl_3$, 30 °C): δ 162.9 (N=*C*H), 158.2 (*C*-OH), 146.2, 136.4 (*ipso*-aniline), 140.5, 136.9,

118.4 (*ipso*-phenol), 127.8, 126.6 (phenol), 129.9, 121.0 (aniline), 35.1, 34.2 ($C(CH_3)_3$), 31.5, 29.5 ($C(CH_3)_3$), 21.0 ($ArCH_3$).

***N*-(4-*tert*-Buthylphenyl)-3,5-di-*tert*-butylsalicylideneamine**

^{1}H NMR (500 MHz, $CDCl_3$, 30 °C): δ 13.80 (1H, s, O*H*), 8.64 (1H, s, N=C*H*), 7.45 (1H, d, *J* = 2.7 Hz, C*H*-phenol), 7.42 (2H, d, *J* = 8.9 Hz, C*H*-aniline), 7.23 (2H, d, *J* = 8.7 Hz, C*H*-aniline), 7.21 (1H, d, *J* = 2.7 Hz, C*H*-phenol), 1.48, 1.34, 1.33 (9H each, s, $C(CH_3)_3$). ^{13}C NMR (100 MHz, $CDCl_3$, 30 °C): δ 163.0 (N=*C*H), 158.3 (*C*-OH), 146.1, 149.8 (*ipso*-aniline), 140.5, 137.0, 118.4 (*ipso*-phenol), 127.8, 126.7 (phenol), 126.2, 120.8 (aniline), 35.1, 34.6, 34.2 ($C(CH_3)_3$), 31.5, 31.4, 29.5 ($C(CH_3)_3$).

***N*-(3-Nitrophenyl)-3,5-di-*tert*-butylsalicylideneamine**

^{1}H NMR (500 MHz, $CDCl_3$, 30 °C): δ 13.13 (1H, s, O*H*), 8.70 (1H, s, N=C*H*), 8.15–8.10 (2H, m, C*H*-aniline), 7.63–7.56 (2H, m, C*H*-aniline), 7.52 (1H, d, *J* = 2.3 Hz, C*H*-phenol), 7.27 (1H, d, *J* = 2.4 Hz, C*H*-phenol), 1.48, 1.34 (9H each, s, $C(CH_3)_3$). ^{13}C NMR (100 MHz, $CDCl_3$, 30 °C): δ 166.1 (N=*C*H), 158.5 (*C*-OH), 150.1, 149.2 (*ipso*-aniline), 141.1, 137.3, 117.9 (*ipso*-phenol), 129.2, 127.4 (phenol), 130.2, 127.9, 121.0, 115.6 (aniline), 35.2, 34.2 ($C(CH_3)_3$), 31.4, 29.4 ($C(CH_3)_3$).

***N*-(3-Chlorophenyl)-3,5-di-*tert*-butylsalicylideneamine**

^{1}H NMR (500 MHz, $CDCl_3$, 30 °C): δ 13.36 (1H, s, O*H*), 8.61 (1H, s, N=C*H*), 7.48 (1H, d, *J* = 2.6 Hz, C*H*-phenol), 7.32 (1H, t, *J* = 7.9 Hz, C*H*-aniline), 7.28 (1H, t, *J* = 1.9 Hz, C*H*-aniline), 7.24–7.21 (2H, m, C*H*-aniline and C*H*-phenol), 7.16 (1H, dd, *J* = 1.0, 6.9 Hz, C*H*-aniline), 1.48, 1.33 (9H each, s, $C(CH_3)_3$). ^{13}C NMR (100 MHz, $CDCl_3$, 30 °C): δ 164.8 (N=*C*H), 158.4 (*C*-OH), 150.1, 135.0 (*ipso*-aniline), 140.8, 137.1, 118.1 (*ipso*-phenol), 128.5, 127.1 (phenol), 130.3, 126.4, 121.2, 119.7 (aniline), 35.1, 34.2 ($C(CH_3)_3$), 31.5, 29.4 ($C(CH_3)_3$).

***N*-(3-Mehylphenyl)-3,5-di-*tert*-butylsalicylideneamine**

^{1}H NMR (500 MHz, $CDCl_3$, 30 °C): δ 13.74 (1H, s, O*H*), 8.63 (1H, s, N=C*H*), 7.45 (1H, d, *J* = 2.4 Hz, C*H*-phenol), 7.28 (1H, t, *J* = 7.7 Hz, C*H*-aniline), 7.22 (1H, d, *J* = 2.4 Hz, C*H*-phenol), 7.13–7.04 (3H, m, C*H*-aniline), 2.39 (3H, s, Ar-CH_3), 1.48, 1.33 (9H each, s, $C(CH_3)_3$). ^{13}C NMR (100 MHz, $CDCl_3$, 30 °C): δ 163.5 (N=*C*H), 158.3 (*C*-OH), 148.7, 139.2 (*ipso*-aniline), 140.5, 137.0, 118.4 (*ipso*-phenol), 127.9, 126.8 (phenol), 129.1, 127.3, 122.0, 118.1 (aniline), 35.1, 34.2 ($C(CH_3)_3$), 31.5, 29.5 ($C(CH_3)_3$), 21.4 (Ar-CH_3).

***N*-(3-Methoxyphenyl)-3,5-di-*tert*-butylsalicylideneamine**

^{1}H NMR (500 MHz, $CDCl_3$, 30 °C): δ 13.64 (1H, s, O*H*), 8.63 (1H, s, N=C*H*), 7.46 (1H, d, *J* = 2.7 Hz, C*H*-phenol), 7.30 (1H, t, *J* = 7.7 Hz, C*H*-aniline), 7.22 (1H, d, *J* = 2.6 Hz, C*H*-phenol), 6.89–6.79 (3H, m, C*H*-aniline), 3.84 (3H, s, OCH_3), 1.48, 1.33 (9H each, s, $C(CH_3)_3$). ^{13}C NMR (100 MHz, $CDCl_3$, 30 °C): δ 163.9 (N=*C*H), 158.3 (*C*-OH), 160.5, 150.1 (*ipso*-aniline), 140.6, 137.0, 118.3 (*ipso*-phenol), 128.1, 126.9 (phenol), 130.1, 113.2, 112.5, 107.0 (aniline), 55.4 (OCH_3), 35.1, 34.2 ($C(CH_3)_3$), 31.5, 29.5 ($C(CH_3)_3$).

***N*-(3-Phenylphenyl)-3,5-di-*tert*-butylsalicylideneamine**

^{1}H NMR (500 MHz, $CDCl_3$, 30 °C): δ 13.69 (1H, s, O*H*), 8.70 (1H, s, N=C*H*), 7.65–7.61 (2H, m, C*H*-aryl), 7.52–7.42 (6H, m, C*H*-aryl), 7.36 (1H, tt, *J* = 7.4, 1.1 Hz, C*H*-aryl), 7.26 (1H, dt, *J* = 7.0, 1.9 Hz, C*H*-aryl), 7.24 (1H, d, *J* = 2.4 Hz, C*H*-aryl), 1.49, 1.34 (9H each, s, C(CH_3)$_3$). ^{13}C NMR (100 MHz, $CDCl_3$, 30 °C): δ 164.0 (N=*C*H), 158.3 (*C*-OH), 149.2, 142.6 (*ipso*-aniline), 140.6 (*ipso*-phenol and *ipso*-phenyl), 137.0, 118.3 (*ipso*-phenol), 130.3, 126.4, 121.2, 119.7 (aniline), 128.8, 127.6, 127.2 (phenyl), 128.1, 126.9 (phenol), 35.1, 34.2 (*C*(CH$_3$)$_3$), 31.5, 29.5 (C(*C*H$_3$)$_3$).

***N*-(3,5-Nitrophenyl)-3,5-di-*tert*-butylsalicylideneamine**

^{1}H NMR (400 MHz, $CDCl_3$, 30 °C): δ 12.71 (1H, s, O*H*), 8.92 (1H, t, *J* = 3.0 Hz, C*H*-aniline), 8.78 (1H, s, N=C*H*), 8.45 (2H, d, *J* = 2.1 Hz, C*H*-aniline), 7.58 (1H, d, *J* = 2.4 Hz, C*H*-phenol), 7.31 (1H, d, *J* = 2.4 Hz, C*H*-phenol), 1.48, 1.35 (9H each, s, C(CH_3)$_3$). ^{13}C NMR (100 MHz, $CDCl_3$, 30 °C): δ 167.9 (N=*C*H), 158.8 (*C*-OH), 151.4, 149.3 (*ipso*-aniline), 141.7, 137.7, 117.6 (*ipso*-phenol), 130.5, 127.9 (phenol), 121.6, 115.8 (aniline), 35.2, 34.3 (*C*(CH$_3$)$_3$), 31.4, 29.4 (C(*C*H$_3$)$_3$).

***N*-(3,5-Trifluoromethylphenyl)-3,5-di-*tert*-butylsalicylideneamine**

^{1}H NMR (400 MHz, $CDCl_3$, 30 °C): δ 12.99 (1H, s, O*H*), 8.69 (1H, s, N=C*H*), 7.77 (1H, s, C*H*-aniline), 7.71 (2H, s, C*H*-aniline), 7.53 (1H, d, *J* = 2.4 Hz, C*H*-phenol), 7.27 (1H, d, *J* = 2.4 Hz, C*H*-phenol), 1.48, 1.34 (9H each, s, C(CH_3)$_3$). ^{13}C NMR (100 MHz, $CDCl_3$, 30 °C): ^{13}C NMR (100 MHz, $CDCl_3$, 30 °C): δ 166.6 (N=*C*H), 158.6 (*C*-OH), 150.4 (*ipso*-aniline), 133.0 (q, *J* = 33.4 Hz, *ipso*-aniline), 141.3, 137.5, 117.9 (*ipso*-phenol), 129.6, 127.5 (phenol), 123.1 (q, *J* = 271 Hz, *C*F$_3$), 121.5 (d, *J* = 2.9 Hz, aniline), 119.8 (m, *J* = 33.4 Hz, aniline), 35.2, 34.3 (*C*(CH$_3$)$_3$), 31.4, 29.4 (C(*C*H$_3$)$_3$).

***N*-(3,5-Chlorophenyl)-3,5-di-*tert*-butylsalicylideneamine**

^{1}H NMR (400 MHz, $CDCl_3$, 30 °C): δ 13.08 (1H, s, O*H*), 8.60 (1H, s, N=C*H*), 7.50 (1H, d, *J* = 2.5 Hz, C*H*-phenol), 7.25 (1H, t, *J* = 1.8 Hz, C*H*-aniline), 7.22 (1H, d, *J* = 2.4 Hz, C*H*-phenol), 7.18 (2H, d, *J* = 1.8 Hz, C*H*-aniline), 1.47, 1.33 (9H each, s, C(CH_3)$_3$). ^{13}C NMR (100 MHz, $CDCl_3$, 30 °C): δ 165.7 (N=*C*H), 158.4 (*C*-OH), 150.8, 135.6 (*ipso*-aniline), 141.0, 137.3, 117.9 (*ipso*-phenol), 129.1, 127.3 (phenol), 126.3, 120.0 (aniline), 35.1, 34.2 (*C*(CH$_3$)$_3$), 31.4, 29.4 (C(*C*H$_3$)$_3$).

***N*-(3,5-mehyl-phenyl)-3,5-di-*tert*-butyl-salicylidene-amine**

^{1}H NMR (400 MHz, $CDCl_3$, 30 °C): δ 13.80 (1H, s, O*H*), 8.63 (1H, s, N=C*H*), 7.44 (1H, d, *J* = 2.4 Hz, C*H*-phenol), 7.21 (1H, d, *J* = 2.4 Hz, C*H*-phenol), 6.94–6.89 (3H, m, C*H*-aniline), 2.35 (6H, s, Ar-CH_3), 1.48, 1.33 (9H each, s, C(CH_3)$_3$). ^{13}C NMR (100 MHz, $CDCl_3$, 30 °C): δ 163.3 (N=*C*H), 158.3 (*C*-OH), 148.6, 139.0 (*ipso*-aniline), 140.4, 137.0, 118.4 (*ipso*-phenol), 127.8, 126.7 (phenol), 128.3, 118.9 (aniline), 35.1, 34.2 (*C*(CH$_3$)$_3$), 31.5, 29.5 (C(*C*H$_3$)$_3$).

***N*-(3,5-Methoxyphenyl)-3,5-di-*tert*-butylsalicylideneamine**

^{1}H NMR (400 MHz, $CDCl_3$, 30 °C): δ 13.59 (1H, s, O*H*), 8.62 (1H, s, N=C*H*), 7.46 (1H, d, *J* = 2.4 Hz, C*H*-phenol), 7.21 (1H, d, *J* = 2.4 Hz, C*H*-phenol), 6.45 (2H, d, *J* = 2.3 Hz, C*H*-aniline), 6.38 (1H, t, *J*

= 2.2 Hz, C*H*-aniline), 3.82 (6H, s, OCH_3), 1.48, 1.33 (9H each, s, C(CH_3)$_3$). ^{13}C NMR (100 MHz, $CDCl_3$, 30 °C): δ 164.0 (N=*C*H), 158.3 (*C*-OH), 161.4, 150.8 (*ipso*-aniline), 140.6, 137.0, 118.2 (*ipso*-phenol), 128.2, 126.9 (phenol), 99.5, 98.9 (aniline), 55.5 (O*C*H$_3$), 35.1, 34.2 (*C*(CH$_3$)$_3$), 31.5, 29.5 (C(*C*H$_3$)$_3$).

***N*-(3,5-*tert*-Butylphenyl)-3,5-di-*tert*-butylsalicylideneamine**

^{1}H NMR (400 MHz, $CDCl_3$, 30 °C): δ 13.88 (1H, s, O*H*), 8.64 (1H, s, N=C*H*), 7.45 (1H, d, *J* = 2.5 Hz, C*H*-phenol), 6.34 (1H, t, *J* = 1.7 Hz, C*H*-aniline), 7.24 (1H, d, *J* = 2.1 Hz, C*H*-phenol), 7.12 (2H, d, *J* = 1.7 Hz, C*H*-aniline), 1.49, 1.34 (9H each, s, C(CH_3)$_3$), 1.37 (18H, s, C(CH_3)$_3$). ^{13}C NMR (100 MHz, $CDCl_3$, 30 °C): δ 163.1 (N=*C*H), 158.3 (*C*-OH), 152.1, 148.2 (*ipso*-aniline), 140.5, 136.9, 118.4 (*ipso*-phenol), 127.7, 126.7 (phenol), 120.7, 115.5 (aniline), 35.1, 35.0, 34.2 (*C*(CH$_3$)$_3$), 31.5, 31.5, 29.5 (C(*C*H$_3$)$_3$).

***N*-(2-Methylphenyl)-3,5-di-*tert*-butylsalicylideneamine**

^{1}H NMR (500 MHz, $CDCl_3$, 30 °C): δ 13.73 (1H, s, O*H*), 8.56 (1H, s, N=C*H*), 7.47 (1H, d, *J* = 2.4 Hz, C*H*-phenol), 7.27–7.21 (3H, m, C*H*-phenol and C*H*-aniline), 7.16 (1H, m, C*H*-aniline), 7.07 (1H, d, *J* = 7.9 Hz, C*H*-aniline), 2.40 (3H, s, Ar-CH_3), 1.49, 1.34 (9H each, s, C(CH_3)$_3$). ^{13}C NMR (100 MHz, $CDCl_3$, 30 °C): δ 163.5 (N=*C*H), 158.4 (*C*-OH), 147.3, 132.2 (*ipso*-aniline), 140.5, 137.0, 118.5 (*ipso*-phenol), 127.9, 126.7 (phenol), 130.6, 126.9, 126.4, 118.0 (aniline), 35.1, 34.2 (*C*(CH$_3$)$_3$), 31.5, 29.5 (C(*C*H$_3$)$_3$), 18.2 (Ar-CH_3).

***N*-(2-*iso*-Propylphenyl)-3,5-di-*tert*-butylsalicylideneamine**

^{1}H NMR (400 MHz, $CDCl_3$, 30 °C): δ 13.58 (1H, s, O*H*), 8.55 (1H, s, N=C*H*), 7.47 (1H, d, *J* = 2.4 Hz, C*H*-phenol), 7.38–7.31 (1H, m, C*H*-aniline), 7.29–7.18 (3H, m, C*H*-phenol and C*H*-aniline), 7.06–6.98 (1H, m, C*H*-aniline), 3.46 (1H, m, Ar-C*H*), 1.49, 1.34 (9H each, s, C(CH_3)$_3$), 1.26 (6H, s, CHCH_3). ^{13}C NMR (100 MHz, $CDCl_3$, 30 °C): δ 164.0 (N=*C*H), 158.2 (*C*-OH), 147.3, 142.2 (*ipso*-aniline), 140.5, 137.0, 118.6 (*ipso*-phenol), 127.9, 126.8 (phenol), 126.8, 126.7, 125.7, 118.6 (aniline), 35.2, 34.2 (*C*(CH$_3$)$_3$), 31.5, 29.5 (C(*C*H$_3$)$_3$), 28.2 (*C*H(CH$_3$)$_2$), 23.2 (CH(*C*H$_3$)$_2$).

***N*-(2-Phenylphenyl)-3,5-di-*tert*-butylsalicylideneamine**

^{1}H NMR (400 MHz, $CDCl_3$, 30 °C): δ 13.09 (1H, s, O*H*), 8.60 (1H, s, N=C*H*), 7.50–7.10 (11H, m, C*H*-aryl), 1.38, 1.32 (9H each, s, C(CH_3)$_3$). ^{13}C NMR (100 MHz, $CDCl_3$, 30 °C): δ 164.0 (N=*C*H), 158.2 (*C*-OH), 146.7, 136.6 (*ipso*-aniline), 140.3, 137.0, 118.4 (*ipso*-phenol), 139.2 (*ipso*-phenyl), 130.5, 129.8, 128.0 (phenyl), 127.9, 126.7 (phenol), 128.5, 127.1, 126.6, 118.9 (aniline), 35.1, 34.1 (*C*(CH$_3$)$_3$), 31.5, 29.3 (C(*C*H$_3$)$_3$).

***N*-(2,6-Di-*iso*-propylphenyl)-3,5-di-*tert*-butylsalicylideneamine**

^{1}H NMR (400 MHz, $CDCl_3$, 30 °C): δ 13.43 (1H, s, O*H*), 8.29 (1H, s, N=C*H*), 7.50 (1H, d, *J* = 2.5 Hz, C*H*-phenol), 7.21–7.12 (4H, m, C*H*-phenol and C*H*-aniline), 3.02 (2H, m, Ar-C*H*), 1.50, 1.34 (9H each, s, C(CH_3)$_3$), 1.18 (12H, s, CHCH_3). ^{13}C NMR (100 MHz, $CDCl_3$, 30 °C): δ 167.5 (N=*C*H), 158.4 (*C*-OH), 146.4, 138.9 (*ipso*-aniline), 140.5, 137.2, 117.7 (*ipso*-phenol), 128.1, 126.6 (phenol), 123.2, 125.2 (aniline), 35.2, 34.2 (*C*(CH$_3$)$_3$), 31.5, 29.5 (C(*C*H$_3$)$_3$), 28.0 (*C*H(CH$_3$)$_2$), 23.6 (CH(*C*H$_3$)$_2$).

***N*-(2,4,6-Triphenylphenyl)-3,5-di-*tert*-butylsalicylideneamine**

^{1}H NMR (500 MHz, $CDCl_3$, 30 °C): δ 12.89 (1H, s, O*H*), 7.95 (1H, s, N=C*H*), 7.72–7.62 (4H, m, C*H*-aryl), 7.49–7.39 (6H, m, C*H*-aryl), 7.38–7.29 (6H, m, C*H*-aryl), 7.28–7.21 (2H, m, C*H*-aryl), 6.56 (1H, d, *J* = 2.4 Hz, C*H*-phenol), 1.37, 1.19 (9H each, s, C(CH_3)$_3$). ^{13}C NMR (100 MHz, $CDCl_3$, 30 °C): δ 169.2 (N=*C*H), 158.1 (*C*-OH), 140.2, 136.5, 117.9 (*ipso*-phenol), 139.8, 138.3 (*ipso*-aniline and *ipso*-phenyl), 139.7, 135.6, 129.9, 128.9, 128.8, 128.3, 127.8, 127.4, 127.0,126.9, 126.4 (aryl), 35.0, 34.0 (*C*(CH_3)$_3$), 31.3, 29.3 (C(*C*H_3)$_3$).

Polymerization Procedure

Cationic polymerization reactions were conducted in a similar manner to that described in Chapter 2.

Characterization

The MWD and NMR spectra of the polymers were determined as described in Chapters 2 and 3.

Results and Discussion

1. The relationship between the electronic properties and the catalytic properties of the *p*- or *m*-substituted phenyl phenoxyimine ligand/MCl_n systems

To examine the relationships between the Hammett substituent constants and the properties of the phenoxyimine ligands, ^{1}H NMR analyses were conducted with a series of ligands having a *p*- or *m*-substituted phenyl moiety. The ^{1}H NMR signals of the protons were observed at approximately 13–14 ppm, which is significantly downfield of the phenol OH group due to the intramolecular interactions of the protons with the imino nitrogen atom.[8,9] ^{1}H NMR analyses of the ligands showed that the chemical shifts of the phenolic protons of the ligands depended on the substituents on the anilinic moieties. A plot of the chemical shifts against the Hammett substituent constants (σ values) showed a linear relationship (Figure 2),[9,10] which indicated that the electric properties of the ligand framework follow the Hammett equation.

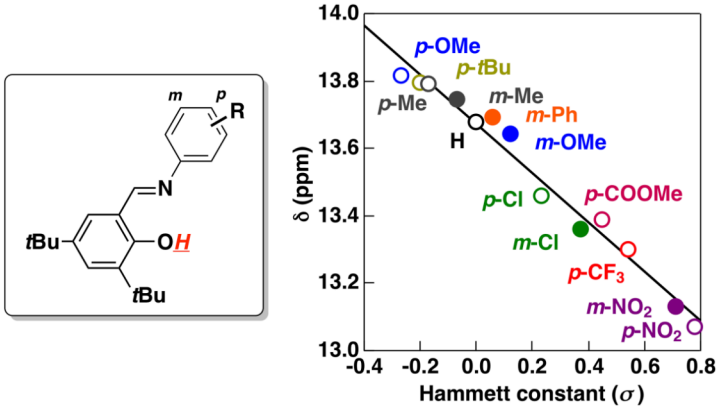

Figure 2. ^{1}H NMR chemical shift values of the phenolic OH protons of the *p*- or *m*-substituted phenyl phenoxyimine ligands (500 MHz in $CDCl_3$ at 30 ºC).

1.1 The catalytic activities of the ligands/$ZrCl_4$ systems

The polymerization of IBVE using initiating systems consisting of $ZrCl_4$ and phenoxyimine ligands with a *p*- or *m*-substituted phenyl ring was found to proceed in a controlled manner regardless of the substituents attached (Table 1). In Chapter 4, the author have demonstrated that the *N*-phenyl phenoxyimine ligand/$ZrCl_4$ initiating system is effective for the controlled cationic polymerization of IBVE in the presence of ethyl acetate in toluene at 0 °C (Table 1, entry 5). Various *N*-aryl phenoxyimine ligands possessing *p*- or *m*-substituents were used for cationic polymerizations under the same conditions. The catalytic solutions were obtained by mixing $ZrCl_4$ and the phenoxyimine ligands. Heterogeneous catalytic solutions were obtained in some cases. After the polymerization was started, however, the polymerization solutions became homogeneous in the early stage of the polymerization (within 3% conversion).[11] In all cases, the polymerizations using the complex catalysts proceeded smoothly and reached over 90% conversion. The polymerization rates depended on the substituents; the reactions using ligands with electron-withdrawing groups, such as CF_3, proceeded faster, while those using ligands with electron-donating groups, such as MeO, proceeded slower (Figure 3A). The M_n values of the obtained polymers increased linearly with the conversion and reached similar values (Table 1, Figure 3B). The MWD curves were relatively narrow, indicating that the polymerizations proceeded in a controlled manner regardless of the ligand used in the initiating system.

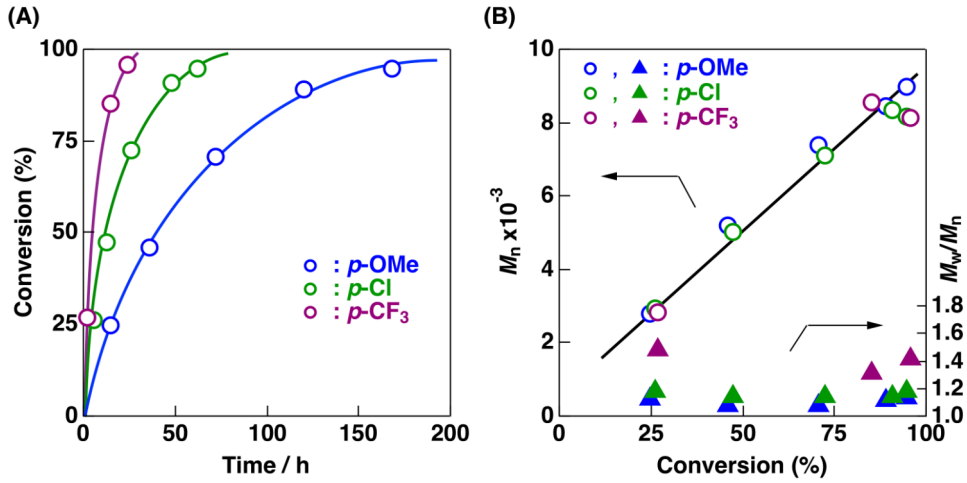

Figure 3. (A) Time–conversion curves of the polymerization and (B) M_n and M_w/M_n values of the polymers obtained using the *p*-substituted phenyl phenoxyimine ligands/$ZrCl_4$ initiating systems ($[IBVE]_0$ = 0.76 M, $[ZrCl_4]_0$ = 5.0 mM, $[ligand]_0$ = 5.0 mM, [ethyl acetate] = 1.0 M, [heptane] = 5.0 vol% in toluene at 0 ºC).

The apparent rate constants (k_{app}), which were determined from the first-order plots of the polymerization reactions using the phenoxyimine ligands, were dependent on the substituents on the anilinic moieties (Figure 4). The all first-order plots were linear. (Figure 4A). The apparent rate constants were calculated from the slope of the plots (k_{app} = [ln(M_0/M)]/[reaction time (h)]). The complexes with an electron-withdrawing group on the phenoxyimine ligand had larger k_{app} values than those with electron-donating groups, most likely because the Lewis acidity of the complexes was enhanced by the

Table 1. Cationic polymerization of IBVE using $ZrCl_4$ and the *p*- or *m*-substituted phenyl phenoxyimine ligands[a]

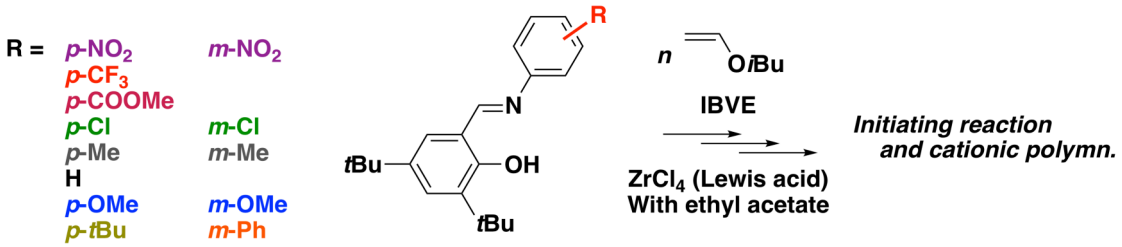

entry	substituent	σ value	time (h)	conv (%)[b]	$M_n \times 10^{-3}$ (calcd)[c]	$M_n \times 10^{-3}$ (obs)[d]	M_w/M_n[d]	meso dyad (%)[e]
1	*p*-NO_2	0.78	24	96	14.7	8.1	1.41	65
2	*p*-CF_3	0.54	40	98	15.0	8.8	1.26	64
3	*p*-COOMe	0.39	50	94	14.5	7.6	1.31	64
4	*p*-Cl	0.23	54	92	14.1	7.9	1.13	63
5	H	0	144	94	14.4	7.9	1.14	62
6	*p*-Me	–0.17	70	95	14.6	9.8	1.21	65
7	*p*-*t*Bu	−0.20	88	93	14.3	9.3	1.23	65
8	*p*-OMe	−0.27	120	91	14.0	8.7	1.11	63
9	*m*-NO_2	0.71	18	96	14.7	6.6	1.33	66
10	*m*-Cl	0.37	48	98	15.0	9.5	1.21	65
11	*m*-OMe	0.12	148	92	14.1	8.3	1.16	64
12	*m*-Ph	0.06	216	95	14.6	6.4	1.21	64
13	*m*-Me	–0.07	80	93	14.4	6.7	1.74	65

[a] $[IBVE]_0 = 0.76$ M, $[ZrCl_4]_0 = 5.0$ mM, $[ligand]_0 = 5.0$ mM, [ethyl acetate] = 1.0 M, [heptane] = 5.0 vol% in toluene at 0 °C. [b] Determined by gas chromatography. [c] Based on the amounts of phenoxyimines. [d] Determined by GPC (polystyrene standards). [e] Determined by ^{13}C NMR analysis.

electron-withdrawing effects of the ligand. A plot of the σ values versus the $\log(k_{R,app}/k_{H,app})$ values (where $k_{R,app}$ and $k_{H,app}$ are the apparent rate constants of the polymerization using phenoxyimine ligands with R- or no substituents on the phenyl group, respectively) showed a curve with a positive slope. The non-linearity of the plot indicates that factors other than the electronic properties of the phenoxyimine ligands affect the polymerization behavior.

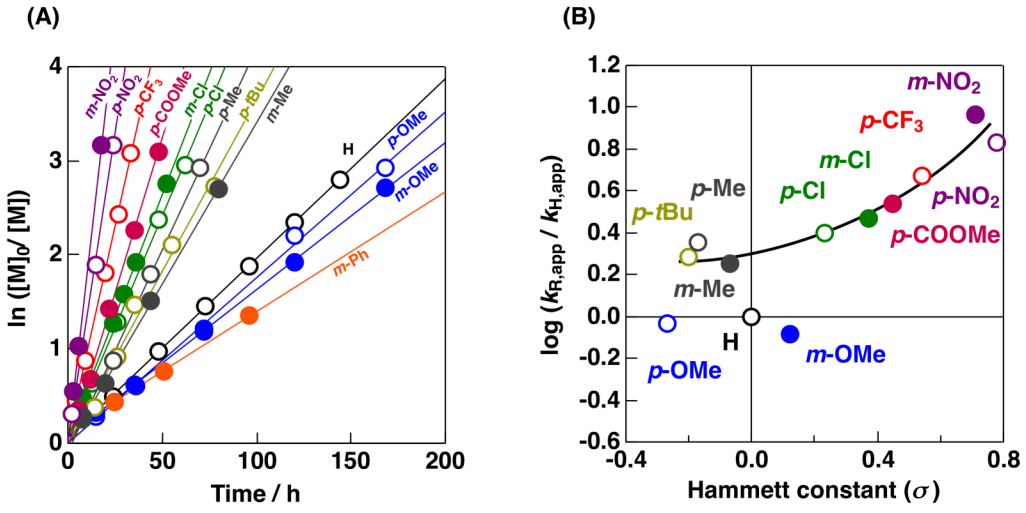

Figure 4. (A) $\ln([M]_0/[M])$–time plots and (B) $\log(k_{R,app}/k_{H,app})$–Hammett substituent constant plot for the polymerization using the *p*- or *m*-substituted phenyl phenoxyimine ligands/$ZrCl_4$ initiating systems ($[IBVE]_0 = 0.76$ M, $[ZrCl_4]_0 = 5.0$ mM, $[ligand]_0 = 5.0$ mM, [ethyl acetate] = 1.0 M, [heptane] = 5.0 vol% in toluene at 0 °C).

The Lewis acid–base interactions between the catalysts and ethyl acetate are likely one of the factors responsible for the non-linearity of the relationship between the Hammett constants and the apparent rate constants. The ^{1}H NMR analyses of the polymerization reaction in $CDCl_3$ at 0 °C (Figure 5) indicated that the catalyst complex and ethyl acetate were in a dissociation (A)-association (B) equilibrium state. The methylene signal of free ethyl acetate was observed at approximately 4.0 ppm, while a signal attributable to the ethyl acetate molecule interacting with a metal complex appeared at 4.6 ppm. From the ratio of the integrals of the imino signal of the catalyst complex and the signal of the ethyl acetate, the ratio of the free catalyst complex (A) and the associated catalyst complex (B) was found to change depending on the ligand structure. Specifically, the proportion of the associated form (B) was higher when ligands with more electron-donating character were used, indicating that stronger Lewis acid catalysts interacted more efficiently with ethyl acetate. The A/B ratio probably affects the polymerization rate because the free catalyst complex (A) and the associated catalyst complex (B) have one and zero vacant coordination sites, respectively. Thus, the difference in the degree of interaction with ethyl acetate among the ligands most likely contributed to the non-linearity of the Hammett plot.

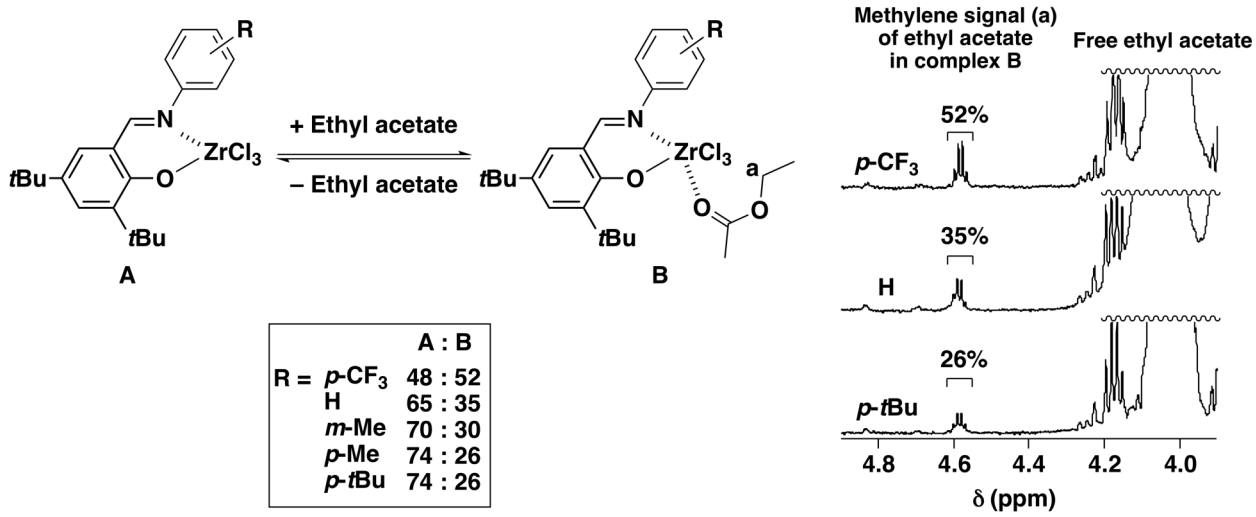

		A : B
R =	*p*-CF_3	48 : 52
	H	65 : 35
	m-Me	70 : 30
	p-Me	74 : 26
	p-*t*Bu	74 : 26

Figure 5. ^{1}H NMR spectra of ethyl acetate (methylene signal: a) with the *p*- or *m*-substituted phenyl phenoxyimine complexes ($[IBVE]_0$ = 0.38 M, $[ZrCl_4]_0$ = 5.0 mM, $[ligand]_0$ = 5.0 mM, [ethyl acetate] = 1.0 M in $CDCl_3$ at 0 ºC).

1.2 The catalytic activities of the ligands/$TiCl_4$ systems

The relationship between the structure of the catalyst and the catalytic activity was investigated in the absence of a Lewis base because the relationship was most likely affected by the interactions of the catalyst with a Lewis base such as ethyl acetate, as shown above. In Chapter 4, the polymerization of IBVE using the *N*-phenyl phenoxyimine ligand/$TiCl_4$ initiating system was demonstrated to proceed in a controlled manner in the absence of a weak Lewis base (Table 2, entry 5) at –78 ºC. Thus, the polymerization was examined using phenoxyimine ligands with various substituents under similar conditions. In each case, the $TiCl_4$ and ligand mixture was transparent. Interestingly, the polymerization of IBVE proceeded in a controlled manner when ligands with any substituents other than a *p*-COOMe group were used (Table 2). The polymerizations proceeded smoothly and reached high conversions. Moreover, the M_n values of the obtained polymers increased linearly with the conversion although the values were larger than those calculated from the amount of ligand. The ineffectiveness of the *p*-COOMe-substituted ligand potentially resulted from the suppression of the Lewis acidity of the metal center by the ester group.

The Hammett plot of the phenoxyimine ligands/$TiCl_4$ initiating systems showed a linear relationship with a positive slope (Figure 6), which was in sharp contrast to the case of the $ZrCl_4$ analogs in the presence of ethyl acetate. The first-order plots of the polymerizations were linear except for the reaction using the *m*-Ph-substituted ligand (Figure 6A). The Hammett plot of the σ values versus the $\log(k_{R,app}/k_{H,app})$

Table 2. Cationic polymerization of IBVE using $TiCl_4$ and the *p*- or *m*-substituted phenyl phenoxyimine ligands[a]

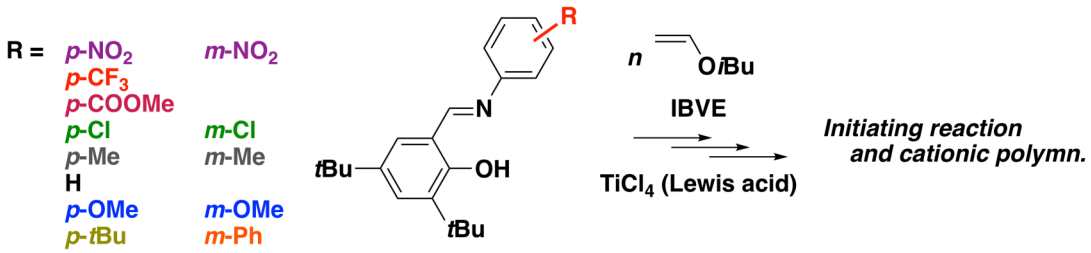

entry	substituent	σ value	time (h)	conv (%)[b]	$M_n \times 10^{-3}$ (calcd)[c]	$M_n \times 10^{-3}$ (obs)[d]	M_w/M_n[d]	meso dyad (%)[e]
1	*p*-NO_2	0.78	0.3	83	12.7	27.7	1.24	71
2	*p*-CF_3	0.54	0.8	96	14.8	30.2	1.07	64
3	*p*-COOMe	0.39	240	16	2.5	–	–	–
4	*p*-Cl	0.23	1.7	89	13.7	29.5	1.05	60
5	H	0	7	94	14.5	29.9	1.11	59
6	*p*-Me	–0.17	21	99	15.2	27.0	1.09	56
7	*p*-*t*Bu	−0.20	19	97	14.9	28.0	1.17	62
8	*p*-OMe	−0.27	20	96	14.7	27.6	1.14	55
9	*m*-NO_2	0.71	0.3	83	12.8	29.6	1.30	72
10	*m*-Cl	0.37	1.5	94	14.4	28.9	1.12	65
11	*m*-OMe	0.12	7	91	14.1	27.5	1.13	63
12	*m*-Ph	0.06	10	80	12.3	20.3	1.30	64
13	*m*-Me	–0.07	19	99	15.2	30.4	1.13	62

[a] $[IBVE]_0$ = 0.76 M, $[TiCl_4]_0$ = 5.0 mM, $[ligand]_0$ = 5.0 mM, [heptane] = 5.0 vol% in toluene at 0 ºC. [b] Determined by gas chromatography. [c] Based on the amounts of phenoxyimines. [d] Determined by GPC (polystyrene standards). [e] Determined by ^{13}C NMR analysis.

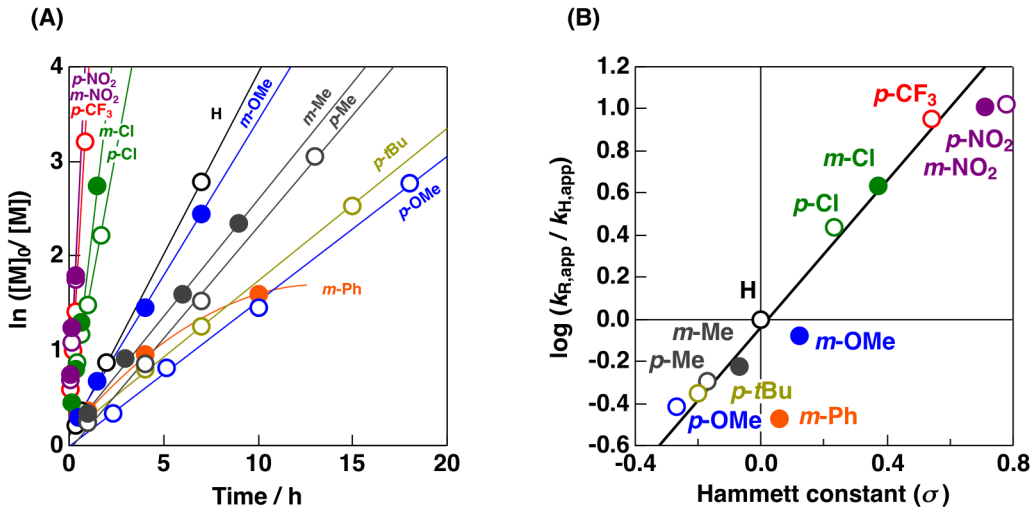

Figure 6. (A) ln([M]$_0$/[M])–time plots and (B) log($k_{R,app}$/$k_{H,app}$)–Hammett substituent constant plot for the polymerization using the *p*- or *m*-substituted phenyl phenoxyimine ligands/$TiCl_4$ initiating systems ([IBVE]$_0$ = 0.76 M, [$TiCl_4$]$_0$ = 5.0 mM, [ligand]$_0$ = 5.0 mM, [heptane] = 5.0 vol% in toluene at –78 ºC).

values of the ligands/$TiCl_4$ initiating systems, as determined from the first-order plots, showed a linear relationship, although the *m*-Ph- and *m*-OMe-substituted ligands deviated from the linear relationship (Figure 6B). The linear relationship clearly indicated that the catalytic activity of the complexes was monotonically related to the electron-withdrawing and electron-donating effects of the substituent on the ligand. In addition, the Hammett σ^+ and σ^- values exhibited more dispersed relationships with the log($k_{R,app}$/$k_{H,app}$) values (Figure 7) than the σ values, which indicated that the catalytic activities of the phenoxyimine ligands/$TiCl_4$ systems were controlled mainly by inductive effects.

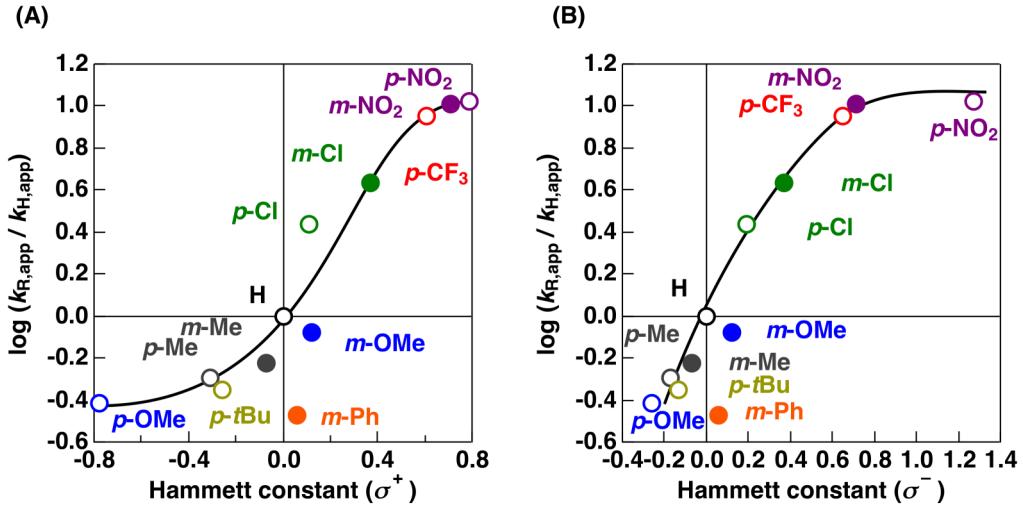

Figure 7. (A) log($k_{R,app}$/$k_{H,app}$)–σ^+ value and (B) log($k_{R,app}$/$k_{H,app}$)–σ^- value plot for the polymerization using the *p*- or *m*-substituted phenyl phenoxyimine ligands/$TiCl_4$ initiating systems ([IBVE]$_0$ = 0.76 M, [$TiCl_4$]$_0$ = 5.0 mM, [ligand]$_0$ = 5.0 mM, [heptane] = 5.0 vol% in toluene at –78 ºC).

1.3 The stereoselectivities in the ligands/$TiCl_4$ systems

The steric and electronic properties of a counteranion are the dominant factors influencing the polymerization behaviors through the ionic interactions between the counteranion and the propagating carbocation. The stereoregularity of a cationic polymerization can also be affected by the properties of the counteranions. Indeed, the counteranion generated from the phenoxyimine complexes with various electronic properties affected the tacticity of the obtained polymers. The ^{13}C NMR analyses indicated that the meso dyad contents of the polymers produced with the phenoxyimine ligands/$TiCl_4$ initiating systems ranged from 55 to 71% (Table 2).

The Hammett plot of the substituent constants versus the logarithm of the meso/racemo ratio [$\log(P_m/P_r)$] show the correlation between the stereoselectivity and the electronic properties of the counteranion (Figure 8). The plots of the σ values and the $\log(P_m/P_r)$ values were fitted with two different curves depending on the substituent positions, except in the case of the *p*-*t*Bu-substituted ligand. The results indicated that the substituent effects, or the electronic properties of counteranions, affected the tacticity of the obtained polymers. Moreover, the plots of the *m*-substituents shows a curve that fits larger P_m/P_r ratios than that of the *p*-substituted analogs. The differences in the positions of the substituents correspond to the difference in the steric hindrance of the counteranions, which affects the stereoregularity. Interestingly, the Hammett plot of the σ^- values versus the $\log(P_m/P_r)$ values for the *p*-substituents showed a linear correlation (Figure 8B). This is probably because a negatively charged counteranion is affected more heavily by resonance effects than a neutral catalyst complex.

The meso dyad contents decreased as the electron-donating effects of the ligands increased (Figure 8). According to the model proposed earlier,[12] the steric repulsion between the counteranion and the incoming monomer and/or the tightness of the growing ion pair determine the stereoregularity of a cationic polymerization. Based on the model, the author expected that an electron-rich catalyst complex would generate an isotactic polymer due to the tight interaction between the counteranion and the carbocation; however, the Hammett plot showed the opposite trend. Specifically, the polymerization using a ligand with a *p*-NO_2 group, a strongly electron-withdrawing group, generated a polymer with a similar meso content to the polymer obtained with the IBVE–HCl/$TiCl_4$ initiating system (m = 72%), and the meso content decreased as the electron-donating nature increased.

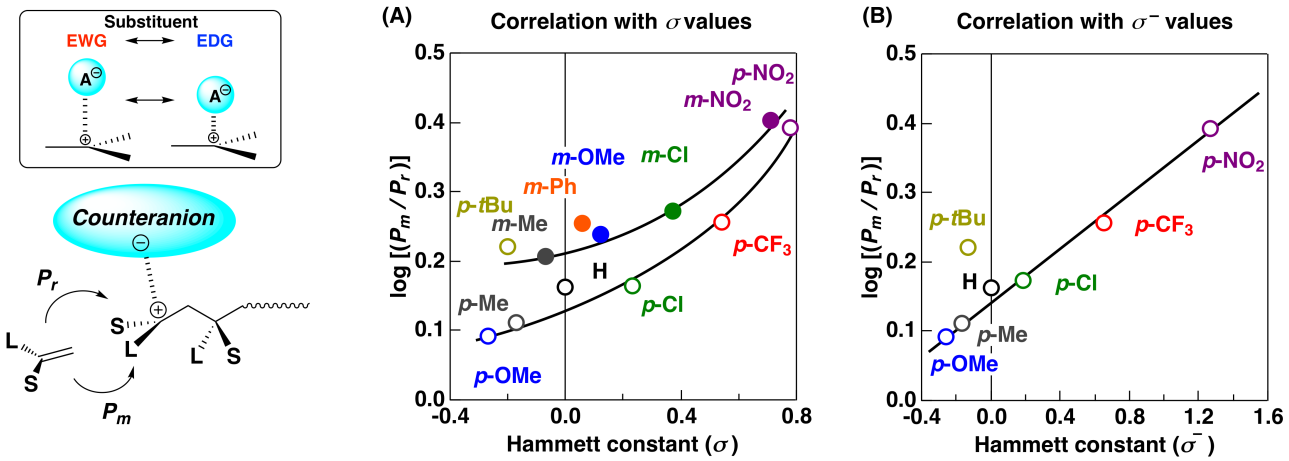

Figure 8. Correlation between meso dyad ratios of the obtained polymers and (A) σ or (B) σ^- values ($[IBVE]_0$ = 0.76 M, $[TiCl_4]_0$ = 5.0 mM, $[ligand]_0$ = 5.0 mM, [heptane] = 5.0 vol% in toluene at –78 ºC).

The substituent effects of the *N*-aryl phenoxyimine ligands with *m,m*-disubstituted phenyl moieties on the tacticity of the obtained polymers exhibited a similar trend to those of the monosubstituted ligands (Table 3). Cationic polymerizations of IBVE using *m,m*-disubstituted ligand/$TiCl_4$ initiating systems proceeded in a controlled manner in toluene at –78 °C. The polymers obtained using ligands with strong electron-withdrawing groups, such as NO_2, CF_3, and Cl groups, showed slightly broader MWDs (Table 3, entries 1–3). The tacticity of the polymers generated using the *m,m*-disubstituted ligands showed a similar trend to what was seen with monosubstituted ligands; the low meso dyad contents were exhibited by the introduction of an electron-donating group onto the ligands. Furthermore, the meso dyad contents of the polymers produced with the *m,m*-disubstituted ligands were slightly larger than those prepared using the corresponding *m*-monosubstituted ligands potentially due to the additive nature of the substituent constants.

Table 3. Cationic polymerization of IBVE using $TiCl_4$ and the *m,m*-disubstituted phenyl phenoxyimine ligands[a]

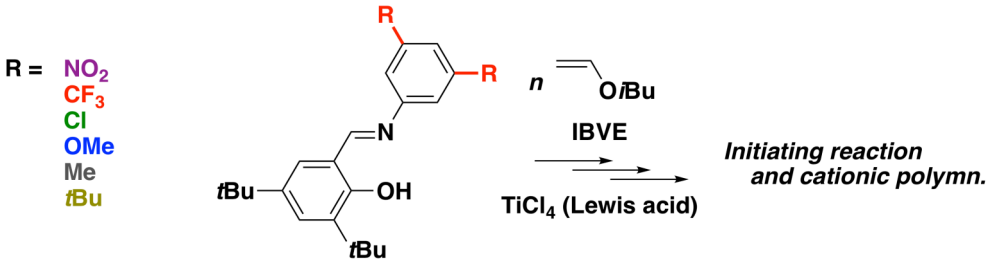

entry	substituent	time (h)	conv (%)[b]	$M_n \times 10^{-3}$ (calcd)[c]	$M_n \times 10^{-3}$ (obs)[d]	M_w/M_n[d]	meso dyad (%)[e]
1	NO_2	0.1	95	14.6	34.7	1.49	75
2	CF_3	0.1	90	13.8	29.3	1.67	73
3	Cl	0.15	89	13.7	27.4	1.40	73
4	OMe	48	80	12.3	16.3	1.25	64
5	Me	76	98	15.1	17.8	1.16	63
6	*t*Bu	50	96	14.7	17.9	1.23	66

[a] $[IBVE]_0$ = 0.76 M, $[TiCl_4]_0$ = 5.0 mM, $[ligand]_0$ = 5.0 mM, [heptane] = 5.0 vol% in toluene at –78 ºC. [b] Determined by gas chromatography. [c] Based on the amounts of phenoxyimines. [d] Determined by GPC (polystyrene standards). [e] Determined by ^{13}C NMR analysis.

2. The relationship between the steric properties and the catalytic properties of the *o*-substituted phenyl phenoxyimine ligand/MCl_n systems

2.1 The catalytic activity of ligands/$ZrCl_4$ systems

o-Substituted phenyl phenoxyimine ligands may exhibit behavior different from that of *p*- or *m*-substituted ligands due to increased steric hindrance. To examine the *o*-substituent effects on the polymerization behavior, cationic polymerizations of IBVE using the *o*-substituted ligands/$ZrCl_4$ initiating systems were conducted via *in situ* complexation in the presence of ethyl acetate in toluene at 0 °C (Table 4). The polymerization using the 2-MePh-substituted ligand proceeded smoothly and reached high conversion of IBVE. The M_n values of the obtained polymers increased linearly with increasing monomer conversion (Figure 9A). In addition, the 2-MePh/$TiCl_4$ concentration corresponded to the M_n values of the obtained polymers, indicating that the cationogen generated *in situ* from 2-MePh and $TiCl_4$ initiated the reaction (Figure 9A). Moreover, the first-order plot was linear (Figure 9B), indicating that the concentration of the propagating species was constant during the polymerization. These results indicate that the polymerization proceeded in a highly controlled manner.

The large number of *o*-substituents caused the fast polymerization (Table 4, Figure 9B). Cationic polymerizations of IBVE using *o*-mono- and *o,o*-disubstituted ligands with alkyl or phenyl groups and $ZrCl_4$ were conducted under similar conditions (Table 4, entries 3–7). The polymerizations proceeded in a controlled manner regardless of the ligands used. An alkyl group generally functions as an electron-donating group; hence, the introduction of an alkyl group to a ligand may decelerate the reaction. However, the introduction of *o*-substituents accelerated the polymerization reaction. Moreover, the *o,o*-disubstituted ligands accelerated the reactions more than their *o*-monosubstituted counterparts. The acceleration effects are

Table 4. Cationic polymerization of IBVE using $ZrCl_4$ and the *o*-substituted phenyl phenoxyimine ligands[a]

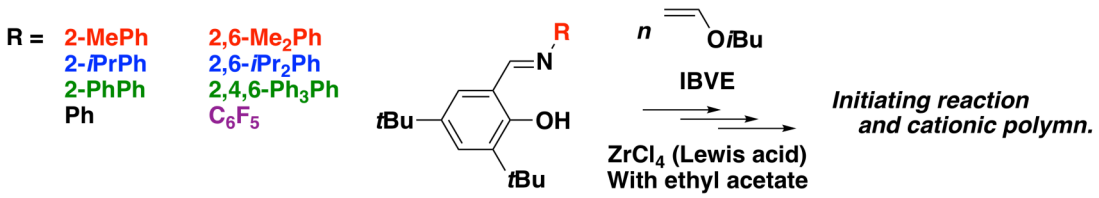

entry	R	time (h)	conv (%)[b]	$M_n \times 10^{-3}$ (calcd)[c]	$M_n \times 10^{-3}$ (obs)[d]	M_w/M_n[d]
1	2-MePh	48	95	14.6	10.6	1.17
2		4	89	6.9	6.9	1.27
3	2-*i*PrPh	96	94	14.5	8.7	1.23
4	2-PhenylPh	96	92	14.2	6.3	1.30
5	2,6-Me_2Ph	28	97	14.9	9.2	1.13
6	2,6-*i*Pr_2Ph	35	98	15.1	12.2	1.13
7	2,4,6-Ph_3Ph	21	94	14.4	13.2	1.28
8	C_6F_5	4	92	14.1	12.7	1.36

[a] $[IBVE]_0$ = 0.76 M, $[ZrCl_4]_0$ = 5.0 mM for entries 1, 3–8, 10 mM for entry 2, $[ligand]_0$ = 5.0 mM for entries 1, 3–8, 10 mM for entry 2, [ethyl acetate] = 1.0 M, [heptane] = 5.0 vol% in toluene at 0 °C. [b] Determined by gas chromatography. [c] Based on the amounts of phenoxyimines. [d] Determined by GPC (polystyrene standards).

likely caused by the rotation of the C–N bond of the ligand.[13] The structural change is probably responsible for the acceleration effects through the steric and/or electronic change to the active site environment. In addition, cationic polymerization using a ligand with a C_6F_5 group, which is expected to exhibit dual-acceleration effects through both electronic and steric properties, proceeded at a rate that was approximately 25 times higher than that of its unsubstituted counterpart (Ph).

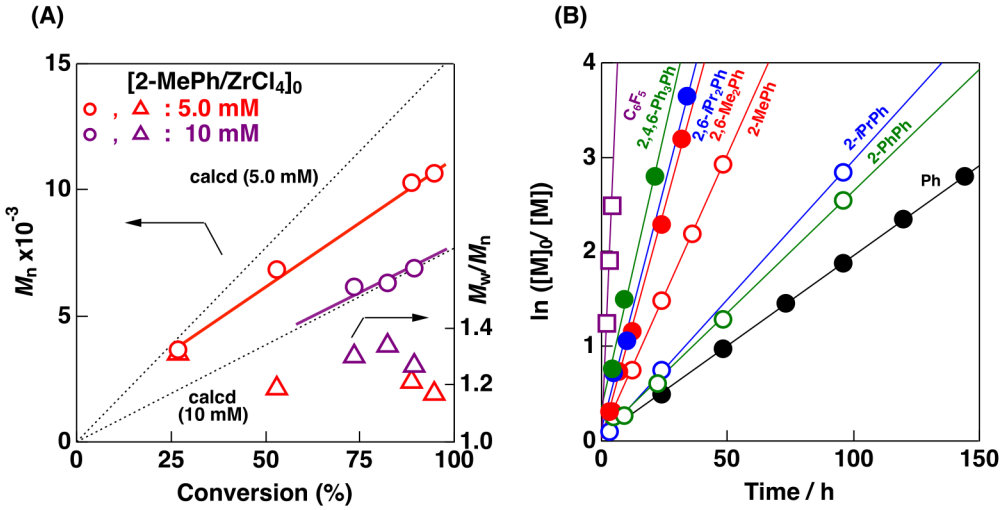

Figure 9. (A) M_n (calculated M_n, dotted line) and M_w/M_n and (B) ln([M]$_0$/[M])–time plots for the polymerization using the *o*-substituted phenyl phenoxyimine ligands/$ZrCl_4$ initiating systems.

2.2 The stereoselectivity in the polymerization of different VEs with ligands/$TiCl_4$ systems

To examine the effects of *o*-substituents on the tacticities of the obtained polymers, cationic polymerizations of VEs were conducted using the *o*-substituted phenyl phenoxyimine ligand/$TiCl_4$ initiating systems (Table 5). First, cationic polymerizations of IBVE were examined in toluene at –78 °C (Table 5). Unlike when $ZrCl_4$ was used, the polymerization using $TiCl_4$ was conducted in the absence of a weak Lewis base. The polymerization behavior considerably depended on the ligand structure (Table 5). The polymerization of IBVE using a 2-MePh- or 2-*i*PrPh-substituted ligand (Table 5, entries 2, 3) proceeded at a slightly faster rate than the reaction using an unsubstituted ligand (Table 5, entries 1), which is similar to what was observed with the *o*-substituted ligand/$ZrCl_4$ initiating systems. In contrast, polymerization was significantly decelerated when 2-PhenylPh-, 2,6-Me_2Ph-, and 2,4,6-Ph_3Ph-substituted ligands were used (Table 5, entries 4, 5 and 7). The steric hindrance of these ligands may be responsible for the deceleration effects, although the polymerization using a 2,6-*i*Pr_2Ph-substituted ligand proceeded smoothly at a moderate rate. ^{13}C NMR analyses indicated that the meso dyad contents of the obtained polymers decreased as the size and number of *o*-substituents decreased (m = 59–74%). However, comparing the polymers generated using the IBVE–HCl/$TiCl_4$ system (m = 72%) suggested that larger substituents had smaller effects on the tacticity. Specifically, the unsubstituted ligand (Table 5, entry 1) was the most favorable for the racemo formation among the ligands examined in Table 5.

Table 5. Cationic polymerization of IBVE using $TiCl_4$ and the *o*-substituted phenyl phenoxyimine ligands[a]

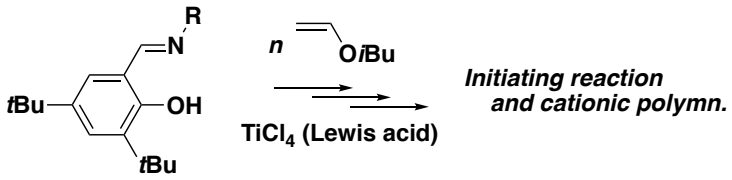

entry	R	time	conv (%)[b]	$M_n \times 10^{-3}$ (calcd)[c]	$M_n \times 10^{-3}$ (obs)[d]	M_w/M_n[d]	meso dyad (%)[e]
1	Ph	7 h	94	14.5	29.9	1.11	59
2	2-MePh	4 h	96	14.8	25.3	1.29	64
3	2-*i*PrPh	5 h	91	14.0	21.1	1.44	67
4	2-PhenylPh	42 h	47	5.3	3.5	1.52	70
5	2,6-Me_2Ph	240 h	30	4.7	7.4	9.72	70
6	2,6-*i*Pr_2Ph	19 h	97	14.9	12.3	1.88	72
7	2,4,6-Ph_3Ph	168 h	64	9.9	41.6	5.33	74
8[f]	no ligand	1 min	96	14.8	14.8	2.00	72

[a] $[IBVE]_0$ = 0.76 M, $[TiCl_4]_0$ = 5.0 mM, $[ligand]_0$ = 5.0 mM, [heptane] = 5.0 vol% in toluene at –78 ºC. [b] Determined by gas chromatography. [c] Based on the amounts of phenoxyimines. [d] Determined by GPC (polystyrene standards). [e] Determined by ^{13}C NMR analysis. [f] $[IBVE–HCl]_0$ = 5.0 mM.

The polymerizations of EVE and IPVE using the *o*-substituted ligand/$TiCl_4$ initiating systems were also significantly affected by the substituents on the ligands. The 2,6-Me_2Ph-substituted ligand/$TiCl_4$ initiating system produced poly(EVE)s and poly(IPVE)s with relatively narrow MWDs (Table 6, entries 2, 6). The unsubstituted ligand (Ph)/$TiCl_4$ initiating system produced polymers with MWDs narrower than those of the polymers obtained using the 2,6-Me_2Ph-substituted ligand/$TiCl_4$ initiating system (Figure 10). In both cases, the M_n values of the obtained poly(EVE) and poly(IPVE) increased linearly with increasing

Table 6. Cationic polymerization of VEs using $TiCl_4$ and the *o*-substituted phenyl phenoxyimine ligands[a]

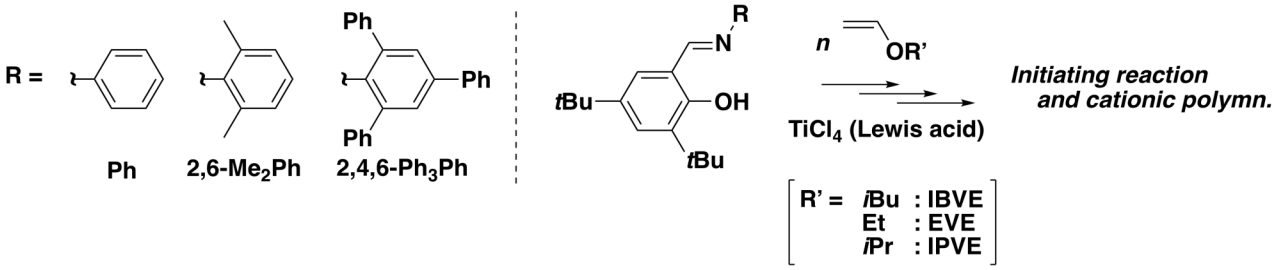

entry	monomer	R	time	conv (%)[b]	$M_n \times 10^{-3}$ (calcd)[c]	$M_n \times 10^{-3}$ (obs)[d]	M_w/M_n[d]	meso dyad (%)[e]
1	EVE	Ph	3 h	96	10.8	23.1	1.07	73
2		2,6-Me_2Ph	168 h	98	11.1	18.1	1.14	79
3		2,4,6-Ph_3Ph	528 h	0	0	–	–	–
4[f]		no ligand	72 h	49	5.5	4.8	1.40	76
5	IPVE	Ph	2 min	92	12.1	25.9	1.11	60[g]
6		2,6-Me_2Ph	2 h	98	13.0	33.6	1.60	60[g]
7		2,4,6-Ph_3Ph	1.5 h	97	12.9	18.6	16.1	81[g]
8[f]		no ligand	30 s	100	13.2	30.9	5.04	82[g]

[a] $[VE]_0$ = 0.76–78 M, $[TiCl_4]_0$ = 5.0 mM, $[ligand]_0$ = 5.0 mM, [heptane] = 5.0 vol% in toluene at –78 ºC. [b] Determined by gas chromatography. [c] Based on the amounts of phenoxyimines. [d] Determined by GPC (polystyrene standards). [e] Determined by ^{13}C NMR analysis. [f] $[IBVE–HCl]_0$ = 5.0 mM. [g] Caluculated from the triad values: $m = mm + (1/2)\,mr$ and $r = rr + (1/2)\,mr$.[14]

monomer conversion, indicating that the polymerization proceeded in a controlled manner. The M_n values were approximately twice those calculated based on the concentration of the phenolic OH hydrogen atoms of the ligands in both cases, which was also observed for the polymerization of IBVE. Notably, the MWDs of the poly(EVE) and poly(IPVE) were narrower than those of the polymers obtained using the IBVE–HCl/$TiCl_4$ initiating system (Figure 10). Thus, the ligand–metal interaction suitably moderated the Lewis acidity of the central metal, triggering the cationic polymerization of VEs in a well-controlled manner. In sharp contrast, the 2,4,6-Ph_3Ph/$TiCl_4$ initiating system led to uncontrolled polymerization of IPVE in a manner similar to what was seen with IBVE. Moreover, no polymer was obtained from EVE when using the 2,4,6-Ph_3Ph system. The steric hindrance of the complex was likely responsible for the uncontrolled propagation reaction and the interruption of the propagating reaction.

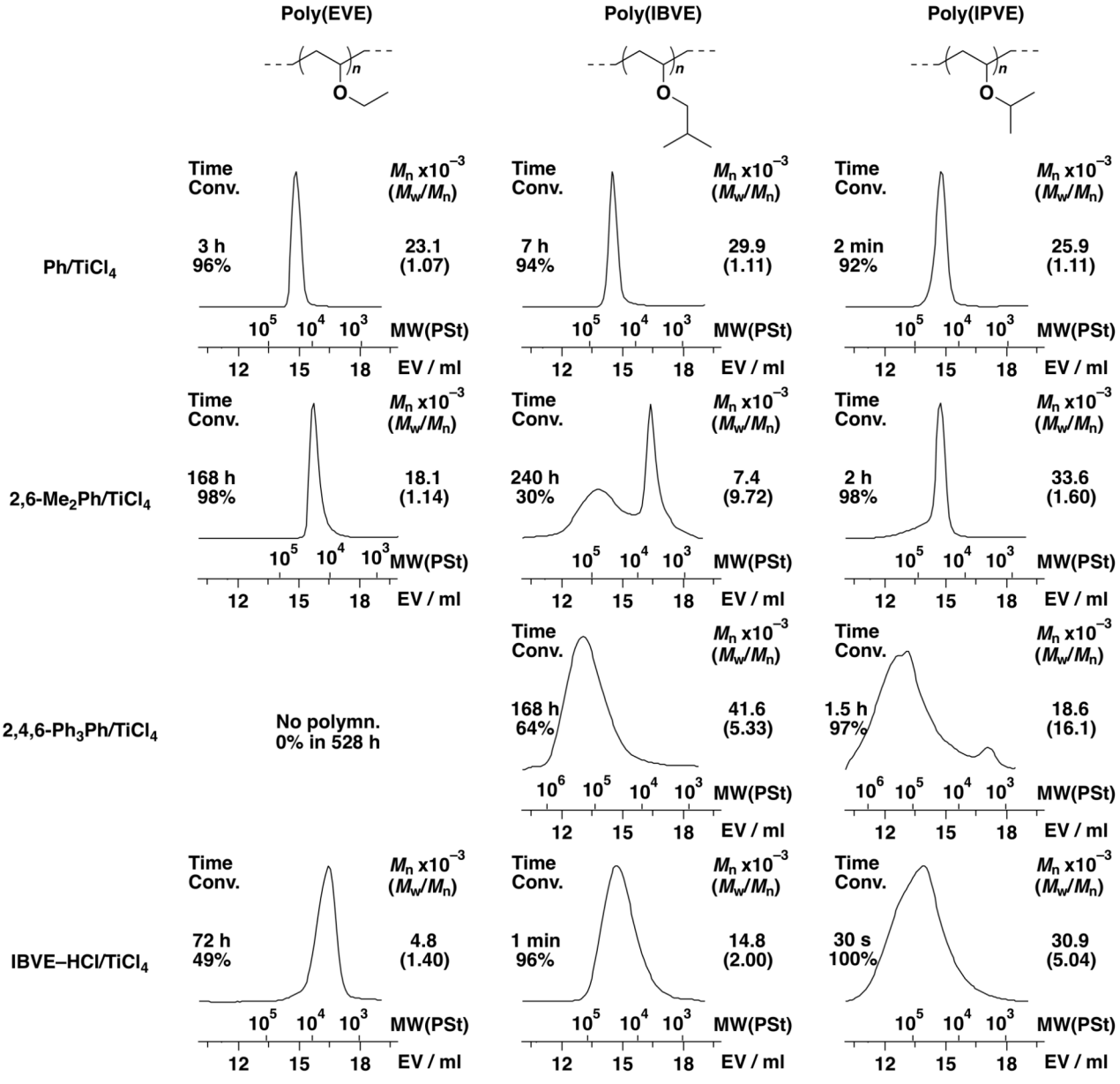

Figure 10. MWD curves for poly(VE)s obtained using the *o*-substituted phenyl phenoxyimine ligands/$TiCl_4$ initiating systems ($[VE]_0$ = 0.76–0.78 M, $[TiCl_4]_0$ = 5.0 mM, $[ligand]_0$ = 5.0 mM in toluene at –78 ºC).

^{13}C NMR analyses of the polymers indicated that the effects of the structures of the ligands on the tacticities of the obtained polymers were highly depend on the VE side chains (Figure 11). The poly(IPVE)s obtained with the Ph and 2,6-Me_2Ph/$TiCl_4$ initiating systems, which proceeded in controlled manners, had notably lower meso contents (m ~ 60%; calculated from the *mm* and *mr* triad contents) than did the polymers obtained using the 2,4,6-Ph_3Ph and IBVE–HCl/$TiCl_4$ initiating systems (m ~ 82%). This trend is similar to the case of the poly(IBVE)s. In contrast, the tacticities of the poly(EVE)s showed small differences regardless of the ligand used. The polymers had meso dyad contents of 73–79%. The smaller side chains of EVE relative to those of IBVE and IPVE are most likely responsible for the smaller effects of the ligand structure on the tacticity.

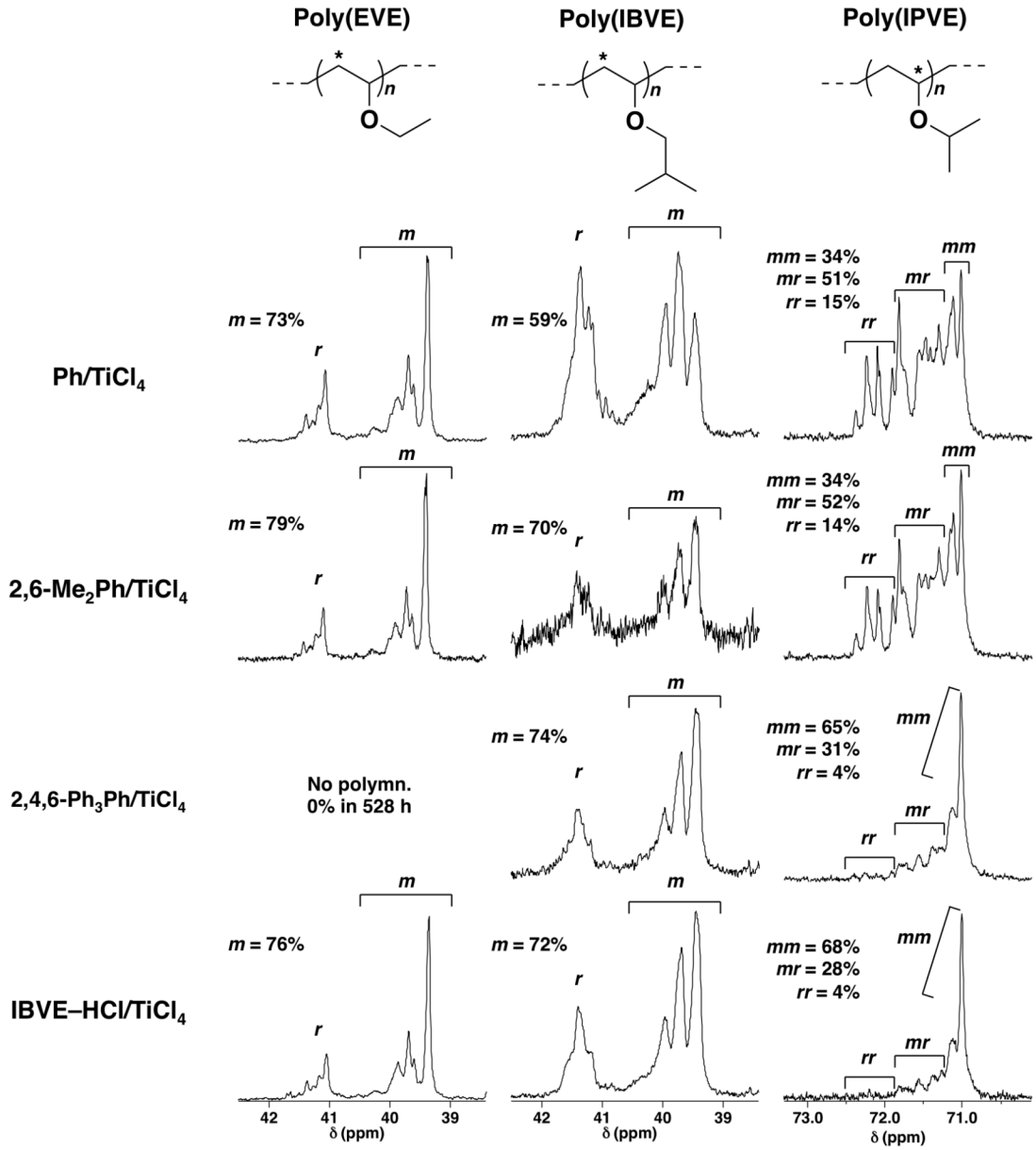

Figure 11. ^{13}C NMR spectra of poly(VE)s obtained with the *o*-substituted phenyl phenoxyimine ligands/$TiCl_4$ initiating systems ($[VE]_0$ = 0.76–0.78 M, $[TiCl_4]_0$ = 5.0 mM, $[ligand]_0$ = 5.0 mM in toluene at –78 ºC; 100 MHz in $CDCl_3$ or 125 MHz in CCl_4/C_6D_6 (9/1 v/v) at 30 ºC).

Conclusion

The substituent effects of various phenoxyimine ligands on the polymerization behavior of the resulting complexes were investigated using the ligand/$ZrCl_4$ or $TiCl_4$ initiating systems by an *in situ* complexation method. In particularly, a linear correlation between the σ values and the $\log(k_{R,app}/k_{H,app})$ values was observed in the polymerization using the *p*- or *m*-substituted phenyl phenoxyimine ligands/$TiCl_4$ initiating systems. This indicated that the electron-withdrawing and donating effects of the substituents directly affected the catalytic activity based on the Lewis acidity of the phenoxyimine complexes. Moreover, the introduction of an electron-donating group onto the ligands decreased the meso dyad values of the obtained polymers. The tight interaction between the electron-donating group-substituted counteranion and the carbocation may cause the racemo formation to be favored. In addition, the Hammett plot of the σ^- versus the $\log(P_m/P_r)$ for *p*-substituents showed a linear correlation, indicating that the negatively charged counteranion was affected by the enhanced resonance effects of the substituent.

The *o*-substituted ligands exhibited polymerization behavior that was different from that of the *p*- and *m*-substituted ligands. The polymerizations using the *o*-substituted ligand/$ZrCl_4$ initiating systems proceeded faster when ligands with larger numbers of *o*-substituents were used. In addition, the polymerization of VEs using ligands with bulky substituents, such as a 2,4,6-Ph_3Ph-substituted ligand, proceeded in an uncontrolled manner (IBVE and IPVE) or did not proceed at all (EVE), depending on the structures of the VEs. *o*-Substituents likely affected the counteranion–carbocation interaction through structural changes caused by the rotation of the C–N bond.

References

1. (a) Hammett, L. P. *J. Am. Chem. Soc.* **1937**, *59*, 96–103. (b) Jaffe, H. H. *Chem. Rev.* **1953**, *53*, 191–261. (c) Brønsted, J. N. *Chem. Rev.* **1928**, *5*, 231–338. (d) Ando, T.; Kim, S.-G.; Matsuda, K.; Yamataka, H.; Yukawa, Y.; Fry, A.; Lewis, D. E.; Sims, L. B.; Wilson, J. C. *J. Am. Chem. Soc.* **1981**, *103*, 3505–33516. (e) Swain, C. G.; Scott, C. B. *J. Am. Chem. Soc.* **1953**, *75*, 141–147.
2. Hansch, C.; Hoekman, D.; Leo, A.; Weininger, D.; Selassie, C. D. *Chem. Rev.* **2002**, *102*, 783–812.
3. Harper, Kaid. C.; Sigman, M. S. *J. Org. Chem.* **2013**, *78*, 2813–2818.
4. (a) Huang, Y.; Wayner, D. D. M. *J. Am. Chem. Soc.* **1994**, *116*, 2157–2158. (b) Kandanarachchi, P.; Sinnott, M. L. *J. Am. Chem. Soc.* **1994**, *116*, 5592–5600. (c) McGrath, J. M.; Pluth, M. D. *J. Org. Chem.* **2014**, *79*, 11797–11801. (d) Bour, J. R.; Camasso, N. M.; Sanford, M. S. *J. Am. Chem. Soc.* **2015**, *137*, 8034–8037. (e) Pulukkody, R.; Kyran, S. J.; Drummond, M. J.; Hsieh, C.-H.; Darensbourg, D. J.; Darensbourg, M. Y. *Chem. Sci.* **2014**, *5*, 3795–3802. (f) He, C.; Ke, J.; Xu, H.; Lei, A. *Angew. Chem., Int. Ed.* **2013**, *52*, 1527–1530. (g) Mueller, J. A.; Sigman, M. S. *J. Am.*

Chem. Soc. **2003**, *125*, 7005–7013. (h) Böhm, V. P. W.; Herrmann, W. A. *Chem. - Eur. J.* **2001**, *7*, 4191–4197.

5. (a) Jencks, W. P.; Gilchrist, M. *J. Am. Chem. Soc.* **1968**, *90*, 2622–2637. (b) Spillane, W. J.; McGrath, P.; Brack, C.; O'Byrne, A. B. *J. Org. Chem.* **2001**, *66*, 6313–6316. (c) Humeres, E.; Debacher, N. A.; Sierra, M. M. S.; Franco, J. D.; Schutz, A. *J. Org. Chem.* **1998**, *63*, 1598–1603. (d) Oh, H. K.; Ku, M. H.; Lee, H. W.; Lee, I. *J. Org. Chem.* **2002**, *67*, 3874–3877.
6. Hansch, C.; Leo, A.; Taft, R. W. *Chem. Rev.* **1991**, *91*, 165–195.
7. (a) Matsugi, T.; Fujita, T. *Chem. Soc. Rev.* **2008**, *37*, 1264–1277. (b) Maiko, H.; Terao, H.; Iwashita, A.; Fujita, T. *Chem. Rev.* **2011**, *111*, 2363–2449.
8. Freedman, H. H. *J. Am. Chem. Soc.*, **1961**, *83*, 2900–2905.
9. (a) Kawato, T.; Koyama, H.; Kanatomi, H.; Isshiki, M. *J. Photochem.* **1985**, *28*, 103–110. (b) Kasumov, V. T.; Medjidov, A. A.; Yayli, N.; Zeren, Y. *Spectrochem. Acta A* **2004**, *60*, 3037–3047. (c) Ahmad, J. U.; Nieger, Martin, Sundberg, M. R.; Leskela, M.; Repo, T. *J. Mol. Struct.* **2011**, *995*, 9 –19.
10. (a) Percy, G. C.; Thornton, D. A. *J. Inorg. Nucl. Chem.* **1972**, *34*, 3357–3367. (b) Saraiva, M. E. L.; Geraldes, C. F. G.; Gil, V. M. S. *Tetrahedron* **1988**, *44*, 163–170.
11. Heterogeneous catalytic solutions were obtained when phenoxyimine ligands with *p*-NO_2, *p*-CF_3, *p*-Cl, *p*-Me, *p*-OMe, and *m*-OMe were used.
12. Kunitake, T.; Aso, C. *J. Polym. Sci., Part A-1 Polym. Chem.* **1970**, *8*, 665–678.
13. Pennington, D. A.; Clegg, W.; Cole, S. J.; Harrington, R. W.; Hursthouse, M. B.; Hughes, D. L.; Light, M. E.; Schormann, M.; Bochmann, M.; Lancaster, S. J. *Dalton Trans.* **2005**, *3*, 561–571.
14. Hatada, K.; Kitayama, T.; Matsuo, N.; Yuki, H. *Polym. J.* **1983**, *15*, 719–725.

Chapter 6

Summary

Designing metal complex catalysts is a powerful tool for the development of novel synthetic methods of various organic compounds with extraordinary selectivity, activity, and atom economy in both industrial and academic fields. To improve a catalytic property, optimize a complex structure, and develop new catalysts and metal-complex-catalyzed reactions, one needs to understand how metals and ligands influence reaction mechanisms and catalytic properties at the molecular level. However, studies of catalyst design using various ligand frameworks have been limited to selected examples in the field of cationic polymerization. The systematic understanding and useful design criteria of metal complex catalysts is insufficient in this field. Thus, the author focused on a systematic understanding of the fundamental aspect of how catalytic structure determines catalytic property and polymerization behavior in cationic polymerization. The objective of this thesis is to comprehensively examine the functions and properties of metal complex catalysts in cationic polymerization.

Part I described the establishment of a new methodology of the *in situ* complexation of metal complex catalysts for living cationic polymerization. In addition, the influences of the central metals on catalytic activities and polymerization behaviors were investigated using the *in situ* complexation method with the combinations of salen-type ligands and various metal chlorides.

Chapter 2 presented the construction of a new methodology for the preparation of metal complex catalysts using various metal chlorides and salphen ligands, which were tetradentate ligands possessing two phenol moieties. The *in situ* complexation method, which was based on ligand exchange reaction, had a dual role: the readily prepared metal complex was used as a catalyst, and *in situ* generated hydrochloric acid was used as an initiator. A series of investigations using various metal chlorides indicated that a vacant site on the central metal of a complex catalyst was important to exert Lewis acidity. In addition, relatively oxophilic metal species were suitable for the fast and quantitative initiation reaction. Particularly, the salphen/$ZrCl_4$ initiating system induced the living cationic polymerization of IBVE through quantitative initiation reaction. Furthermore, the usability of salphen ligand frameworks was confirmed by the occurrence of controlled cationic polymerization using the combinations of ligands with various substituents and $ZrCl_4$.

Chapter 3 described the structural effect of ligands on the catalytic property and the scope of metal chlorides available for the *in situ* complexation method. The polymerization performed with the salen system proceeded at an approximately ten times smaller rate than that of the salphen system. Moreover, salen ligands had a potential to provide an appropriate catalytic environment for a wider variety of metal species than salphen ligands. Indeed, $FeCl_3$, a metal chloride that was not suited for the initiating system using

salphen ligands, efficiently generated a metal complex catalyst via the complexation with salen ligands and produced polymers with narrow MWDs. Thus, tailoring the ligand framework to the metal species was highly important for the design of metal complex catalysts with sufficient stabilities and desirable catalytic properties.

In part II, the author demonstrated the ligand screening using various bidentate ligand frameworks for investigating appropriate ligands for controlled cationic polymerization. The relationship between the catalytic structure and the catalytic property in controlled cationic polymerization was also investigated using the Hammett equation under optimized conditions.

Chapter 4 addressed the screening for finding an appropriate ligand scaffold in cationic polymerization. The results of the polymerizations using various ligands/$ZrCl_4$ initiating systems indicated the usefulness of the [*N*,*O*]-type phenoxyimine ligand frameworks, which had a similar structure with a salen-type ligand. In particular, the *N*-aryl phenoxyimine ligand with *t*Bu groups on the phenol moiety was effective in terms of the controllability of the polymerization, catalyst solubility, catalytic activity, and ease of derivatization. The optimization of reaction conditions led to the expansion of the applicable metal species for controlled cationic polymerization. In addition, the phenoxyimine/$ZrCl_4$ systems were effective for the controlled polymerization of various monomers including St derivatives. The easily tunable electronic properties and stereochemical properties were also useful for the controlled bulk polymerization.

In Chapter 5, the author investigated the catalytic structure–property relationships of the phenoxyimine complexes by the Hammett correlation. In cationic polymerization, catalyst and counteranion were responsible for polymerization behaviors, such as polymerization rate and stereoselectivity. Theoretical understanding of the ligand structure-catalytic property relationships and the catalytic reaction mechanisms was highly efficient for the development of functional catalysts. Correlation analyses of the series of experiments indicated that the substituents on the *N*-aryl phenoxyimine ligands affected the polymerization rate and stereoselectivity. Moreover, a linear correlation was observed between the Hammett substituent constants and the polymerization rates. In addition, the tacticity of product polymers also correlated to the Hammett substituent constants. The tight interaction between the electron-donating group-substituted counteranion and the carbocation possibly induced a racemo-favored route. In contrast, the polymerization behavior using *o*-substituted ligands exhibited a trend different from those using *p*- or *m*-substituted ligands. The structural change, which was caused by the rotation of the C–N bonding, most likely triggered the acceleration effect.

In conclusion, this thesis described the development of a new methodology of the *in situ* complexation of metal complex catalysts for living cationic polymerization and the catalytic

structure-property relationship based on the substituent effect in controlled cationic polymerization. Tailoring the ligand framework to the metal species was highly important for the design of metal complex catalysts with sufficient stabilities and appropriate Lewis acidities. Specifically, both the electronic and steric properties of complex catalysts and counteranions were closely related to the catalytic activity and the stereoselectivity, most likely due to the ionic interaction between counteranion and propagation carbocation. The author hopes that the research conducted in this thesis will be a clue for an elaborate design of a metal complex catalyst with advanced features.

List of Publications

1. Sensho Kigoshi, Arihiro Kanazawa, Shokyoku Kanaoka, and Sadahito Aoshima
   "*In Situ* and Readily Prepared Metal Catalysts and Initiator for Living Cationic Polymerization of Isobutyl Vinyl Ether: Dual-Purpose Salphen as a Ligand Framework for $ZrCl_4$ and an Initiating Proton Source"
   Polym. Chem., **2015**, *6*, 30–34.
   (Corresponding to Chapter 2)

2. Sensho Kigoshi, Arihiro Kanazawa, Shokyoku Kanaoka, and Sadahito Aoshima
   "Salen- and Salphen-Type Ligand/MCl_n Initiating Systems for the Controlled Cationic Polymerization of Isobutyl Vinyl Ether: Effects of the Ligand Framework"
   to be submitted.
   (Corresponding to Chapters 2 and 3)

3. Sensho Kigoshi, Arihiro Kanazawa, Shokyoku Kanaoka, and Sadahito Aoshima
   "Appropriate Ligand Frameworks for Controlled Cationic Polymerization of Isobutyl Vinyl Ether"
   to be submitted.
   (Corresponding to Chapter 4)

4. Sensho Kigoshi, Arihiro Kanazawa, Shokyoku Kanaoka, and Sadahito Aoshima
   "Structure–Property Relationship of Phenoxyimine Ligands/MCl_n Initiating System for Cationic Polymerization of Vinyl Ether"
   to be submitted.
   (Corresponding to Chapter 5)